Reviews in Mineralogy & Geochemistry
Vol. 74 pp. 211-278, 2012

Supplementary Cementitious Materials

Ruben Snellings, Gilles Mertens and Jan Elsen

Department of Earth and Environmental Sciences
Katholieke Universiteit Leuven
B-3001 Leuven, Belgium

e-mail: ruben.snellings@epfl.ch

INTRODUCTION

The current widespread use of calcium silicate or aluminate hydrate binder systems in the construction industry finds its roots in the Antique world where mixtures of calcined lime and finely ground reactive (alumino-)silicate materials were pioneered and developed as competent inorganic binders. Architectural remains of the Minoan civilization (2000-1500 BC) on Crete have shown evidence of the combined use of slaked lime and additions of finely ground potsherds to produce stronger and more durable lime mortars suitable for water-proof renderings in baths, cisterns and aqueducts (Spence and Cook 1983). It is not clear when and where mortar technology evolved to incorporate volcanic pumice and ashes as a functional supplement. A plausible site would be the Akrotiri settlement at Santorin (Greece), where archeological indications of strong ties with the Minoan culture were found and large quantities of suitable highly siliceous volcanic ash were present. This so-called Santorin earth has been used as a pozzolan in the Eastern Mediterranean until recently (Kitsopoulos and Dunham 1996). Evidence of the deliberate use of this and other volcanic materials by the ancient Greeks dates back to at least 500-400 BC, as uncovered at the ancient city of Kamiros, Rhodes (Efstathiadis 1978; Idorn 1997). In the subsequent centuries the technological knowledge was spread to the mainland (Papayianni and Stefanidou 2007) and was eventually adopted and improved by the Romans (Mehta 1987). The Roman alternatives for Santorin earth were volcanic pumices or tuff found in neighboring territories, the most famous ones found in Pozzuoli (Naples), hence the name pozzolan, and in Segni (Latium). Preference was given to natural pozzolan sources, but crushed ceramic waste was frequently used when natural deposits were not locally available. The exceptional lifetime and preservation condition of some of the most famous Roman buildings such as the Pantheon or the Pont du Gard constructed with the aid of pozzolan-lime mortars and concrete testify to both the excellent workmanship reached by Roman "engineers" and to the durable properties of the utilized binder materials.

In designing the binder mixes Romans seem to have paid much attention to a very thorough grinding and mixing of components and to the granulometric gradation of the aggregate with an increased proportion of fines (Day 1990). This principle of extending the range of particle sizes to improve space filling is based on the so called Apollonian concept and has more recently been applied to the binder phase in modern concrete to achieve ultra-high strength concretes (Scrivener and Kirkpatrick 2008). The utilization of lime-pozzolan binders recovered gradually after the decline of the Roman Empire, particularly due to their hydraulic capability of hardening underwater. However, pozzolan-lime binders were gradually replaced by Portland cement based binders over the course of the 19th and early 20th century (Blezard 2001).

1529-6466/12/0074-0006$10.00 DOI: 10.2138/rmg.2012.74.6

More recently, especially since the 2nd half of the 20th century, the addition to Portland cement of natural or artificial materials able to react with lime to produce a cementitious product has received renewed attention. The production of Portland clinker being an energy-intensive process, in which raw materials are typically burned at 1450 °C, renders the economic advantages of replacing a substantial part of the clinker by cheap naturally available pozzolans or industrial by-products obvious. The replacement of a part of the cement clinker does not need to have negative effects on the mechanical and durability performance of the so-called blended cement. To the contrary, many studies have indicated that particularly the durability of blended cements is substantially improved. An overview of the technological effects of using blended cements is included in the present chapter. A more recent important incentive to increase and optimize the incorporation of supplementary cementitious materials (SCMs) in blended cements is the problem of climate change associated with the anthropogenic emission of greenhouse gasses. Additional to the need of reaching high temperatures in the cement kilns, the release of CO_2 by decomposition of limestone results in an average ratio of 0.87 kg CO_2 emitted per kg of Portland cement produced (Damtoft et al. 2008). It is estimated that with a current annual cement production of 2.8 billion tonnes the cement industry alone is responsible for 5-7% of the anthropogenic emissions. Future prospects foresee a drastic increase in Portland cement production in developing countries. Therefore, the contemporary cement industry is faced with the challenges of producing more sustainable, less energy intensive products without sacrificing the mechanical or durability performance of the end product. The societal incentives and associated emission quotas in order to reduce global CO_2 emissions are rapidly evolving into an all-important issue for the cement industry (Damtoft et al. 2008; Habert et al. 2010). In response, the currently most common development with limited interference in the conventional production process is the increased blending of supplementary cementitious materials or pozzolans with Portland cement (Gartner 2004).

The utilization of industrial by-products available in large and regular quantities of suitable consistent composition, i.e., ground granulated blast furnace slags from iron smelting and coal or lignite fly ashes from electricity production, has been firmly established in many countries. However, the supply of high quality SCM by-products is limited and many local sources are already fully exploited. In addition, a decline in production of blast furnace slags and fly ashes is expected due to future developments in steel and electricity production (Scrivener and Kirkpatrick 2008). An illustration of the evolution of the clinker substitution in France is given by Habert et al. (2010). Figure 1 shows that since the early 70's the total replacement percentage has remained stable at 20%, while the main cement replacement materials have shifted from slag and fly ash to limestone. Alternatives to the traditional industrial by-product SCMs are to be found on the one hand in an increased usage of naturally occurring SCMs and on the other hand in the expansion of the range of industrial by-products or societal waste to substitute for clinker. The development of cement and concrete prescriptions and standards towards more performance based conditions highlights the generally accepted view that the utilization of a wider array of SCMs at higher replacement percentages should be allowed and judged on the eventual performance of the end product (Hooton 2008; Kaid et al. 2009).

Natural SCMs or pozzolans are abundant in certain locations and are extensively used as an addition to Portland cement in countries such as for example Italy, Germany, Greece and China. Compared to traditional industrial SCMs they are characterized by a larger range in composition and a larger variability in physical properties. The application of natural pozzolans in Portland cement is mainly controlled by the local availability of suitable deposits and the competition with the accessible traditional industrial by-product SCMs. In part due to the exhaustion of the latter sources and the extensive reserves of natural pozzolans available, partly because of the proven technical advantages of an intelligent use of natural pozzolans, their use is expected to be strongly expanded in the future (Mehta 1987; Damtoft et al. 2008).

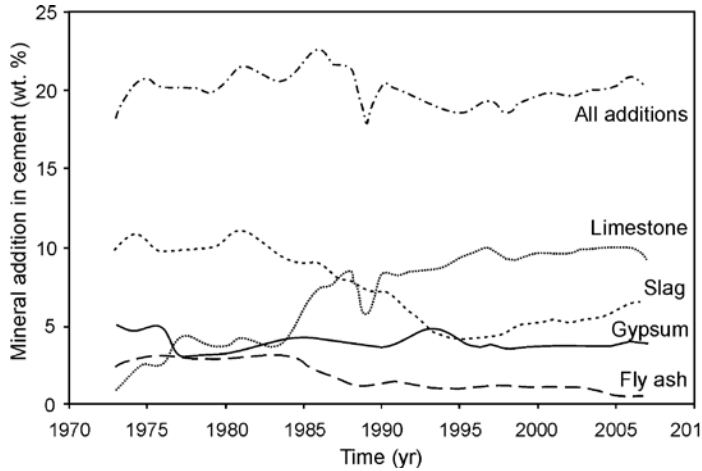

Figure 1. Evolution of clinker substitution materials in France from 1973 to 2007 (Habert et al. 2010).

A substantial part of the by-products and waste materials generated by present-day society have the potential of being utilized in construction materials. Immobilization of harmful metals in waste materials by incorporation in the high pH environment of hydrated cement offers interesting perspectives for application. Apart from avoiding costs of waste disposal and environmental pollution, lowering cement costs and increasing the product sustainability, some materials may also beneficially affect the microstructure and the mechanical and durability properties of mortars and concrete (Meyer 2009). Recently, a substantial amount of research has been dedicated to improve the understanding of the behavior of a broadened range of waste materials in cement and concrete products and to explore the potential applications. This review will be limited to waste materials or by-products which are already extensively employed as reactive binder components, e.g., fly ashes and blast furnace slags, and have successfully passed the development and testing stage. For a recent review of the usage of by-product or waste materials as aggregate, the reader is referred to the comprehensive survey of Siddique (2008).

The potential of clinker substitution by SCMs to decrease production costs and to increase sustainability and durability of the end-products is reflected in the large and steadily growing numbers of peer-reviewed papers published on the subject. Excellent general literature reviews which have been remarkable sources of information for the present paper have been published earlier by Massazza (1974, 2001), Sersale (1980, 1993), Takemoto and Uchikawa (1980), Swamy (1986), Malhotra and Mehta (1996) and Siddique (2008).

This literature review will mainly consider more recent insights and research findings and put them into perspective with the previously existing knowledge on supplementary cementitious materials. Though the combined use of chemical admixtures and SCMs is common, a thorough treatment on the effect of chemical admixtures on cement properties would require a separate review. Also, no account is made of the different methodologies for testing the reactivity of SCMs or pozzolans. Instead, here, a general definition and classification of SCMs is presented first, followed by sections treating the physico-chemical properties of specific SCM groups. A detailed account of recent developments in the understanding of the pozzolanic reaction mechanism and kinetics has been provided, together with a general overview of the reaction products encountered. Finally, a concise outline of the properties of SCM-blended cement binders is offered.

DEFINITION AND CLASSIFICATION OF SUPPLEMENTARY CEMENTITIOUS MATERIALS

Definition

The group of supplementary cementitious materials comprises materials that show either hydraulic or pozzolanic behavior. A hydraulic binder is a material that can set and harden submerged in water by forming cementitious products in a hydration reaction. Iron blast furnace slags commonly show a "latent hydraulicity," i.e., their hydraulic activity is relatively low compared to Portland cement and activation by chemical or physical means is needed to initiate and accelerate the hydration reaction (Regourd 1986; Lang 2002). Blast furnace slags can be chemically activated by addition of alkali-hydroxides, sulfates in the form of gypsum or anhydrite or more frequently by the addition of lime or lime-producing materials such as Portland cement. It should be noted that hydraulic materials can replace Portland cement up to a much larger extent than materials showing pozzolanic behavior.

A pozzolan is generally defined in ASTM C618 as a siliceous or siliceous and aluminous material which, in itself, possesses little or no cementitious value but which will, in finely divided form and in the presence of moisture, react chemically with calcium hydroxide (lime) at ordinary temperature to form compounds possessing cementitious properties (Mehta 1987). It should be remarked that the definition of a pozzolan imparts no bearing on the origin of the material, only on its capability of reacting with lime and water. A quantification of this capability is comprised in the term pozzolanic activity.

The pozzolanic activity is by convention described as a measure for the degree of reaction over time between a pozzolan and Ca^{2+} or $Ca(OH)_2$ in the presence of water. Physical surface adsorption is not considered as being part of the pozzolanic activity, because no irreversible molecular bonds are formed in the process (Takemoto and Uchikawa 1980). The driving force underlying the pozzolanic activity is the difference in Gibbs free energy between the initial and final reaction stages, while the reaction kinetics are governed by the activation energy barrier which needs to be surmounted to proceed in the reaction (Felipe et al. 2001). It should be remarked that the bulk properties of the end product (i.e., mortar, concrete etc.) are not directly related to the SCM inherent pozzolanic activity. Physical bulk properties such as permeability and mechanical strength are more strongly dependent on the type, shape, dimensions and distribution of reaction products and pores than on the extent of the lime-pozzolan reaction (Takemoto and Uchikawa 1980; Massazza 2001). The former factors are mainly affected by the mix design and curing conditions and can thus be controlled. However at equal binder preparation conditions, the pozzolanic activity remains a primary factor that controls the capability of a material to engage in the formation of cementitious compounds and in consequence also the contribution of the material to the binder performance.

Classification

The general definition of supplementary cementitious material embraces a large number of materials which vary widely in terms of origin, chemical and mineralogical composition, and typical particle characteristics. Although it is generally accepted that the hydraulic or pozzolanic activity of SCMs depends largely on their physico-chemical properties rather than their origin (Sersale 1993), classifications of SCMs according to their activity or their performance in concrete (e.g., Mehta 1989) have known little success. Still more commonly accepted is the classification based on the origin of the SCM (Massazza 2001) and this will be followed here.

Two broad categories can be distinguished, on the one hand materials of a natural origin and on the other hand materials of man-made or artificial origin. The former group consists of materials that can be used as SCM in their naturally occurring form. In most cases they only need conditioning of particle characteristics by sieving and grinding processes. Typical natu-

ral SCMs are pyroclastic rocks, either diagenetically altered or not, and highly-siliceous sedimentary rocks such as diatomaceous earths. The group of artificial SCMs includes materials which have undergone structural modifications as a consequence of manufacturing or production processes. Artificial SCMs can be produced deliberately, for instance by thermal activation of kaolin-clays to obtain metakaolin, or can be obtained as waste or by-products from high-temperature processes such as blast furnace slags, fly ashes or silica fume. A general genetic classification scheme is presented in Figure 2. Natural SCMs are subdivided into materials of primary volcanic origin and materials of sedimentary origin. The volcanic materials utilized are generally pyroclastics and can be altered by diagenetic processes to zeolite-rich tuffs. The sedimentary rocks comprise chemical and detrital sediments. Both biochemically deposited SCMs such as diatomaceous earths and deposits resulting from the circulation of hydrothermal fluids are included in the former category. Naturally burned clays, such as gliezh, are an example of the use of detrital sediments. Some individual materials, e.g., Danish moler and French gaize, cannot be distinctively categorized as either a natural or artificial SCM because their natural pozzolanic activity is commonly enhanced by thermal treatment. Here, they are included together with the artificial SCMs. Other materials, such as Sacrofano earth, containing components of mixed natural origins (volcanic, detritic and biogenic) are classified under the category of materials of sedimentary origin. The classification of artificial SCMs is conveniently based either on the industrial processes producing the SCMs or on the original materials that are thermally treated to intentionally manufacture SCMs. Some waste materials with the potential to become more widely used as SCM in the future, but which need further experimental evaluation are also mentioned in the classification scheme.

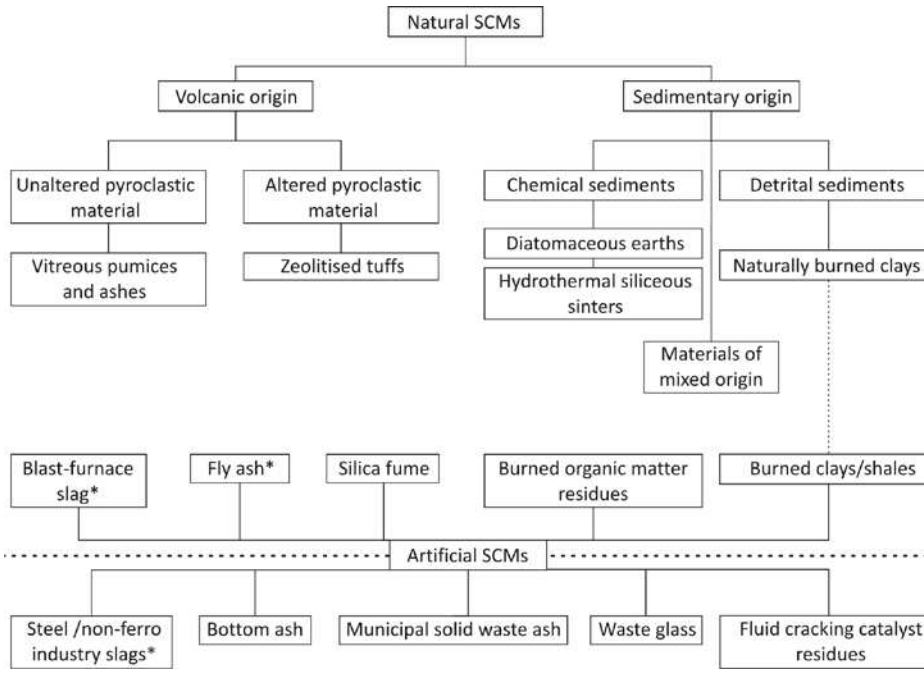

Figure 2. General classification scheme of supplementary cementitious materials. * denotes materials which can present hydraulic activity, all other materials display pozzolanic behavior. A selection of promising SCMs still largely under development are positioned below the dashed line (modified after Massazza 2001).

Within a group of SCMs of the same origin there can be considerable variability in the physico-chemical properties. The extent of variability depends on the SCM origin. The large compositional variability of volcanic extrusive rocks is a reflection of the natural variability in magmatic and diagenetic processes leading to their present condition. In contrast, the characteristics of silica fume produced in the controlled manufacturing of silicon metal and ferrosilicon alloys show much more consistency. Apart from differences in variability, separate groups show characteristic ranges of chemical composition. Figure 3 illustrates the chemical composition and typical variability for the most commonly used groups of SCMs in a CaO-SiO_2-Al_2O_3 ternary variation diagram. Alkalis, MgO and Fe_2O_3 content are ignored in this diagram. The figure can also be instrumental in estimating the impact of SCM incorporation on the blended cement chemistry and can eventually be used to predict reaction product assemblages (cf. infra).

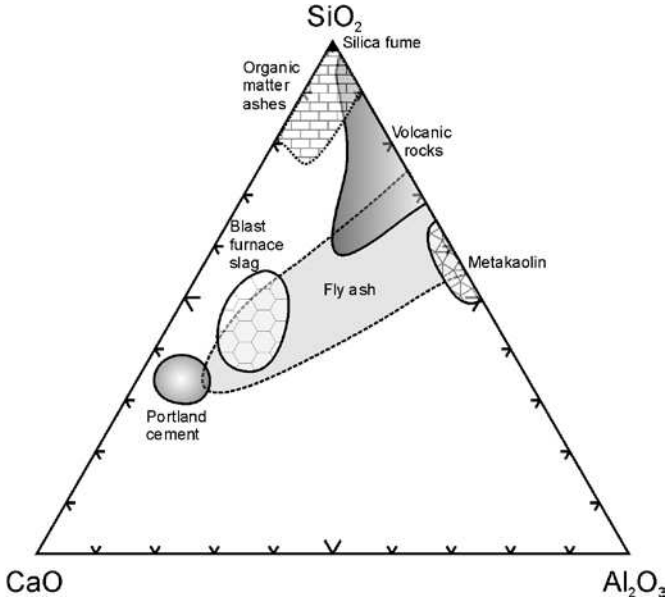

Figure 3. Ternary CaO-SiO_2-Al_2O_3 diagram (wt% based) situating the chemical constitution of the major SCM groups (modified after Glasser et al. 1987).

MINERALOGY AND CHEMISTRY OF SCMS

Natural SCMs

The great majority of natural pozzolans in use today is of volcanic origin, mainly owing to the widespread availability of volcanic rocks in many countries. In Figure 4 the global distribution of volcanic rocks can be compared with the reported occurrences of natural pozzolan deposits. It is apparent that the overwhelming majority of these deposits are located in areas of Cenozoic volcanic activity. However, not all volcanic rocks are suitable as pozzolanic material. Pyroclastic materials resulting from explosive eruptions such as ashes or pumices show higher pozzolanic activity owing to their higher glass content and highly porous or vesicular nature. The eruption type largely depends on the magma viscosity which is related to the "acidity" (i.e., SiO_2 content) of the magma. In general, more siliceous magma produces more explosive volcanism and products with better pozzolanic properties. Coarser highly vesicular pyroclastic

Figure 4. Global distribution of volcanic rocks (grey areas) and deposits of reported natural supplementary cementitious materials (black dots).

material forms pumice-type deposits. Finely divided materials are transported further away from the volcanic source and are deposited as ash layers.

Subsequent to the deposition of the pyroclastic material, diagenetic alteration of the vitreous material to crystalline zeolites can occur under certain circumstances. The resulting zeolite-bearing rocks are often coherent tuffs and present, when ground to sufficient fineness, high pozzolan activities. As the likelihood of a material having undergone diagenetic alteration increases with its age, zeolitized tuffs tend to become more abundant in rocks of increasing geologic age throughout the Neogene (Gottardi and Obradovic 1978). The type of zeolites formed and the quality of the zeolitized rocks is largely related to the composition of the original vitreous material. Regional differences are therefore common and are ultimately related to the type of volcanism and the corresponding geological situation.

The utilization of materials of sedimentary origin is scarcer, which is evidently related to the general stability at ambient conditions of the mineral assemblages deposited as sediments. However, in some specific conditions sediments rich in pozzolanically active components can be formed during deposition, e.g., diatomaceous earths, or due to subsequent alteration, e.g., naturally burned clays.

Topical reviews on natural pozzolans and their applications can be found in Cook (1986a), Day (1990), Malhotra and Mehta (1996), Colella et al. (2001) and Massazza (2001, 2002).

Unaltered pyroclastic materials. The major pozzolanically active component of unaltered pyroclastic pumices and ashes is a highly porous glass (Ludwig and Schwiete 1963). The easily alterable, or highly reactive, nature of these ashes and pumices limits their occurrence largely to recently active volcanic areas. Most of the traditionally used natural pozzolans belong to this group, i.e., volcanic pumice from Pozzuoli, Santorin earth and the incoherent parts of the German trass. The international (IUGS) classification of glassy or aphanitic rock types based on the chemical composition has been applied to natural pozzolans of volcanic origin. The reported chemical data of 150 unaltered pyroclastic materials and 83 zeolitized rocks used as natural pozzolanic material were plotted in a total alkali over SiO_2 diagram on a recalculated 100% volatile-free basis in Figure 5. A large spread of data indicates the variability in composition. SiO_2 being the major component, most natural unaltered pumices and ashes fall in the intermediate (52-66 wt% SiO_2) to acid (> 66 wt% SiO_2) composition range. The

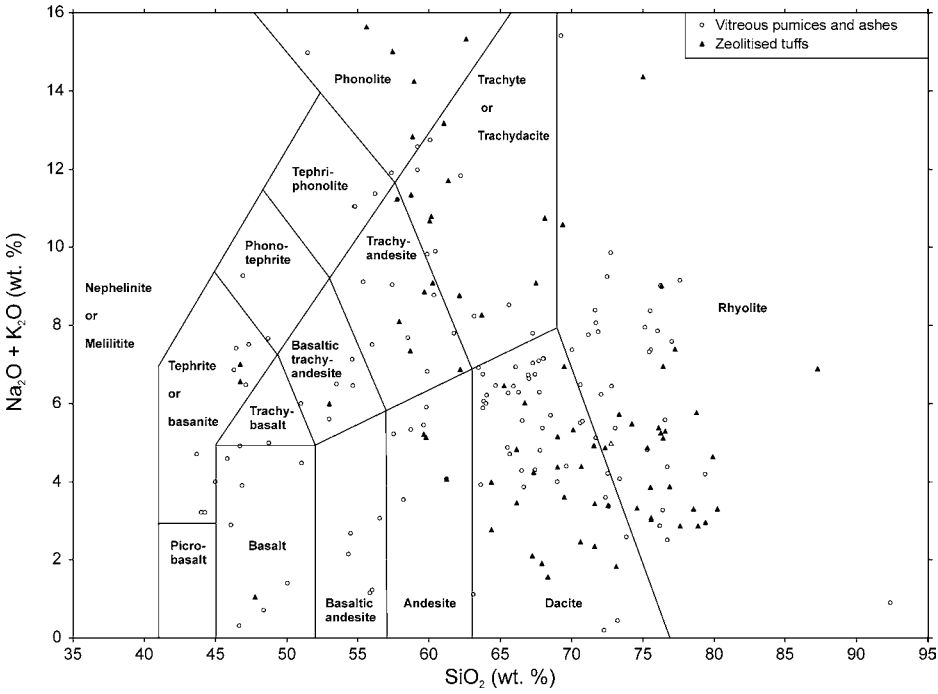

Figure 5. IUGS classification (Le Maître et al. 1989) of vitreous rock types based on chemical composition on an anhydrous basis.

predominant rock types are dacite and rhyolite, representing respectively 29% and 21% of the reported analyses. Basic (45-52 wt% SiO_2) and ultrabasic pyroclastics (< 45 wt% SiO_2) are less commonly used as natural pozzolans, and represent only 15% of the reported analyses. The total alkali content is variable and linked to the regional type of volcanism. It can reach levels higher than 11 wt% on an anhydrous basis in Neapolitan pozzolans (e.g., Battaglino and Schippa 1968), Moroccan "leucitite" (Hilali et al. 1981 in Day 1990) or pumicite from Idaho (Asher 1965 in Day 1990).

A synthesis of the collected chemical data of the unaltered pyroclastics is shown as a series of box plots in Figure 6. Apart from SiO_2 as the main component, Al_2O_3 is present in substantial amounts in most reported pozzolans. Most samples contain Fe_2O_3 and MgO in minor proportions, which is typical of more acid rock types. CaO and alkali concentrations are usually modest, but can vary substantially depending on for instance the presence of calcite as a secondary phase. Loss on ignition (LOI) is generally low but can reach values over 10 wt% in some trasses and tuffs which probably contain substantial amounts of unreported zeolites and/or clay minerals.

A summarizing representation of the collected chemical data of the unaltered pyroclastics is shown as a series of box plots in Figure 6. Apart from SiO_2 as the main component, Al_2O_3 is present in substantial amounts in most reported pozzolans. Most samples contain Fe_2O_3 and MgO in minor proportions, which is typical for more acid rock types. CaO and alkali concentrations are usually modest, but can vary substantially depending on for instance the presence of calcite as a secondary phase. Loss on ignition (LOI) is generally low but can reach values over 10 wt% in some trasses and tuffs which probably contain substantial amounts of unreported zeolites and/or clay minerals.

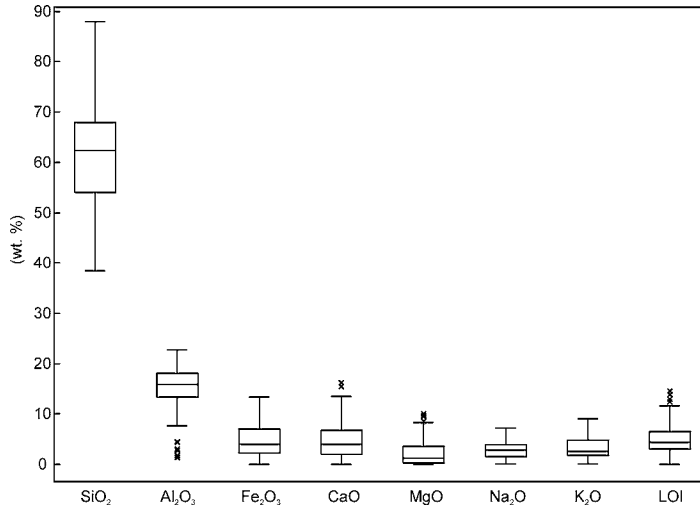

Figure 6. Box plots of the distribution of collected chemical data (N = 150) of unaltered pyroclastic materials investigated as pozzolanic material. Crosses are outliers.

The mineralogical composition of unaltered pyroclastic rocks is mainly determined by the presence of phenocrysts and the chemical composition of the parent magma. Additionally, the pyroclastic material can become intermixed with the constituents of detrital or biochemical sediments during deposition. Finally, some limited alteration can have occurred after deposition. The major component is volcanic aluminosilicate glass typically present in quantities over 50 wt%. Unaltered pyroclastics containing significantly less volcanic glass, such as the trachyandesite from Volvic (France) with only 25 wt% are reported to be less reactive (Mortureux et al. 1980). Within a group of unaltered natural pozzolans with similar volcanic origin and composition, a correlation between amorphous phase content and pozzolanic activity has been observed (Mehta 1981). The glass SiO_2 content ranges between 45 and 75 wt% and its chemical composition can differ slightly from the bulk composition through the incorporation of lithophile elements in high-temperature phenocrysts (e.g., Ca in anorthite). Mielenz et al. (1950) reported that basaltic glass appeared to be inferior to more acid glasses in terms of pozzolanic activity. Akman et al. (1992) confirmed the better performance of natural pozzolans of rhyolitic and trachytic composition over more basaltic pozzolans. Apart from the glass content and its morphology associated with the specific surface, also defects and the degree of strain in the glass phase appear to be important for the pozzolanic activity (Mehta 1981). The impact of the latter parameters remains unclear due to difficulties in their experimental quantification.

Typical associated minerals present as large phenocrysts are members of the plagioclase feldspar solid solution series varying between albite and anorthite depending on the parent magma composition. In pyroclastic materials in which alkalis predominate over Ca, K-feldspar such as sanidine or albite Na-feldspar were identified (Neapolitan pozzolans). Leucite is present as phenocrysts in the K-rich, silica-poor Latium pozzolans (Costa and Massazza 1974). Quartz is usually present in minor quantities in acidic pozzolans, while pyroxenes and/or olivine phenocrysts are often found in more basic materials. Xenocrysts or rock fragments incorporated during the violent eruptional and depositional events are also encountered. Zeolite and clay minerals are often present in minor quantities as alteration products of the volcanic glass. While zeolitization in general is beneficial for the pozzolanic activity, clay formation or argillitization

has adverse effects on the performance of lime-pozzolan blends or blended cements (Massazza 1974; Sersale 1980; Akman et al. 1992; Türkmenoğlu and Tankut 2002). Other early diagenetic products reported are opal CT (a more or less disordered interlayering of the SiO_2 polymorphs cristobalite and tridymite) and secondary calcite. The former shows elevated pozzolanic activity, the latter is not a pozzolan but can contribute to the material performance of Portland cement by reacting with calcium-aluminate-hydrate reaction products (cf. infra; Matschei et al. 2007a; Matschei and Glasser 2010) or acting as a filler material.

Another type of unaltered volcanic pozzolanic material is perlite, a volcanic glass containing relatively high amounts of water. Perlite is typically rhyolitic, containing around 75 wt% SiO_2, 10-15% Al_2O_3 and additional alkalis. The pozzolanic activity of ground perlite from deposits in Turkey (Erdem et al. 2007) and China (Yu et al. 2003) was evaluated to be high.

Altered pyroclastic materials. Diagenetic alteration of pyroclastic deposits by alkaline fluids results in the formation of micrometer size zeolite minerals (Fig. 7). Alteration by less alkaline fluids usually leads to the development of clay minerals. The recrystallization of the volcanic glass often results in a more compact and coherent tuffaceous rock. Zeolites are members of the tectosilicate group and possess open, porous framework structures of corner-sharing AlO_4 and SiO_4 tetrahedra. The aluminosilicate tetrahedra are arranged in rings which are three-dimensionally connected to form open cages and channels running through the crystal. The substitution of Al^{3+} for Si^{4+} imposes a net negative framework charge, which is compensated by exchangeable cations in cages and channels. Water molecules are sequestered in the cages due to charge-dipole interactions. Zeolitization can occur in a range of geological environments. The most important zeolitization processes in terms of deposit volume are due to circulation of saline-alkaline lacustrine waters, of alkaline ground water or of hydrothermal fluids and due to low-grade burial diagenesis metamorphism (Hay and Sheppard 2001).

The range in chemical composition of the zeolitized pyroclastic materials used as pozzolans broadly coincides with that of their unaltered counterparts (Fig. 8). The most prominent difference is the higher loss on ignition due to the formation of zeolite and/or clay minerals containing substantial amounts of water. On an anhydrous base, the altered pyroclastics used as

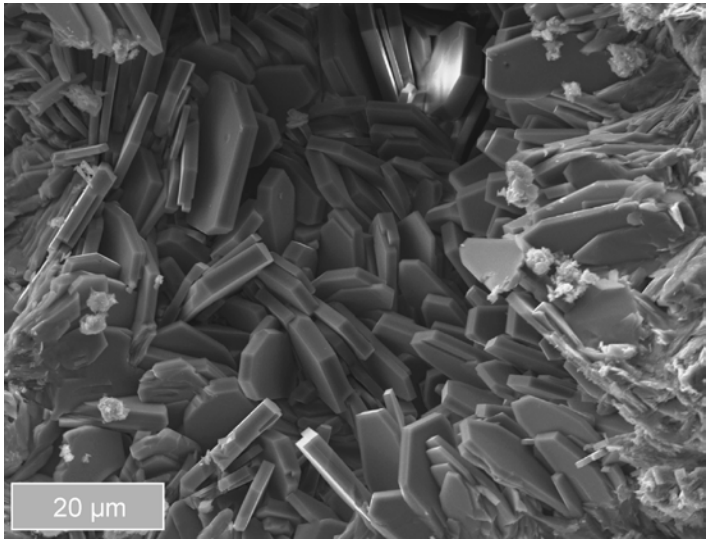

Figure 7. SEM picture of typical micrometer-size "coffin"-shaped clinoptilolite crystals formed as alteration product of volcanic glass in a tuff sample from Karacaderbent, Turkey.

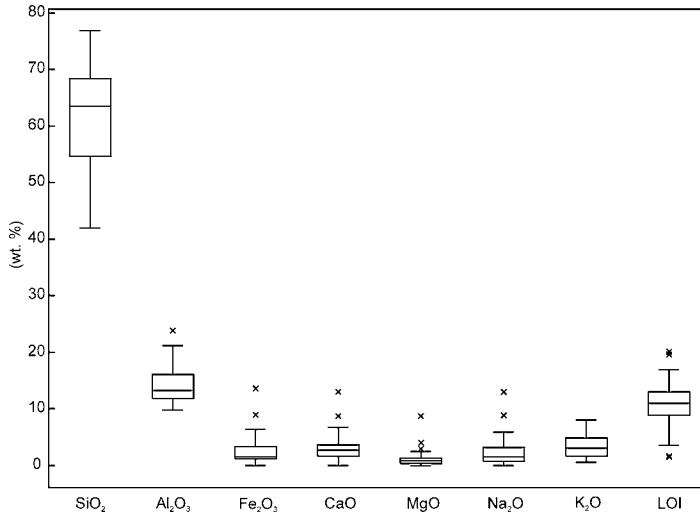

Figure 8. Box plots of the distribution of collected chemical data (N = 83) of zeolitized pyroclastic materials investigated as pozzolanic material.

pozzolans tend to be more siliceous and contain somewhat more alkalis. A comparison of the unaltered and altered pyroclastics in a ternary diagram in Figure 9 corroborated this observation in that a larger proportion of the unaltered pumices and ashes are shifted towards the CaO and Al_2O_3 apices. This can be linked with the fact that zeolitized rocks used as pozzolans are mostly reported from regions with products of more siliceous or alkali-rich volcanism. More siliceous zeolitized rocks are encountered in the Balkan region (e.g., Držaj et al. 1980;

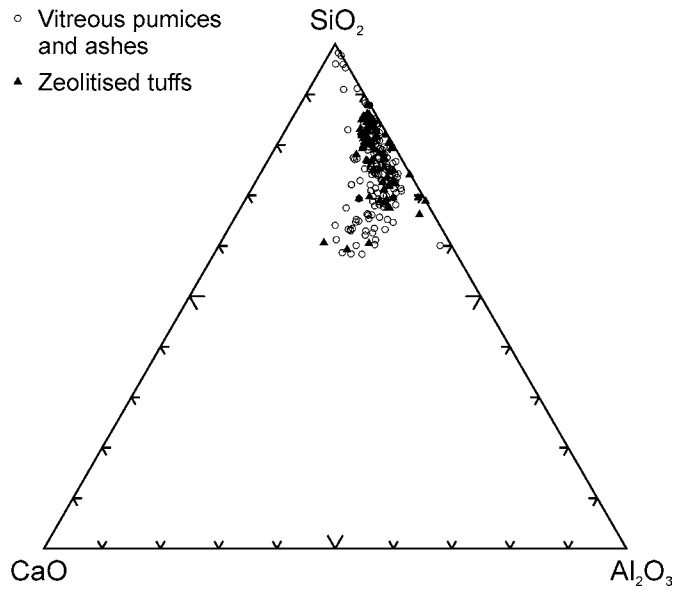

Figure 9. Ternary CaO-SiO_2-Al_2O_3 diagram (wt% based) comparing the chemical composition of unaltered and zeolitized pyroclastics used as pozzolanic material.

Naidenov 1991; Janotka et al. 2003), Greece (e.g., Kitsopoulos and Dunham 1996; Fragoulis et al. 1997; Stamatakis et al. 1998; Perraki et al. 2003) and in the Turkey-Iran volcanic chain (e.g., Canpolat et al. 2004; Yilmaz et al. 2007; Uzal et al. 2010; Ahmadi and Shekarchi 2010). In the Circumpacific siliceous zeolite deposits utilized or evaluated as pozzolans occur for instance in New Zealand, the Philippines (Mertens et al. 2009), Japan (Takemoto and Uchikawa 1980), the western United States (Mielenz et al. 1950), Mexico (Rodriguez-Camacho and Uribe-Afif 2002) and Ecuador (Mertens et al. 2009). Zeolite deposits of trachytic to phonolitic composition are situated on the Italian peninsula (e.g., Sersale and Frigione 1987; Liguori et al. 2003) and in the Eifel region in Germany (e.g., Liebig and Althaus 1998).

The type of zeolite assemblage formed during alteration depends on a number of factors. Most important are the temperature of formation, the chemical composition of the volcanic glass and the zeolitizing fluid (Chipera and Apps 2001). Zeolites are not the thermodynamically most stable phases and form because of faster reaction kinetics. The most widespread siliceous zeolites are clinoptilolite, mordenite and erionite. These zeolites are observed to form in the alteration of siliceous glasses, whereas the common more aluminous zeolites, phillipsite, chabazite, analcime and heulandite (alumina-rich polymorph of clinoptilolite) form from the alteration of more basic glasses. Heulandite-clinoptilolite is by far the most frequently (up to 60%) identified zeolite mineral in natural zeolite-rich pozzolans. The compositional flexibility of this zeolite in terms of Si-Al and exchangeable cation composition promotes its formation. Mordenite was identified as a major constituent in about 10% of the altered natural pozzolans and is a silica-rich zeolite with a predominance of Na over Ca and K as exchangeable cation. Most of the identified chabazite and phillipsite pozzolans are derived from alkali-rich, intermediate to basic pyroclastics occurring in Italy or Germany and together make out 25% of the reported occurrences. Phillipsite is usually formed in K-rich volcaniclastics such as the Neapolitan Yellow Tuff. Analcime is a Na-rich zeolite which can be formed by the reaction of volcanic glass or zeolite precursors with Na-rich fluids and commonly occurs together with quartz. The eventual zeolite content of the tuff is a function of the original amount of volcanic glass and the extent of the zeolitization process. Altered pyroclastic materials can consist of several types of zeolite and zeolites are often associated with other alteration products such as opal A (amorphous), opal CT, clay minerals and authigenic feldspar and the original pyrogenic phenocrysts (cf. supra).

The main pozzolanically active phases are considered to be the zeolite and silica-polymorphs together with relict volcanic glass. Zeolite is reported to be more reactive than its unaltered vitreous counterpart (Sersale and Frigione 1987). The pozzolanic activity of a zeolitized pozzolan seems to be a function of a number of variables. First of all, the content of zeolite and other active phases is important (Liguori et al. 2003), next the reactivity of the zeolite itself depends on its crystallinity (Snellings et al. 2010b), and its framework and exchangeable cation composition (Caputo et al. 2008; Mertens et al. 2009; Snellings et al. 2009). Silica-rich zeolites have been found to render the blended cements more performant in terms of strength and durability than aluminous zeolites (Huizhen 1992; Fragoulis et al. 1997; Rodriguez-Camacho and Uribe-Afif 2002; Caputo et al. 2008), which can be linked with larger amounts of calcium-silicate-hydrate reaction products (C-S-H) being formed. Furthermore, clinoptilolite tuffs exchanged to Na or K were more reactive than tuffs exchanged to Ca (Luke 2007; Mertens et al. 2009). A classification solely based on the presence of a particular zeolite type does not seem to be meaningful due to the variability in zeolite content, composition and crystallinity in tuffs.

(Bio)chemical sediments. This category comprises both biogenic sediments, resulting from the deposition of (micro-) organism skeletons, as well as chemical precipitates resulting from the circulation of hydrothermal waters. Diatomaceous earths are the principal biogenic materials that show pozzolanic activity. They mainly consist of siliceous skeletons or frustrules

of diatom micro-organisms together with variable amounts of calcareous biogenic material and detrital sediment such as clay minerals. The diatoms can be deposited in lacustrine and marine waters. The depositional environment influences the size of the diatoms, those of fresh-water origin generally being smaller and more pozzolanically reactive (Stamatakis et al. 2003). The distribution of chemical data of 22 diatomaceous earths is presented in Figure 10. The silica content is usually high but can drop significantly because of mixing of siliceous diatoms with calcareous material. In reported impure diatomaceous earths calcite contents may reach 50 wt% or more. The presence of feldspars, clay minerals and finely divided iron(hydr)oxides is evidenced by significant amounts of Al_2O_3 and Fe_2O_3. The levels of alkalis and MgO are usually very low.

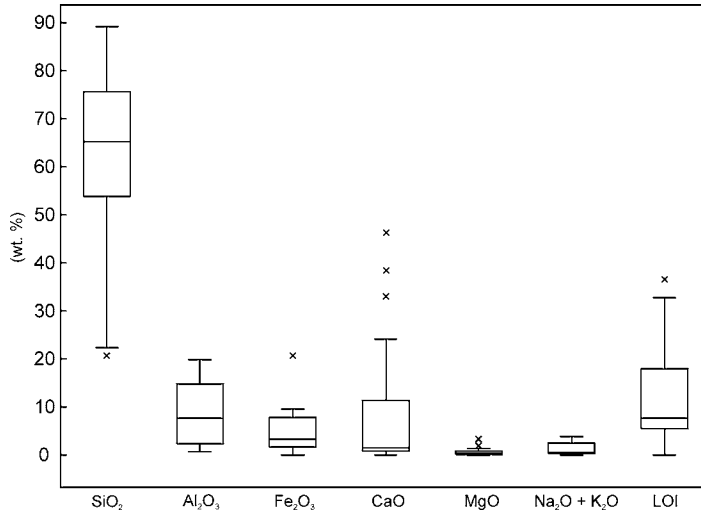

Figure 10. Box plots of the distribution of collected chemical data of diatomaceous earths (N = 22) materials investigated for application as pozzolanic material.

Diatom frustrules are composed of opal A. The higher the opal A content of the diatomaceous earth, the higher the pozzolanic activity and the better the performance. The pozzolanic activity of diatomaceous earths containing large amounts of clay minerals, such as Danish "moler," can be improved by thermal decomposition of the clay minerals (Johansson and Andersen 1990). In calcite-rich diatomites the reduced amount of opal A can be partially compensated by a filler effect of the calcareous compounds (Stamatakis et al. 2003). The intricate surface morphology and high porosity of the disk-shaped diatom frustrules (Fig. 11) results in typically elevated specific surface areas and water demand, limiting the incorporation of diatomite earths to about 15% without usage of water-reducing agents such as superplasticizers (Stamatakis et al. 2003; Degirmenci and Yilmaz 2009).

Interest in some hydrothermal siliceous sinters has been raised principally because of their high silica content. Deposits considered for utilization as pozzolanic material are located in New Zealand, Japan (Takemoto and Uchikawa 1980) and Turkey (Davraz and Gunduz 2005, 2008). Opal A is the main constituent together with some quartz and the material is described as a pumiceous, porous rock demonstrating a high specific surface area.

Materials of detrital and mixed origin. Detrital sediments are usually largely composed of stable mineral compounds derived from the erosion and weathering of other rocks. In these

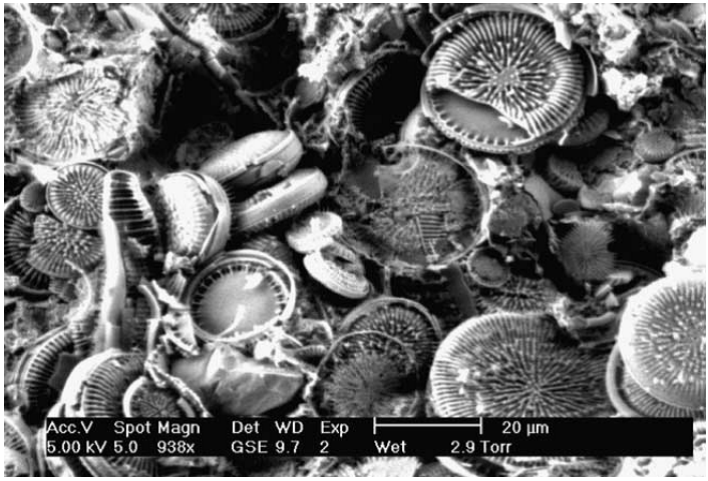

Figure 11. SEM picture of disk-shaped diatom frustules from Giannota, Greece. [Used by permission of Elsevier, from Fragoulis et al. (2005), *Cement and Concrete Composites*, Vol. 27, Fig. 1, p. 206.]

sediments, it is rather uncommon to find pozzolanically reactive compounds such as reworked volcanic glass fragments or diatoms in sufficient quantities to be suitable for application. Some exceptional materials of detrital or mixed origin have nevertheless been used as a pozzolan. One is the Sacrofano earth of mixed origin which can be found near Viterbo (Italy) and shows a very high SiO_2 content around 85-90 wt%. Volcanic particles, diatoms and some crystalline minerals present were severely altered by acid fluids infiltrating the uppermost layers of the deposit and leaving essentially a dessicated pozzolanically reactive silica gel (Massazza 2001). Other reactive materials deriving from detrital rocks are naturally burned clays such as porcellanite from Trinidad (Day 1990) and gliezh from Central Asia (Kantsepolsky et al. 1969). The former is thought to have formed by spontaneous combustion of bituminous or lignitic clays and the latter are shales burned by natural subsurface coal fires (Massazza 2001). Gaize is a sedimentary rock occurring in the French Ardennes and Meuse valley. It has a high proportion of quartz and biogenic siliceous material and a substantial amount of clay. Gaize is generally calcined before use as a pozzolan (Cook 1986a). Table 1 shows an overview of the chemical composition of several particular natural pozzolans. In Figure 12 natural pozzolans of a sedimentary origin can be compared in a CaO-SiO_2-Al_2O_3 ternary plot. The presence of calcite in some diatomaceous earths is illustrated by the mixing trend occurring between the CaO and SiO_2 apices. The majority of other pozzolans are characterized by their high SiO_2 content.

Thermally activated SCMs

The use of natural pozzolans was traditionally limited to the regions where they were locally available. To produce water-proof lime-based binders in other regions, people traditionally resorted to blends of thermally activated clays or soils and lime. Usually waste streams of clay pottery, bricks or tiles were recycled as pozzolanic additive. The widespread use of these thermally activated pozzolans before the advent of Portland cement can be illustrated by their presence in e.g., the flooring fundaments of the San Marco basilica in Venice or the Hagia Sophia in Istanbul (Zendri et al. 2004). Crushed brick pozzolans remains continued as a traditional building material in some countries, e.g., under the name of surkhi in India, homra in Egypt and sarooj in Oman (Cook 1986b; Al-Rawas et al. 1998). In modern construction, large volumes of purposely burned clays have been used in the construction of large scale structures such as dams (Jones 2002). The excellent pozzolanic properties of kaolinite-rich materials

Table 1. Overview of the chemical composition of natural pozzolans of sedimentary origin.

pozzolana	origin	Al_2O_3	SiO_2	Fe_2O_3	CaO	Na_2O	K_2O	MgO	SO_3	LOI	SUM	ref.
Sacrofano earth	Italy	3.1	89.2	0.8	2.3	-	-	-	-	4.7	100.1	1
Gliezh	USSR	12.4	72.8	5.1	2.8	0.4	1.7	1.1	1.5	-	97.8	2
Gaize	France	7.1	79.6	3.2	2.4	-	-	1.0	0.9	5.9	100.1	3
Silica sinter	Japan	2.4	87.7	0.5	0.2	0.1	0.1	0.2	0.1	4.1	95.4	4
Silica sinter	Turkey	2.6	92.5	0.1	0.3	1.1	0	0	0.1	1.9	98.6	5

1: Battaglino and Schippa (1968); 2: Kantsepolsky et al. (1969); 3: Lea (1970);
4: Takemoto and Uchikawa 1980; 5: Davraz and Gunduz 2005

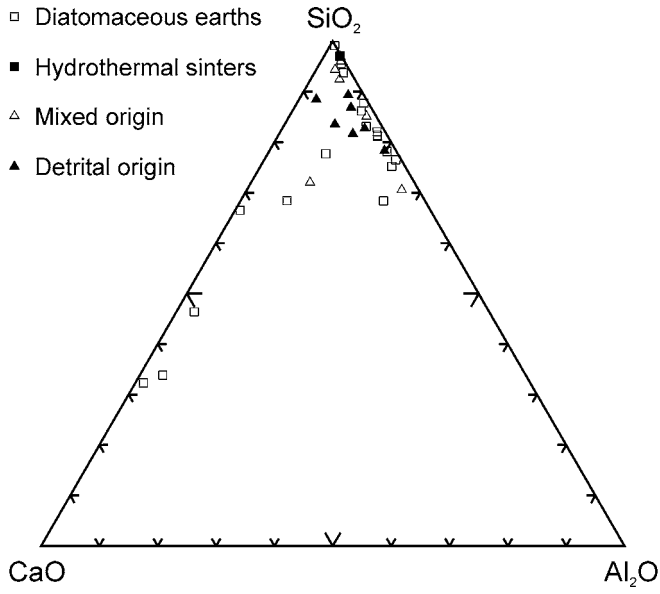

Figure 12. Ternary CaO-SiO_2-Al_2O_3 diagram (wt% based) illustrating the distribution in chemical composition of a selection of natural pozzolans from a sedimentary origin.

burned under controlled conditions, better known as metakaolin, has drawn renewed attention towards deliberately thermally activated clays. The pozzolanic properties of burned clays and shales have been reviewed by Cook (1986b), more specific reviews on metakaolin can be found in Sabir et al. (2001), Jones (2002) and Siddique (2008).

Next to burned clays, shales and soils, burned agricultural residues consisting predominantly of amorphous silica have received considerable attention as pozzolan for construction purposes in rural areas deprived of other SCMs. General reviews are presented by Cook (1986c) and Siddique (2008).

Burned clays and shales. Clays are defined as sediments which consist primarily of particles smaller than 2 μm. The constituting particles are mostly phyllosilicates incorporating a considerable amount of water. These minerals are commonly termed clay minerals and are composed of sheets of tetrahedrally (T) coordinated SiO_4 and AlO_4 connected to sheets of octahedrally (O) coordinated cations such as Al^{3+} or Mg^{2+} to form T-O or T-O-T layers. Depending on the layer charge, exchangeable interlayer cations can be present between the compound layers. Water is present as H_2O in the interlayer and as $(OH)^-$ in the octahedral

layer. During burial, clays compact to coherent mud rock and eventually shale when cleavage is developed. Clay minerals are the common product of chemical weathering of primary igneous minerals such as feldspars or form during low-temperature diagenetic alteration. Depending on the weathering conditions and the chemical composition of the altered material, various clay minerals form. Commonly encountered clay minerals are kaolinite, smectites, illite, chlorite and palygorskite-sepiolite. General chemical compositions of common clay minerals, lateritic soils and red mud waste are given in Table 2. Untreated clays show unsatisfactory pozzolanic activity and low technological performance. According to He et al. (2000), this is due to the stability of their crystal structures, their high specific surface requiring a high water to binder ratio for a desired workability, and the platy particle morphology and preferential cleavage. Non-pozzolanic micro- and nanoscale clay particles were observed to change the cement paste structure by serving as preferential substrates for C-S-H nucleation. Addition of smectite and palygorskite resulted in a more open, interconnected cement pore structure compared to the addition of silica fume (Lindgreen et al. 2008). Only kaolinite and smectite are reported to show good pozzolanic activity when fired at appropriate temperatures (Mielenz et al. 1950; Ambroise et al. 1985; He et al. 1995; Liebig and Althaus 1997).

The pozzolanic activity of thermally activated clay minerals is closely linked with their behavior during heating. Optimal activation is achieved through amorphization of the clay mineral upon complete dehydroxylation of the octahedral sheet. Overheating results in particle agglomeration and crystallization of inactive high-temperature phases. The temperatures at which dehydration, dehydroxylation and recrystallization occur are determined by the clay mineral structure and composition. Most important in the formation of a pozzolanically active material is the temperature range of dehydroxylation which depends on the bonding of the hydroxyl groups in the octahedral sheet. The thermal strength of these bonds increases from Fe-OH over Al-OH to Mg-OH. The formation of recrystallization products depends mainly on the chemical composition of the raw materials. The commonly formed minerals are mullite, cordierite, enstatite and cristobalite (Emmerich 2010). The thermal behavior of the various common clay minerals is illustrated in Figure 13.

The T-O clay mineral kaolinite, $Al_2Si_2O_5(OH)_4$, does not contain exchangeable cations or interlayer water. The temperature of dehydroxylation (endothermal) of kaolinite depends on the structural layer stacking order. Disordered kaolin dehydroxylates between 530 and 570 °C, ordered between 570 and 630 °C. Dehydroxylated disordered kaolinite shows higher pozzolanic activity than ordered (Kakali et al. 2001; Bich et al. 2009). Upon dehydroxylation kaolinite transforms into metakaolin, a complex amorphous structure which retains some long-range order due to layer stacking (Bellotto et al. 1995). Much of the aluminum contained in the octahedral layer becomes tetrahedrally and pentahedrally coordinated (Justnes et al. 1990; Rocha and Klinowski 1990; Fernandez et al. 2011). Upon further heating a defect Al-Si spinel and

Table 2. Characteristic chemical compositions for a selection of clay minerals, a laterite soil and red mud waste.

Material	SiO_2	Al_2O_3	Fe_2O_3	TiO_2	CaO	MgO	Na_2O	K_2O	H_2O	SUM
Kaolinite	46.6	39.5							14.0	100.1
Illite	54.0	17.0	1.9			3.1		7.3	12.0	95.3
Montmorillonite	43.8	18.6			1.0		1.1		36.1	100.6
Palygorskite	58.4	6.2				14.7			19.7	99.0
Chlorite	30.3	17.1	15.1			25.4			12.1	100.0
Laterite	3	10	75						10	98.0
Red mud	5.0	15	26.6	15.8	22.2	1.0	1.0	0.0	12.1	98.7

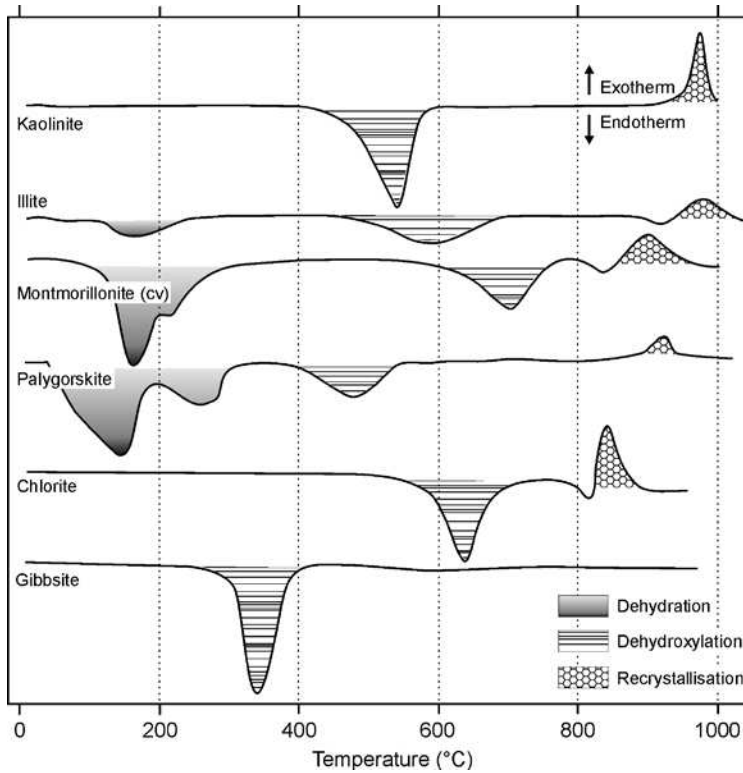

Figure 13. Representative differential thermal analysis (DTA) curves for common clay minerals and gibbsite (modified after Cook 1986b).

eventually mullite are formed. Reported optimal activation temperatures vary between 550 °C (He et al. 1994) and 850 °C (Ayub et al. 1988) for varying durations, however most values cluster around 650-750 °C (Murat 1983; Ambroise et al. 1987; De Silva and Glasser 1992; Kakali et al. 2001; Chakchouk et al. 2009). In comparison with other clay minerals kaolinite shows a broad temperature gap between dehydroxylation and recrystallization, this much favors the formation of metakaolin. Also, because the Al-OH groups of the kaolinite octahedral sheets are directly exposed to the interlayer, structural disorder can be attained more easily upon dehydroxylation of kaolinite than in T-O-T clay minerals (Fernandez et al. 2011). If the raw clay material is sufficiently pure, metakaolin is a highly active SCM which can be used in high-performance, high-strength binders to improve the compressive and flexural strength and increase durability and resistance to chemical attack (Siddique 2008). For low-cost applications kaolinite deposits or tropical soils of lower purity can be used (e.g., Cara et al. 2006; Kakali et al. 2001; Badogiannis et al. 2005). Highly active metakaolin can also be produced from paper sludge waste or oil sand fine tailings. Paper sludge waste is mainly composed of cellulose fibers, kaolinite and calcite. Calcination at 700 °C for 2-5 hours decomposes and volatilizes the organic material and activates the kaolinite while no calcite decarbonation occurs (Péra and Amrouz 1998; Frias et al. 2008). In some cases the clay fraction of oil and tar sands consists mainly of kaolinite. The separated fine tailings can be valorized by controlled firing and production of metakaolin (Wong et al. 2004). Alternatively, kaolinite can be activated by mechanochemical (Vizcayno et al. 2009) or acid treatment. Aluminum extraction from calcined kaolin by sulfuric acid results in a dealuminated kaolin with high pozzolanic activity (Mostafa et al. 2001).

Smectites are a group of T-O-T clay minerals containing exchangeable cations and showing the remarkable capability to absorb water between the layers and swell. Isomorphous substitutions in the tetrahedral and octahedral sheets as well as the interlayer cation type influence the dehydration and dehydroxylation behavior. Dehydration occurs below 300 °C and is associated with the release of water bound to outer surfaces and coordinated to interlayer cations. Dehydroxylation temperature depends on the type of cations contained in the octahedral sheet (Fe < Al < Mg) and their arrangement. When the cations contained in the octahedral sheet are mainly trivalent (Al^{3+}, Fe^{3+}) then only two out of three cation positions are filled and the clay minerals are termed dioctahedral. The disposition of the hydroxyl groups with respect to the resulting vacancy defines two kinds of configurations: *cis*-vacant when both hydroxyls are located on one side of the vacancy and *trans*-vacant when they are located on either side (Tsipursky and Drits 1984). Dehydroxylation of smectites which show mainly *cis*-vacant octahedral sheets occurs at temperatures around 700 °C, 150-200 °C above the dehydroxylation of *trans*-vacant octahedral sheets. Smectites contain predominantly *cis*-vacancies while illite clay minerals are mostly *trans*-vacant (Drits et al. 1995). Recrystallization starts above 850 °C, depending on the chemical composition of the clay. The reported optimal activation temperature ranges for montmorillonite-rich clays are typically higher and narrower defined when compared to kaolinite: 800-830 °C for 1-5 hours (Mielenz et al. 1950; He et al. 1996; Liebig and Althaus 1997; Habert et al. 2009). Overheating to recrystallization temperatures is easily attained and is together with the variable chemical composition a complicating factor in thermal activation. Activated montmorillonite has been observed to be a good pozzolanic material, incorporation into lime or Portland cement based binders contributed significantly to the compressive strength (He et al. 1995; Liebig and Althaus 1997).

Other clays are reported to be less pozzolanically active upon thermal activation. The dehydroxylation of illite, a T-O-T clay mineral with a composition intermediate between mica and smectite, occurs at relatively low temperatures (580 °C). However dehydroxylation does not result into a collapse of the structure into a largely amorphous state before recrystallization into spinel and corundum occurs (He et al. 1995). In consequence, the resulting calcined material shows much lower pozzolanic activity than that formed from less stable smectites or kaolinite.

Mg-rich T-O-T clays of the palygorskite-sepiolite group contain both interlayer and zeolite water and show complex dehydration reactions. The release of zeolite water and adsorbed water proceeds simultaneously at low temperature (Fig. 13) and is succeeded by the release of interlayer water. Dehydroxylation of palygorskite occurs below 500 °C, sepiolite dehydroxylates at 820 °C, simultaneously with decomposition and recrystallization into enstatite and cristobalite. The pozzolanic activity was observed to be low (He et al. 1996). The T-O-T octahedral sheet in chlorite clay minerals tends to dehydroxylate at rather high temperatures due to the elevated Mg content. Recrystallization into spinel and olivine occurs at low temperatures leaving a narrow window for thermal activation.

Natural clay deposits often contain more than one type of clay mineral. Habert et al. (2009) observed that ideal activation of all different clay minerals in a mixture is difficult, because recrystallization of previously activated clay can occur when a second one is activated. Furthermore they found that optimal activation and recrystallization temperatures were lowered in the impure mixtures with respect to the purified materials.

In tropical climates, intense chemical weathering leaches out silica, alkaline earths and alkalis from soils to leave a residue of aluminum and ferric (hydr)oxides. The resulting soils are bauxites and laterites, respectively. Calcination of laterites at 750 °C has been reported to produce a pozzolanically active material which improved the compressive strength of blended cements (Péra et al. 1998). Red mud waste obtained from the extraction of aluminum from bauxites can be transformed into a pozzolanically active material by calcination in the range

of 600-800 °C (Péra et al. 1997). Dehydroxylated aluminum and ferric hydroxides tend to produce cementitious reaction products when contacted with lime.

Oil shales are fine-grained sedimentary rocks containing 5-65% of organic material and detrital minerals such as clay minerals, quartz and calcite. If the level of organic material is sufficient, oil shales can be combusted and utilized for electricity production or as alternative raw material in the production of Portland cement. Depending on the type of organic material, the oil can also be extracted by pyrolysis. The resulting ashes can show hydraulic or pozzolanic activity. In ashes abundant in calcium, hydraulic calcium silicates (β-C_2S) and aluminates were observed to form (Smadi and Haddad 2003). The pozzolanic activity of the low calcium ashes is strongly linked to the original mineralogy of the shale and the burning conditions (Ish-Shalom et al. 1980). Inactive phases such as quartz and mica can represent an important fraction of the ash and lower the pozzolanic activity (Feng et al. 1997).

Although waste ceramic material has been utilized intensively as a pozzolanic additive in the past, contemporary ceramic waste does not find the same application. Modern ceramic production usually involves controlled firing at elevated temperatures between 900-1050 °C, which are invariably above the optimal activation temperature of the original clay minerals (Baronio and Binda 1997). In most cases significant high-temperature recrystallization occurs and in consequence the pozzolanic activity is relatively low, resulting in lowered compressive strength values upon increasing replacement of Portland cement (Wild et al. 1997; Lavat et al. 2009).

Burned organic matter residues. Ashes of burned agricultural residues can be used as an inexpensive alternative material for partial replacement of Portland cement or lime. While a large proportion of agricultural residues are recycled for fertilization or stock feed purposes, some is utilized as fuel or left as waste. Firing leads to the decomposition of the organic carbon and a concentration of the silica in the residue. Under controlled firing conditions a highly active pozzolan material can be produced (Mehta 1977). The elevated specific surface area and considerable surface roughness are often associated with a high water demand of the ashes and necessitate the use of superplasticizers when the replacement percentage of optimally fired ashes is more than 10-20%. The yield of production of a pozzolanic material from organic residues is determined by two factors: the inorganic residue after ignition or ash content and the silica content of the inorganic residue. Typical inorganic residue fractions and silica contents are enlisted in Table 3 for common agricultural residues. The greatest yield can be expected for the calcination of rice husks. Upon firing, a highly siliceous material with a very large surface area can be obtained. Some of the enlisted materials such as corn or rice straw face strong competition from the utilization as stock feed (Cook 1986c).

Table 3. An overview of ash content of plant parts and silica content of the ash (modified after Cook 1986c).

Plant	Part of plant	Ash (%)	Silica (%)
Sorghum	Leaf sheath	12.55	88.7
Wheat	Leaf sheath	10.48	90.56
Corn	Leaf blade	12.15	64.32
Sugar cane	Bagasse	14.71	73
Sugar cane	Straw		62
Sunflower	Leaf and stem	11.53	25.32
Rice	Husk	22.15	93
Rice	Straw	14.65	82
Palm	Fibers and shells		65

A ternary plot of reported chemical compositions of various organic material ashes in Figure 14 demonstrates the highly siliceous nature of rice husk ash compared to other residues. The level of soil derived impurities can often reach significant levels and can become concentrated in the inorganic residue upon firing. This can lead to a dilution of the active components in the ash (Cordeiro et al. 2008). Also soil and climate conditions can influence the ash and silica contents of the residue (Biricik et al. 1999).

The pozzolanic activity of the inorganic residue is strongly affected by the firing temperature. Optimal activation is achieved when the cellulose and other combustibles are removed and the pore structure and associated large surface area (25-40 m²/g) of the silica-rich skeleton are preserved (Jauberthie et al. 2000) (see Fig. 15). The dissolution of the silica is strongly linked with the concentration of silanol groups at the surface (Nair et al. 2008). Over-heating leads to reductions in specific surface and to transformation of the amorphous silica to crystalline high-temperature silica polymorphs such as cristobalite and tridymite. Firing should therefore be performed in an oxidizing atmosphere at temperatures above 400 °C to decompose the organic material (James and Rao 1986) but, for rice husk ash, below 700 °C to avoid the formation of cristobalite and tridymite (Hamdan et al. 1997). Prolonged exposure to elevated temperatures leads to a collapse of the pore structure and to decreased recrystallization temperatures (Cook 1986c). The sensitivity of the activated material to the firing conditions and the utilization of agricultural residues as fuel for domestic or industrial purposes have been primary obstacles to the widespread application of organic material ashes as a pozzolanic material. Therefore, recently, research focus shifted to the beneficiation of ashes of organic residues used as fuel.

The sensitivity of the activated material to the firing conditions and the utilization of agricultural residues as fuel for domestic or industrial purposes have been primary obstacles to the widespread application of organic material ashes as a pozzolanic material. Therefore, recently, research focus shifted to the beneficiation of ashes of organic residues used as fuel. Sugar cane bagasse and straw ashes resulting from uncontrolled combustion in boilers of

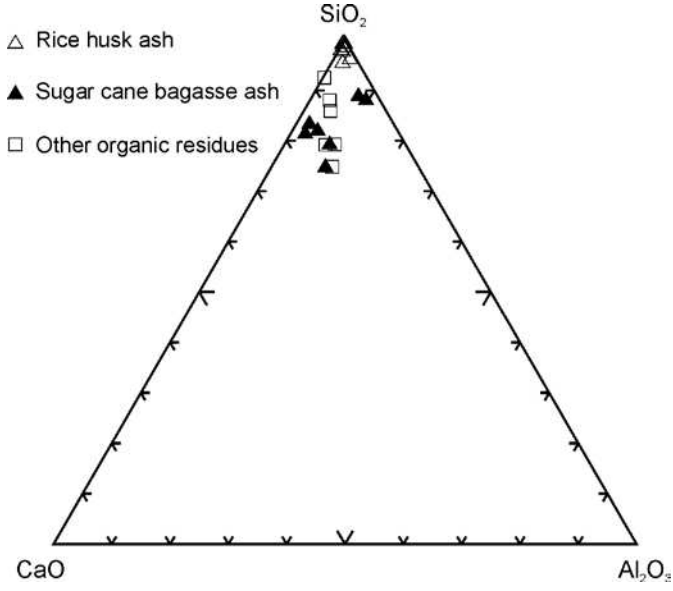

Figure 14. CaO-SiO_2-Al_2O_3 ternary diagram (wt% based) of chemical composition of reported organic residue ashes.

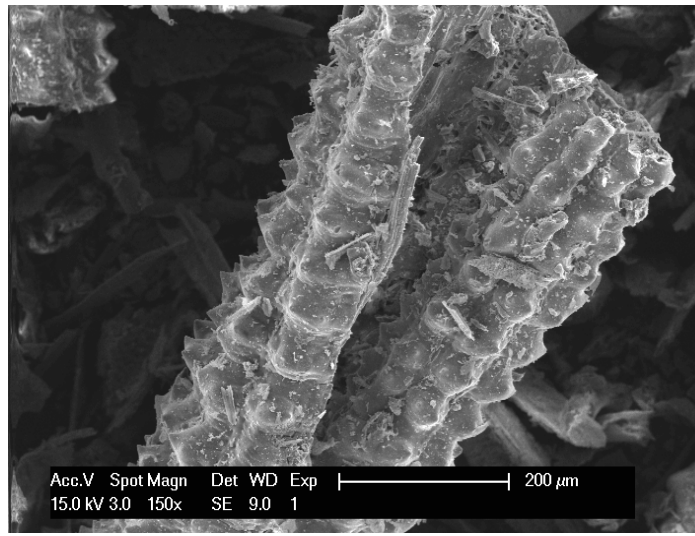

Figure 15. SEM picture of fragments of the highly-porous silica-rich skeletons of rice husks after uncontrolled burning in a field furnace.

sugar and alcohol factories at 700-900 °C were found to behave pozzolanically when finely ground (Cordeiro et al. 2008, 2009a; Chusilp et al. 2009; Morales et al. 2009). Also the ashes of uncontrolled firing of rice husks (De Sensale 2006; Cordeiro et al. 2009b), rice husks and eucalyptus bark (Tangchirapat et al. 2008) and palm oil residue (Tangchirapat et al. 2009) show pozzolanic activity when finely ground.

By-product SCMs

The valorization of industrial and societal waste in construction materials is one of the main routes for progress in increasing the sustainability of present-day society. A large diversity of waste materials can be considered and applications can range from low-value products such as aggregates to high-value products such as some SCMs. In this section, the properties of the most widely used industrial by-product SCMs are reviewed. The widespread success of blast furnace slags, coal and lignite fly ash and silica fume can serve to corroborate the view that construction materials will increasingly become a primary target for disposal of industrial and societal waste. The extensive experience and knowledge built up over years of using these established by-product SCMs should be considered as valuable when proceeding into a future expansion of the range of waste materials suitable for construction purposes.

Blast furnace slags. The most widely utilized slags in cements are obtained as a by-product in the extraction of pig iron in blast furnaces. Blast furnace slags commonly present latent hydraulic behavior if they are quenched sufficiently rapidly as a vitreous phase from the melt at 1350-1550 °C to below 800 °C and finely ground. The first hydraulic cements incorporating blast furnace slags were pioneered in the 2nd half of the 19th century in Germany, first as $Ca(OH)_2$-slag blends, later on as SCM in Portland cement. Nowadays, blast furnace slags are mostly used in combination with Portland cement and, being latent hydraulic, can constitute a much larger proportion of the blended cement than pozzolanic materials. In addition, blast furnace slags present marked cementitious properties when activated by either lime, alkali hydroxides, sodium carbonates or sodium silicates (water glass) and calcium or magnesium sulfates (e.g., supersulfated slag cements). Over recent years the activation of various types of slags has received much attention as potential alternative for Portland cement, a detailed

account of the progress made is however out of the scope of this chapter. Topical reviews on blast furnace slags in cements are available (Smolczyk 1980; Regourd 1986, 2001; Lang 2002).

The chemical composition of a slag varies widely depending on the composition of the raw materials in the iron production process. Silicate and aluminate impurities from the ore and coke are combined in the blast furnace with a flux which lowers the viscosity of the slag. In the case of pig iron production the flux consists mostly of a mixture of limestone and forsterite or in some cases of dolomite, the latter for reasons of economy. In the blast furnace the slag floats on top of the iron and is decanted for separation. Slow cooling of slag melts results in an unreactive crystalline material consisting of an assemblage of Ca-Al-Mg silicates. To obtain the slag hydraulicity, the slag melt needs to be rapidly cooled or quenched below 800 °C in order to prevent the crystallization of merwinite and melilite (Regourd 1986). To cool and fragment the slag a granulation process can be applied in which the molten slag is subjected to jet streams of water or air under pressure. Alternatively, in the pelletization process the liquid slag is partially cooled with water and subsequently projected into the air by a rotating drum. Pumiceous, porous pellets are produced in which the mostly glassy fraction finer than 4 mm can be used as a supplementary cementitious material. The coarser, typically more crystalline fraction can be used as lightweight aggregate. The pelletization process is more economical in terms of water consumption during the cooling process and energy needed to dry the slurry of quenched slag fragments but is usually less effective in obtaining high glass contents (Taylor 1990) compared to the granulation process. In order to obtain a suitable reactivity, the slag fragments are ground to reach the same fineness as the Portland cement.

The main components of blast furnace slags are CaO (30-50%), SiO_2 (28-38%), Al_2O_3 (8-24%) and MgO (1-18%) (Regourd 2001). In a CaO-SiO_2-Al_2O_3 ternary diagram (Fig 16, Fig. 3) the blast furnace slags can be situated somewhere in between typically pozzolanic materials such as natural SCMs or silica fume and Portland cements, indicating the "latent hydraulicity" of the slags. In general, increasing the CaO content results in raised slag basicity and an

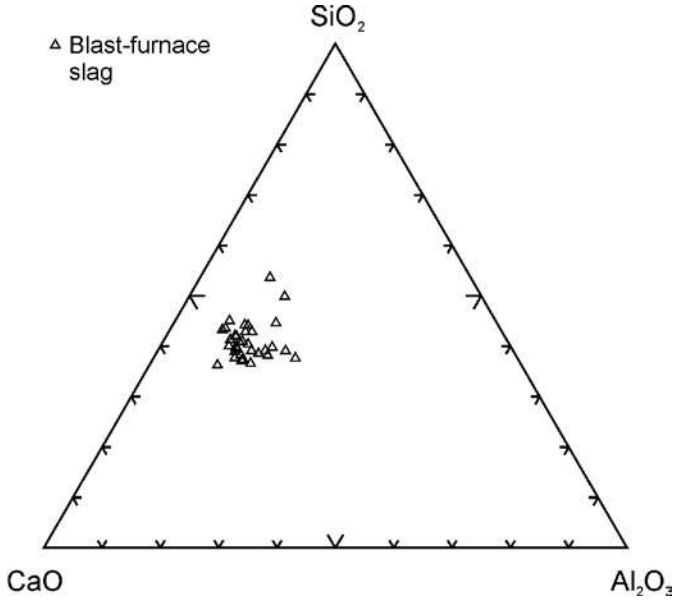

Figure 16. Ternary diagram (wt% based) of the compositional distribution of a selection of blast furnace slags.

increase in compressive strength of the binder, the MgO and Al_2O_3 contents show the same effect up to respectively 10-12% and 14% beyond which no further improvement can be observed. Also higher levels of alkali lead to strength improvement, especially at early ages. Other minor components such as MnO and TiO_2 exert a negative effect on the hydraulic character of the slag. Several compositional ratios or so-called hydraulic indices have been used to correlate slag composition with hydraulic activity; the latter being mostly expressed as the binder compressive strength. Normative compositional requirements have also been formulated based on a number of hydraulic indices, for instance the EN-197-1 norm requires a $(CaO+MgO)/SiO_2$ larger than 1, the German and Japanese standard demand a $(CaO+MgO+Al_2O_3)/SiO_2$ larger than respectively 1 and 1.4. However, the relationship between the hydraulic indices and compressive strength are very roughly defined and do not allow an accurate prediction of compressive strength solely based on the slag chemical composition for a series of slags originating from different production sites (Lang 2002). Other parameters which have been often included in multiple regression analyses for strength prediction are the slag fineness and glass content (e.g., Douglas et al. 1990; Escalante et al. 2001; Pal et al. 2003; Bougara et al. 2010).

The glass content of slags suitable for blending with Portland cement typically varies between 90-100% and depends on the cooling method and the temperature at which cooling is initiated. The glass structure of the quenched slag largely depends on the proportions of network-forming elements such as Si and Al over network-modifiers such as Ca, Mg and to a lesser extent Al. The network-forming atoms are tetrahedrally coordinated by oxygen atoms and show a varying degree of polymerization or connectivity depending on the ratio of network-forming to network-modifying elements. Increased amounts of network modifiers lead to higher degrees of network depolymerization and reactivity (Goto et al. 2007). The rate of cooling influences the amount of structural defects in the glass phase, the higher the cooling rate, the more defects and the higher the reactivity. The presence of small amounts of finely dispersed crystalline material has been observed to improve the reactivity of the slag (Demoulian et al. 1980; Frearson and Uren 1986), especially when dendritic crystallization of merwinite ($Ca_3Mg(SiO_4)_2$) occurs. The Al-enrichment of the glass near the merwinite crystallites and the mechanical stress and presence of nucleation sites introduced by the phase separation are suggested to enhance the slag reactivity.

Another common crystalline constituent of blast furnace slags is melilite, a solid solution between gehlenite ($Ca_2Al_2SiO_7$) and åkermanite ($Ca_2MgSi_2O_7$). The $CaO\text{-}SiO_2\text{-}Al_2O_3$ phase diagram at 10% MgO (Fig. 17) shows that most blast furnace slags will initially crystallize melilite, other minor components which might form during progressive crystallization are belite (Ca_2SiO_4), monticellite ($CaMgSiO_4$), rankinite ($Ca_3Si_2O_7$), (pseudo-) wollastonite ($CaSiO_3$) and forsterite (Mg_2SiO_4). The α' and β-polymorphs of belite and possibly also melilite show hydraulic activity and can contribute to the compressive strength. Minor amounts of reduced sulfur are commonly encountered as oldhamite (CaS) (Scott et al. 1986). The reducing environment that blast furnace cements can provide are often advantageously used for waste stabilization (Roy 2009). Deleterious free lime (CaO) or periclase (MgO) are usually not present in blast furnace slags.

Fly ash. Coal fly ash is a gigascale material (Scheetz and Earle 1998). Over one billion tons of by-products are generated annually during the combustion of coal (Kutchko and Kim 2006). These by-products include mainly dry bottom ash, wet bottom boiler slag, economizer ash, fly ash and flue gas desulphurization or scrubber sludge. Of these by-products, the annual production of fly ash is estimated around 500 millions of tons (Joshi and Lothia 1997). Coal is not exclusively composed of organic matter, which produces the energy during coal firing in power plants. It also contains a variable amount of inorganic material. This intermixed inorganic material may remain unaffected or will be transformed during combustion. It will then be concentrated in the by-products. Besides coal fly ash, other types of fly ash; for instance

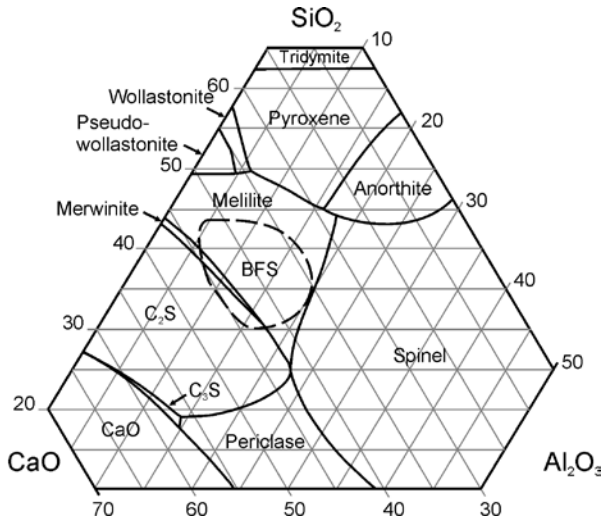

Figure 17. Phase diagram of the CaO-SiO_2-Al_2O_3 system (wt% based) at 10 wt% MgO, the blast furnace chemical composition distribution largely falls into the melilite field (modified after Satarin 1974).

Municipal Solid Waste Incineration (MSWI) fly ash exist. However, coal fly ash is by far the most widely used and investigated type of fly ash. Therefore most attention will go to coal fly ash in what follows. It will simply be designated as "fly ash" hereafter. Much of the information in the following paragraphs is taken from the valuable work of Joshi and Lothia (1997) and Sear (2001) who made extensive reviews of the production, the use and the properties of fly ash.

From all coal combustion products (CCP), coal fly ash (CFA), also designated as fly ash (FA) or pulverized fuel ash (PFA) is most widely used as a supplementary cementitious material. Fly ash is produced when C-rich sediments are burned at temperatures reaching 1450 °C or higher. Whereas the carbon-based materials are mainly transformed to gaseous compounds as CO_2, H_2O, NO_X and SO_2, most of the minerals that are present in the burned sediments will not be volatilized. Instead, they may undergo various chemical, physical and mineralogical changes. Whereas some of the primary minerals remain unaffected during the burning process, others will melt, become amorphous and/or recrystallize to form secondary minerals. These materials are then recovered at the bottom of the furnace/boiler or from the flue gases by electrostatic or mechanical precipitators or bag houses (Joshi and Lothia 1997). Fly ash is the material recaptured from the exhaust gases of power plants using pulverized coal as a combustion product. Fly ash is generally subdivided in categories following the national or international standards. It is a versatile, heterogeneous material that is extensively researched regarding all its intrinsic properties, its use as a supplementary cementitious material or for multiple other applications.

Since the beginning of the 20th century, fly ash has been recognized as a pozzolanic constituent (Joshi and Lothia 1997). Initially, only the Ca-poor fly ashes resulting from the burning of bituminous coal were considered as supplementary cementitious materials. However, from about the middle of the 20th century, also the more Ca-rich fly ashes were considered as a cement replacement material. The actual use of fly ash dates back to more than 50 years ago (Sear et al. 2003). Besides scientific research dealing with fly ash characterization, many studies were done on the various applications of fly ash. A considerable portion of this research focuses on its use as a supplementary cementitious material in cement or concrete, even though other uses increasingly attract attention. Most of the scientific work focuses on the physical/

mechanical properties of cement/fly ash mixtures (e.g.: Papadakis 1999; Papadakis 2000; Maltais and Marchand 1997; Erdoğdu and Türker 1998; Grzeszczyk and Lipowski 1997; Payá et al. 1997), investigates the durability of fly ash use (e.g.: Bijen 1996; Lilkov et al. 1997; Papadakis 2000; Roy et al. 2001), or studies the hydration reactions more in general (e.g., Sharma and Pandey 1999; Lilkov et al. 1997; Papadakis 1999; Maltais and Marchand 1997). Although the suitability of some types of fly ash may still be a matter of debate (Papadakis 2000; Sear et al. 2003), the use of fly ash in concrete is generally considered as beneficial from an ecological, economical and technological point of view.

In addition to the use as a SCM in traditional calcium silicate or aluminate hydrate binders, fly ash has many other applications. Amounts of 5-15% are generally cited as the proportion of fly ash used in concrete compared to the global amount of fly ash produced. Some European countries consume up to 100% of their production (Queralt et al. 1997), whereas other countries as Israel seem to have already reached a much lower maximum for the addition of fly ash to cement clinker or concrete (Nathan et al. 1999). Mainly in Europe, other applications account for the use of increasingly large amounts of this secondary raw material. Due to its bulk mineralogy and chemistry, it can serve as a source of raw materials for large-volume, low-tech applications (Scheetz and Earle 1998). As fly ash is a complicated heterogeneous material (Vempatie et al. 1994) of variable quality (Sakai et al. 2005), a detailed knowledge of the physical and chemical characteristics is generally required (Vempatie et al. 1994) before use. The numerous cementitious applications of fly ash include grouts, block manufacture and road sub-base and base construction (Sear et al. 2003). High proportions of fly ash can also be incorporated in dams, walls, girders, roller-compacted concrete pavements and parking areas (Manz 1998; Sakai et al. 2005). However, large amounts of fly ash can also be used for land reclamation (Mondragon et al. 1990; Sear et al. 2003). Moreover, increasing efforts are done to use the material for technologically valuable applications as for the manufacture of monolithic ceramics (Mondragon et al. 1990; Queralt et al. 1997; Ilic et al. 2003) or for alkali-activated materials (Puertas and Fernández,-Jiménez 2003; Bakharev 2005) with a significant compressive strength. Other high-tech applications include the production of zeolites (Mondragon et al. 1990; Murayama et al. 2002) or its use for phosphate immobilization from agricultural activities (Grubb et al. 2000). Instead of using fly ash as a bulk resource, some authors (Cheriaf et al. 1999; Vassilev et al. 2003) suggest to separate several fractions for different uses. The ultra-fine fraction (0.1-1 μm) could for instance be used in high performance concretes (Sear 2001), cenospheres as a strong lightweight inert filler material (Sear 2001) or for specific aerospace applications (Mondragon et al. 1990). The magnetic fraction for instance could be competitive as ferro-pozzolan for the production of dense concretes (Vassilev et al. 2004). Bottom ash, another secondary raw material formed during coal combustion is also used in concrete as a low-cost replacement material for sand or as a base in road construction. Bottom ash is also used as a fertilizer (Cheriaf et al. 1999). Future research will be required to ensure the continuous proper application of coal combustion waste products as fly ash, considering for instance a changing fly ash composition. The types of fuel used in the future will change and diversify and blends of fuels will be used (Steenari and Lindqvist 1999; Koukouzas et al. 2007). Thereby, the nature of the fly ash will inevitably be affected, requiring an adapted utilization. Moreover, other coal combustion by-products such as bottom ash will probably gain more interest in the future, as they are potentially appropriate as secondary raw material for various applications. Other types of fly ash such as MSWI fly ash could similarly be used more often in the future (Kirby and Rimstidt 1993; Ferreira et al. 2003).

The quality of the fly ash varies widely (Sakai et al. 2005). Depending on the burning temperature, the coal type, the processing and many other factors, fly ash exhibits different physical, chemical and mineralogical properties (Erdoğdu and Türker 1998; Vassilev et al. 2003). These will in turn affect the properties of the concrete or other products in which they are used. The first standards were introduced to classify fly ashes in order to reduce this variability

for fly ash users. In 1953-1954, the ASTM standard C350 for fly ash as an admixture was introduced (Malhotra 1993; Manz 1998). In 1960 it was extended to the use of fly ash as a pozzolan. The ASTM standard C618 was introduced in 1968 and covers both natural pozzolans and fly ashes for their use as mineral admixtures in Portland cement concrete. A first British standard BS 3892 was introduced in 1965 in which fly ash was treated as a fine aggregate with three classes of fineness for use in concrete. It was revised afterwards. In 1995, a common specification for EU countries, EN 450, was introduced for fly ash used in concrete. Particular for this common European norm compared to the BS 3892, is the definition of the Activity Index, imposing a minimum strength for fly ash/Portland Cement mixtures. Also the ASTM standard, C618 requires both fly ash/Portland cement and fly ash/lime mixtures to achieve a minimum strength after 28 or 7 days respectively.

The ASTM C618 defines three categories of mineral admixtures; Class N, Class F and Class C. Class N includes mainly the group of natural pozzolans. Class F fly ash is a siliceous type of fly ash mainly obtained from the combustion of bituminous or hard coals. The main part of the fly ash used in concrete is of this type. Class C fly ash is richer in calcium and results primarily from the combustion of lignite or brown coal. Whereas the classification in ASTM C618 of mineral admixtures in Portland cement concrete derives from a genetic differentiation, some authors (Mehta 1983, 1989; Joshi and Lothia 1995, 1997; Manz 1998) repeatedly suggested making a distinction based on the properties of the admixtures. Joshi and Lothia therefore proposed to define one class of "pozzolanic but non-self cementitious" materials and another class of "pozzolanic and self cementitious" or "hydraulic" materials. The two classes would in that case be distinguished by their difference in loss on ignition.

It is generally believed that there is a close relationship between the properties of supplementary cementitious materials (as fly ashes) and their mineralogy (Vassilev and Vassileva 1996; Manz 1998). The mineralogy of fly ashes is in general not considered in the norms. This is due to a lack of quantitative analytical data (Ward and French 2006) and/or knowledge of mineralogical analysis techniques (Manz 1998). However, reliable methodologies for mineral quantification have been developed (Winborn et al. 2000) and can be used to establish correlations with the Activity Index and other relevant parameters. It is therefore reassuring that an increasing number of studies systematically use quantitative mineralogical information for interpreting data.

Pulverized Fuel Ash may also be classified as "low-lime" and "high-lime" fly ashes (Dhir 1986). This classification roughly corresponds to the ASTM class F and C fly ashes respectively. An alternative classification was proposed by Roy et al. (1981) and has been adopted by others (Goodarzi 2006). Three major groups of oxides are defined; $SiO_2 + Al_2O_3 + TiO_2$ (sialic); $CaO + MgO + Na_2O + K_2O + (BaO)$ (calcic) and $Fe_2O_3 + MnO + P_2O_5 + SO_3$ (ferric). The fly ash compositions are plotted in a ternary diagram where the three major classes sialic, calcic and ferric, are defined next to the intermediate classes ferrocalsialic, ferrosialic, calsialic and ferrocalcic.

Fly ash is composed of mainly spherical particles ranging in size from less than 1 to about 300 μm (Fig. 18). These particles form upon rapid cooling of droplets of viscous, molten or even vaporized mineral matter that was initially present in the combustion product. The major consequence of the rapid cooling is that only few minerals will have time to crystallize and that mainly amorphous, quenched glass remains. Nevertheless, some refractory minerals in the pulverized coal will not melt (entirely) and remain crystalline. In the following sections, the physical, chemical and mineralogical properties of fly ashes in general and of their discrete constituents in particular will be discussed.

The average specific gravity of fly ash is estimated around 2.2 with a standard deviation of about 0.3. The BET specific surface area may range from less than 0.5 to more than 10 m^2/g.

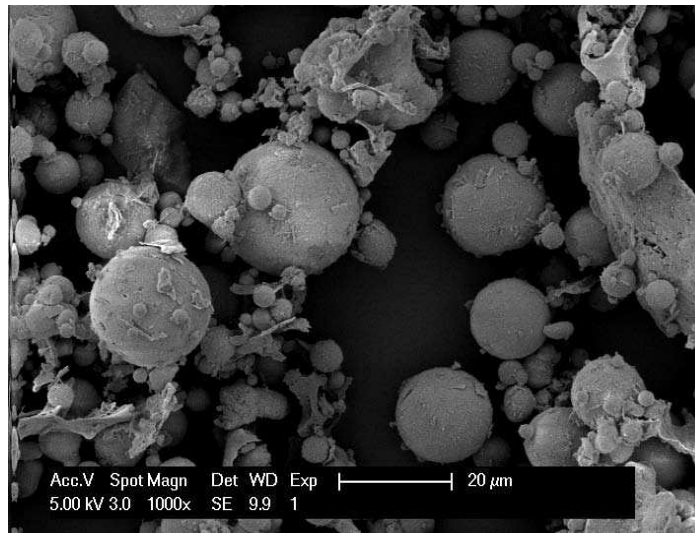

Figure 18. SEM picture of a typical fly ash with its mostly spherical and some angular particles.

Average Blaine surface areas are in the order of 0.35 m²/g and are relatively less divergent compared to tabulated BET surface areas. When pulverized, the specific gravity of the fly ash increases to about 2.7 as hollow particles break up (Dhir 1986). There also seems to be a direct relation between specific gravity of the bulk fly ash and its mineralogy. Higher quartz and mullite contents account for a lower specific gravity (Joshi and Lothia 1997). The particle size distribution appears to be strongly dependent on the method of collection (Dhir 1986). Fly ashes collected from electrostatic precipitators are two to five times finer compared to fly ashes from mechanical separators. The former type is therefore more generally used as a SCM. The fineness of fly ash is often expressed as the fraction passing a 45 µm wet sieve. It also serves as a routine measure for quality control and to assure uniformity in fly ash supply. A substantial correlation exists between the fineness of the fly ash (% retained on a 45 µm sieve) and its Activity Index (Dhir 1986).

However, fly ash is a heterogeneous material. Physically distinct particles can be distinguished. 1 to 2 wt% (Sear 2001) or 15 to 20 vol% (Vassilev and Vassileva 1996) of the fly ash consist of hollow spherical particles known as cenospheres. Cenospheres have diameters ranging from 50 to 200 µm, with a wall thickness of approximately 10% of their radius (Sear 2001). Cenospheres form when trapped organics, carbonates, sulfides, sulfates or hydrosilicates decompose or water evaporates and induces an expansion while the particle is still in a viscous state (Kolay and Singh 2001; Kutchko and Kim 2006). They appear to be more characteristic for fly ashes obtained from coals enriched in finely dispersed illite and quartz (Vassilev and Vassileva 1996). Their density is very low and ranges from 250 to 800 kg/m³. If the fly ash is stored in a lagoon, the cenospheres will float at the surface. The Blaine surface area of cenospheres collected from such a lagoon in Dahuna, India, is about 0.05 m²/g (Kolay and Singh 2001) and thereby much lower than the surface area of the bulk fly ash. This is explained by their nearly perfect spherical shape and their hollow structure. Because of their particular properties, cenospheres are used for specific applications as in lightweight constructions. As cenospheres are hollow, they have good isolating properties. Plerospheres are like cenospheres, but instead of being empty, they contain smaller spherical or other particles. Dermaspheres are defined as plerospheres that have crystal nuclei of mullite, hematite and other minerals,

covered with amorphous aluminosilicate envelopes (Vassilev and Vassileva 1996). Ferrospheres are spherical particles enriched in iron, be it amorphous or crystalline. Spheroïds are a specific type of spheres that look more porous or vesicular particles, with sizes ranging from 10 to 80 μm (Vassilev and Vassileva 1996). Ramsden and Shibaoka (1982) made their own classification of fly ash particles and defined seven categories; (1) unfused detrital minerals, (2) irregular-spongy particles, (3) vesicular colorless glass, (4) solid glass, (5) dendritic iron oxide particles, (6) crystalline iron oxide particles and (7) unburned char particles.

Like in most other supplementary cementitious materials, SiO_2, Al_2O_3, Fe_2O_3 and occasionally CaO are the main components present in fly ashes. A selection of fly ash compositions is plotted in Figure 19. Following the ASTM classification, a main distinction can be made between Class F and Class C fly ashes. The relatively more CaO-rich Class C fly ashes plot further away from the SiO_2-Al_2O_3 border of the diagram compared to the Class F fly ashes. The ASTM standard requires the sum of SiO_2, Al_2O_3 and Fe_2O_3 to be greater than 70% for Class F and greater than 50% for Class C fly ashes.

The mineralogy of fly ashes is very diverse. The main phases encountered are a glass phase, together with quartz, mullite and the iron oxides hematite, magnetite and/or maghemite. Other phases often identified are among others; cristobalite, anhydrite, free lime, periclase, calcite, sylvite, halite, portlandite, rutile and anatase. The Ca-bearing minerals anorthite (feldspar), gehlenite, åkermanite and various calcium silicates and calcium aluminates identical to those found in cement clinker can be identified in Ca-rich fly ashes. These, mainly type C, fly ashes may have hydraulic properties, as they contain minerals that react with water to form calcium-silicate/aluminate hydrates with binding properties. A similar mineralogical composition to that of coal fly ash is found in Municipal Solid Waste Incinerator ash (Kirby and Rimstidt 1993). For fly ashes in general, the Ca-minerals, free lime, periclase and sulfate minerals are probably most critical towards their properties (Sear et al. 2003). There appears to be a strong relation between the mineralogy of the fly ashes and the mineralogy of the feed coals (Ward and French

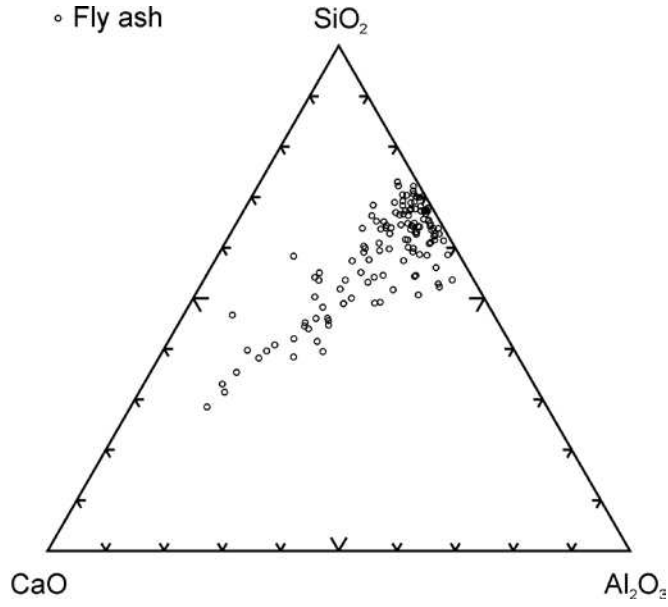

Figure 19. The reported chemical compositions of fly ashes plotted into a CaO-SiO_2-Al_2O_3 ternary diagram (wt% based).

2006; Koukouzas et al. 2007) as well as their combustion temperature (Koukouzas et al. 2007). This is also true for alternative fuel sources. Wood chips, being rich in Ca, will generate Ca-rich fly ashes, whereas the combustion of biomass rich in alkalis will generate fly ashes containing minerals alkali-bearing minerals.

Three large groups of components are identified in fly ashes; (1) an organic char fraction, (2) an inorganic amorphous and (3) an inorganic crystalline fraction.

1) Char particles are concentrated in the larger grain size fractions (Kutchko and Kim 2006). The char fraction mainly consists of carbon and correlates with the Loss on Ignition (LOI). Whereas the relative abundances of the main elements in the fly ash are chiefly dependent on the source of the pulverized fuel, the LOI is strongly dependent on the burning process. During the "boosting period," i.e., at the start-up of the power plant, an increase of the LOI is generally observed (Sear 2001). About 90% of this LOI is due to unoxidized elemental carbon. Older power stations also tend to yield high LOI fly ashes. The same goes for modern low NO_x burners. In general, lower temperatures correspond to lower NO_x values, but higher unburned carbon. LOI values may range from less than 1 to more than 20%, although values of maximum 6 or 7% are accepted by most standards for fly ash in Portland cement concrete.

2) The glass or inorganic amorphous phase in fly ashes may represent up to 90% of the total weight. An average value is probably in the order of about 60 to 80 wt%. Its quantity can be accurately determined from Quantitative X-Ray Diffraction (QXRD) measurements using an internal standard. Microscopic methods are often not suitable for quantifying fly ashes as the glass and crystalline phases are generally intimately intermixed (Ward and French 2006). The glass phase is principally composed of silica and alumina, although many other constituents are present. The silica is present as cross-linked tetrahedra, thereby showing a short- but no long-range ordering (Bijen 1996). The basicity of the glass phase can be calculated through the same formula as that used for blast furnace slag employed in German and Japanese concrete (Sakai et al. 2005):

$$basicity = \frac{\left(CaO + MgO + Al_2O_3\right)}{SiO_2} \tag{1}$$

Sakai et al. (2005) found that when the glass content of the fly ash is low, its basicity tends to decrease. Moreover, there appears to be an inverse correlation between the mullite content and the amount of amorphous material in fly ashes (Sakai et al. 2005). Obviously, higher mullite contents result in lower quantities of amorphous material with a lower average basicity. Compared to granulated blast furnace slags, fly ashes have low basicities. Some authors (Bijen 1996; Manz 1998; Ward and French 2006) consider the amorphous part as the "active part." It is likely that the amorphous fraction is not composed of a single glass phase, but that it consists of different phases with a dissimilar composition (Nathan et al. 1999).

3) A tremendous work was done by Vassilev and Vassileva (1996) and Vassilev et al. (2003), who discussed the origin and occurrence of all minerals and groups of minerals found in 11 Bulgarian fly ashes. Their data include an exhaustive list of minerals, which is relevant for all studies on fly ash mineralogy. Individual fly ash particles, with the exception of plerospheres, are chemically fairly homogeneous (Gieré et al. 2003). Nevertheless, bulk fly ash is heterogeneous and differences in chemistry are observed between size fractions and between the categories of fly ash particles defined earlier. Cenospheres for instance are more silica-, alumina- and potassium-rich and poorer in calcium compared to the bulk fly ash (Vassilev and Vassileva 1996; Sear 2001). Ferrospheres are obviously rich in Fe and Fe-bearing minerals. Element partitioning in fly ashes induces important differences in chemistry and mineralogy among the

size fractions. Many comprehensive papers deal with this partitioning (Filipidis and Georgakopulos 1992; Vassilev and Vassileva 1996; Erdoğdu and Türker 1998; Hower et al. 1999; Gieré et al. 2003; Vassilev et al. 2004; Chen et al. 2005) and the environmental/toxicological issues related with the finest fly ash particles (Coles et al. 1979; Tazaki et al. 1989). Magnetic or other separable fractions have also been studied separately (Hower et al. 1999; Vassilev et al. 2004).

The majority of trace elements in fly ash is found in the fines (Vassilev and Vassileva 1996). Moreover, there is a clear correlation with the mineralogy, as accessory minerals are mainly identified in the smaller grain size fractions. In these smaller fractions, trace elements may form discrete mineral phases (Vassilev and Vassileva 1996). Crystalline particles as small as 20 nm have been observed by Transmission Electron Microscopy (TEM) (Chen et al. 2005). Toxic elements that are volatilized during the combustion can also be absorbed on the surface of very small particles (Gieré et al. 2003). More in particular, glass particles tend to attract many trace elements, due to their reactive surface (Dudas and Warren 1987). It has been mentioned that the composition of the glass fraction is probably not uniform throughout the fly ash. The same is true for the crystalline components. In a TEM-study dedicated to the composition of the mullite phase, Gomes and François (2000) discovered that its composition is very heterogeneous. However, from the determination of the lattice parameters by X-ray diffraction, an average mullite composition can be obtained (Cameron 1977). Similarly, the composition of magnetite can also vary between individual fly ash particles (Gomes et al. 1999).

Silica fume. Silica fume is a by-product of the silicon metal and ferro-silicon alloy industries, the terms "condensed silica fume" and "microsilica" are also used. It is an excellent supplementary cementitious material with a high pozzolanic activity due to a high content of SiO_2 in amorphous form and a very fine particle size distribution (0.1-0.2 μm average diameter). Major reviews on silica fume and its applications in concrete can be found in Mehta (1986), Kjellsen et al. (1999), Fidjestol and Lewis (2001), Justnes (2002), Chung (2002) and in Justnes (2007).

Silica fume is produced during the reduction of quartz at high temperatures in electric arc furnaces. High purity quartz is heated to 2000 °C together with coal, coke or wooden chips to remove the oxygen. One of the reactions involves the formation of SiO vapor which oxidizes and condenses in the form of very small amorphous silica spheres. The first experiments on the use of silica fume in concrete were carried out at the Norwegian Institute of Technology in Trondheim (1950) but extensive research started only in the 1970's and widespread commercial use of silica fume in concrete started in the 1980's. Important production countries at this moment are China, Norway, South Africa, USA, Canada, Spain, Russia and France.

Unlike other thermally activated supplementary cementitious materials such as for example fly ash, silica fume from one production source has nearly no variation in chemical composition over time, because of the use of relatively pure raw materials. The SiO_2 content varies with the silica content of the alloy being produced and should be higher than 85% for silica fumes suitable for use as pozzolan (ASTM C 1240). In general, the chemical composition of silica fume is not complex and consists usually of more than 90% of SiO_2 (85-99%). Other oxides such as Fe_2O_3, Al_2O_3, CaO, MgO, Na_2O and K_2O are normally below 1.0%, the value for the loss on ignition varies between 1.0% and 2.0%.

Silica fume consists essentially of an amorphous silica structure and a very large peak can be observed centered at about 4.4 Å using X-ray powder diffraction. The silica fume particles are spherical in shape and using electron microscopy it was shown that they have an average diameter size between 0.1 and 0.2 μm (Fig. 20). Silica fume has an approximate value of 2.2 g/cm³ for the specific gravity and a very high surface area value of about 20-22 m²/g as measured with BET N_2-adsorption.

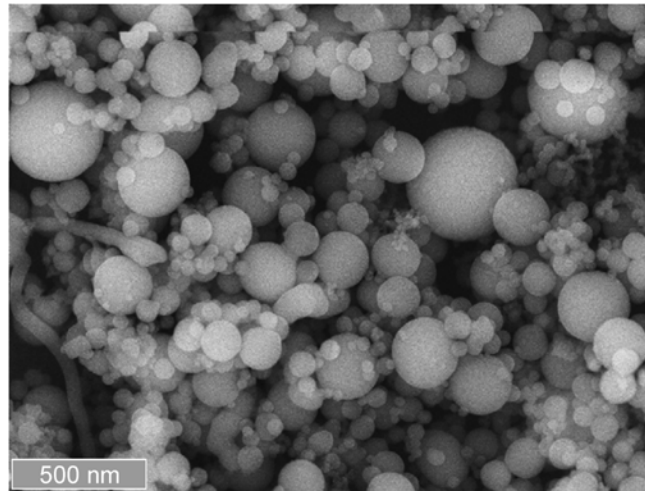

Figure 20. SEM picture of a typical silica fume with average particle diameter of 0.1 μm. [Used by permission of Elsevier, from Jo et al. (2007), *Construction and Building Materials*, Vol. 21, Fig. 1, p. 1352.]

THE POZZOLANIC REACTION

The recombination of an (alumino-)silicate or aluminate material and Ca^{2+} or $Ca(OH)_2$ in the presence of water into hydrated reaction products with binding properties can be schematically formulated in cement chemistry notation (A = Al_2O_3, C = CaO, H = H_2O, S = SiO_2; hyphenation denotes variable stoichiometry) as:

$$AS + CH + H \rightarrow C\text{-}S\text{-}H + C\text{-}A\text{-}H \quad (2)$$

The driving force behind this simplified reaction is the difference in Gibbs energy between the reactants and the eventual products. The reaction rate is however, determined by the individual elementary steps or processes in the reaction. The reaction step with the slowest rate of conversion is the rate-controlling process and is typically the one with the highest activation energy barrier. It is generally accepted that the initial rate-controlling process consists of the release or dissolution of silica from the pozzolan. The increasing pore solution saturation degree eventually gives rise to heterogeneous nucleation and growth of the C-S-H reaction products at the pozzolan surface. Subsequent to the formation of a layer of reaction products enveloping the reactant grains, the reaction rate is commonly assumed to be limited by the diffusion of ions through the growing and densifying layer of products (Kondo et al. 1976; Držaj et al. 1978; Takemoto and Uchikawa 1980). Most published reviews on supplementary cementitious materials do not treat the subject of the mechanism of the pozzolanic reaction in detail, but tend to focus on material properties defining the activity and performance of pozzolans. However, difficulties are met when trying to compare and relate the activity controlling properties among SCMs of different origin (e.g., Mehta 1987; Sersale 1993). In this respect, empirically established relationships between pozzolan properties and activity remain limited to materials of a similar origin. To determine which material properties are of importance and when they become essential in the pozzolanic reaction, a detailed knowledge of the pozzolanic reaction mechanism is needed. In this particular area much work remains to be done. Unraveling the impact of the heterogeneous group of SCMs on cement hydration will constitute one of the major challenges in cement science for years to come. As a starting point, in the following sections, the traditional views on the pozzolanic reaction are combined with recent fundamental insights into the dissolution of minerals developed in geochemistry (Lasaga 1998; Dove et al. 2005).

The pozzolanic reaction mechanism

A general overview of the different stages in the pozzolanic reaction can be obtained by monitoring the rate at which heat is evolved during the reaction. The rate of heat evolution is closely related to the actual rate of reaction provided that the reactions are exothermal (Gartner et al. 2002). In Figure 21 an idealized heat release curve for the pozzolanic reaction between silica and $Ca(OH)_2$ is presented. Three main stages can be recognized. The duration of each of the stages and also the shape of the heat release curve vary significantly depending on the experimental conditions and the pozzolanic activity of the material. The initial sharp peak occurring directly after mixing (stage I) lasts only for several minutes and is followed by a period of low activity designated as the induction period (stage II). Renewed activity defines the initiation of stage III, which can be divided tentatively in parts of an accelerating and a decelerating reaction rate. The induction period usually lasts only for several hours to some days. The duration of stage III is indefinite. In some cases the reaction can proceed at very low rates for extended periods of years to decades (e.g., Taylor et al. 2010).

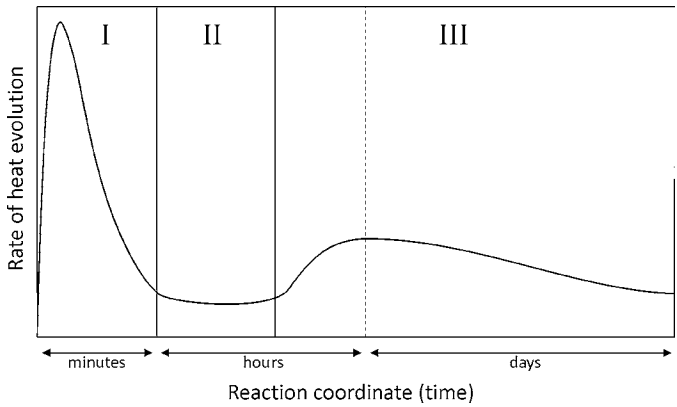

Figure 21. Schematic overview of the rate of heat release during the pozzolanic reaction of silica and $Ca(OH)_2$. Stage I, represents the initial dissolution period. Stage II corresponds to the induction period and stage III is the phase in which the main reaction occurs.

I. Initial dissolution period and aluminosilicate dissolution. Both lime-based and Portland cement based binders have in common that initial fast dissolution of $Ca(OH)_2$ or clinker minerals in water rapidly results in an alkaline solution saturated in $Ca(OH)_2$. In $Ca(OH)_2$-based systems the solution pH is usually around 12.4, while in Portland cement based systems the solution may reach values of 13.7 when abundant soluble alkalis were released from the clinker minerals. At alkaline pH above 10.7 the solubility of silica and silicates (i.e., amount of silica in solution) increases continuously with pH (Iler 1979; Knauss and Wolery 1988) and pozzolans will be subjected to dissolution. The silicate dissolution rate at high pH is governed by processes of hydration, deprotonation, ion-adsorption and hydrolysis at the mineral-water interface. Greenberg (1961) concluded that the rate-controlling step in the pozzolanic reaction was the hydrolysis of surface silica groups. To understand and predict the kinetics of dissolution, the molecular details and energetics of the actual pathway that links reactants and products via the activated complex need to be known. The activation energy is the energy difference between the activated complex or transition state and the reactants. *Ab initio* quantum mechanical calculations of finite molecular clusters clarified the pathway to dissolution of silicates and aluminosilicates at high pH in recent years (cf. Xiao and Lasaga 1994; Lasaga 1998). The generally accepted reaction pathway for the hydrolysis of the bridging bond (O_{br}) in a

$(HO)_3$-Si-O_{br}-Si-$(OH)_3$ (Q_1) cluster is illustrated in Figure 22 and the corresponding energetics are given in Figure 23 (Morrow et al. 2009). In alkaline conditions the silanol groups at the silicate surface are partially deprotonated. Xiao and Lasaga (1996) have shown that nucleophilic hydroxyl attack on a neutral Si-OH surface group is equivalent to hydrolysis of a deprotonated Si-O^- surface group. Both situations result in a H-bonded H_2O adsorption onto the negatively charged Si-O^- site (RC or reaction precursor complex). The key step in the reaction is the formation of a negatively charged fivefold coordinated trigonal bipyramidal Si species. To form this reaction intermediate (INT) the reaction has to pass through a transition state (TS1) and surmount the associated large energy barrier (calculated to be 110 kJ/mol in the gas phase; Morrow et al. 2009). The Si-O_{br} bond in the formed intermediate state is significantly weakened and the energy barrier associated with the final step of bond breakage is much smaller (22 kJ/mol in gas phase; Morrow et al. 2009).

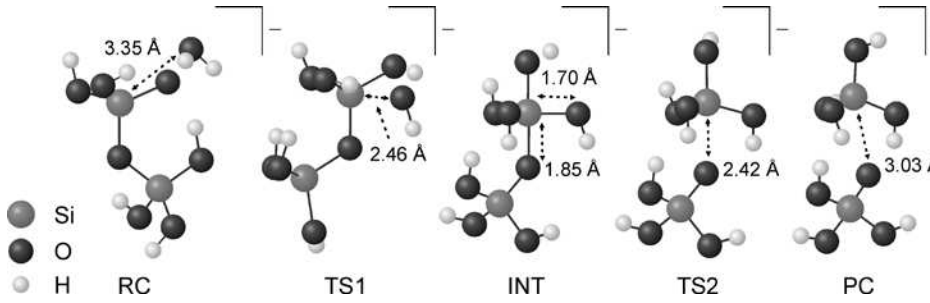

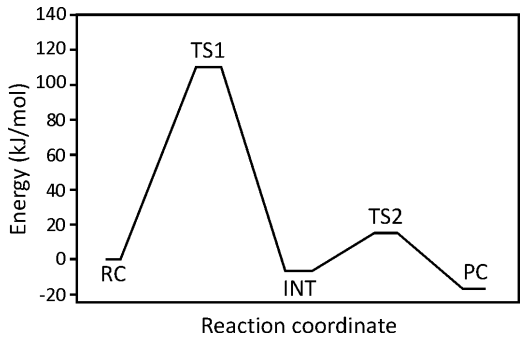

Figure 22 (*above*). Reaction stages along the reaction profile for the hydrolysis of a deprotonated Si-O-Si species (Morrow et al. 2009). RC is the reaction precursor complex, TS1 and TS2 are transition states, INT is an intermediary state and PC the product complex.

Figure 23 (*to the left*). Energy profile for the Si-O-Si hydrolysis reaction shown in Figure 22 (modified after Morrow et al. 2009).

The activation energy of Si-O_{br}-Si hydrolysis in larger clusters where the considered Si atoms are doubly (Q^2) or triply (Q^3) connected to neighbor Si atoms via Si-O_{br}-Si bonds (e.g., Fig. 24) was investigated by Pelmenschikov and co-workers for dissolution by H_2O attack (Pelmenschikov et al. 2000, 2001) and by Criscenti et al. (2006) for dissolution by H_3O^+ attack on a Q^3 cluster. The calculations indicated that the activation energy increased with connectivity (up to 205 kJ/mol for a Q^4 cluster), this was attributed to resistance of the remaining bridging bonds against relaxation of the partially uncoupled Si species (Pelmenschikov et al. 2000). In the neutral silanol state the breakage of the Si-O_{br}-Si bond is expected to be followed by a very fast condensation or rehealing reaction. The experimentally determined activation energy of silicate dissolution (67-92 kJ/mol; Knauss and Wolery 1988; Brady and Walther 1990; Dove and Crerar 1990; Walther 1996) would then be associated with the hydrolysis of the last Si-O_{br}-Si bonds (Q^1 and/or Q^2) (Criscenti et al. 2006). In an alkaline medium the rehealing reaction is suggested to be partially prevented by the deprotonation of the formed Si-OH HO-Si defect (Pelmenschikov et al. 2001).

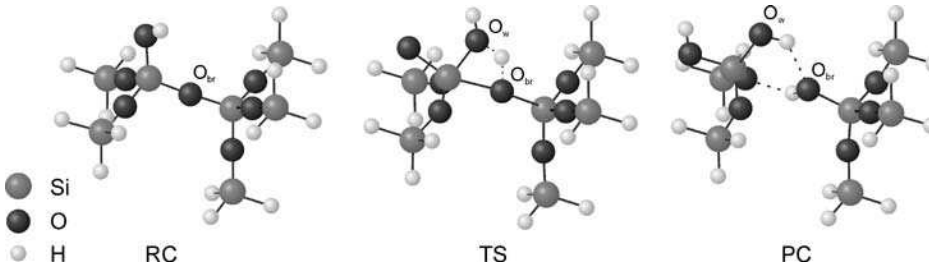

Figure 24. Reaction profile for the hydrolysis of a Q^3 connected Si-O_{br}-Si bond at the (111) β-cristobalite surface (Pelmenshikov et al. 2000). O_{br} stands for bridging oxygen. O_w was originally part of the attacking water molecule.

Morrow et al. (2009) compared the pathways of dissolution of aluminosilicate Q^1 clusters with the earlier reported silicate dissolution mechanism. At high pH dissolved Al is fourfold coordinated (Swaddle et al. 2005), only one transition state was found for the dissolution and release of $Al(OH)_4^-$. This step corresponded with the formation of a fivefold coordinated almost trigonal bipyramidal Al species with a much lengthened Al-O_{br} bond interaction (Fig. 25). At acid and neutral pH the barrier heights of Si-O_{br}-Si hydrolysis (resp. 63 and 146 kJ/mol) were considerably higher than that of Al-O_{br}-Si linkages (resp. 38 and 39 kJ/mol). This is supported by the experimental observation of leaching of Al from the surface of feldspars at low pH (Stillings and Brantley 1995). However, at high pH there was no significant difference (79 kJ/mol for both), which is in agreement with the observation that little or no Al depletion occurs on aluminosilicate surfaces at high pH (Hamilton et al. 2001).

The dissolution rates of silicate minerals were observed to be affected by the solution pH or, equivalently, by the distribution of protonated, neutral or deprotonated groups at the mineral surface. Based on such a surface speciation model and transition state theory (cf. Lasaga 1998) the pH dependence of the dissolution rate of quartz can be predicted (Dove 1994; Nangia and Garrison 2008). However, for mixed oxides containing Si-O_{br}-Si linkages such as aluminosilicate feldspars, the activities of the leached cations in solution should be included into the model (Oelkers 2001). For orthosilicates and minerals without silicate linkages, dissolution rates can be correlated with the solvation-water exchange constant of the non-silicate cations (Westrich et al. 1993). Background cations in solution change the aluminosilicate surface speciation by adsorption and proton exchange reactions. At high pH, alkali and alkaline-earth cations are drawn to the negatively charged surface by electrostatic attraction (Iler 1979). Both

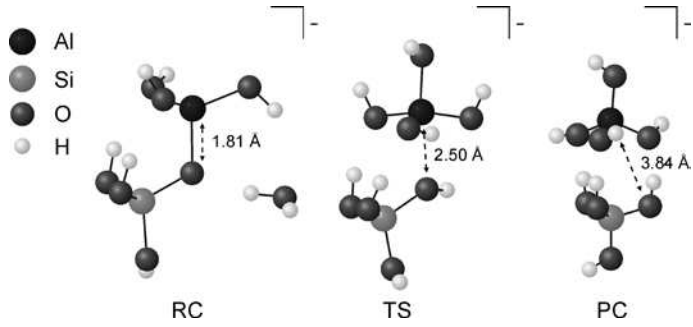

Figure 25. Reaction stages along the reaction profile for hydrolysis of a deprotonated Al-O_{br}-Si (Morrow et al. 2009). RC is the reactant complex, TS the transition state and PC the product complex.

experimental (Sjöberg 1989; Dove and Crerrar 1990) and computational (Strandh et al. 1997) results show that the adsorption of cations generally leads to enhanced dissolution rates and weakened bridging bonds of the Si or Al species with the lattice. In general, alkaline-earth cations in solution bind more strongly to the mineral surface and remain only partially hydrated. Alkali cations retain significant water shielding upon interaction and would increase dissolution rates by increasing the reaction frequency compared to alkaline-earth cations which show slower exchange of solvation water (Dove 1999).

When water is added to dry blended cement or lime-SCM binders, dissolution of clinker constituents, SCMs or lime occurs at first in far-from-equilibrium, highly undersaturated conditions. The initial fast dissolution rate subsequently slows down significantly until a $Ca(OH)_2$ saturated solution is reached. In terms of silicate dissolution theory, this parabolic dissolution rate behavior has been attributed to the rapid initial dissolution of fine particles or sites with high surface energy (Brantley 2008). Other models explain the parabolic rate behavior by the formation of a leached surface layer due to non-stoichiometric dissolution or by the precipitation of a protective membrane at the mineral surface through which dissolved ions must diffuse (Schott and Petit 1987). The latter two models are very similar to the mechanisms invoked to explain the occurrence of the induction period during alite hydration (see below; Gartner et al. 2002; Bullard et al. 2011). More recently a mechanistic model for mineral dissolution was formulated to enable the prediction of dissolution rates depending on the saturation state of the solution (Dove et al. 2005; Lasaga and Lüttge 2005). This model is based on concepts borrowed from crystal growth theory where dissolution can be regarded as the inverse of crystal growth. Dissolution occurs as the result of horizontal step retreat at incomplete surface layers and of vertical removal of atoms at plain surfaces or at the intersection of dislocation or point defects with the surface (Fig. 26). Three different regimes of mineral dissolution can be distinguished depending on the dominant mechanism of dissolution. At very high undersaturation, two-dimensional pits or vacancy islands can nucleate at perfect surfaces without any dislocations present. However, the activation energy barrier for this mechanism is high and is expected to occur for only a very short time in cementitious systems (Juilland et al. 2010). Closer to equilibrium, two-dimensional pitting on plain surfaces will end. However, step nucleation can proceed at dislocation defects due to the associated strain field. Eventually, when the saturation degree reaches near-equilibrium, only step retreat is possible. No more steps can form at the surface or near dislocation defects. Step nucleation only occurs at crystal edges and the crystal becomes progressively smoother and edges more rounded (Brantley 2008). In this model the dissolution rate depends on the density of steps present or nucleated at the surface and the velocity of step retreat at the surface. Both parameters are a function of the degree of solution undersaturation, thus the dissolution rate will decrease sharply when the undersaturation degree

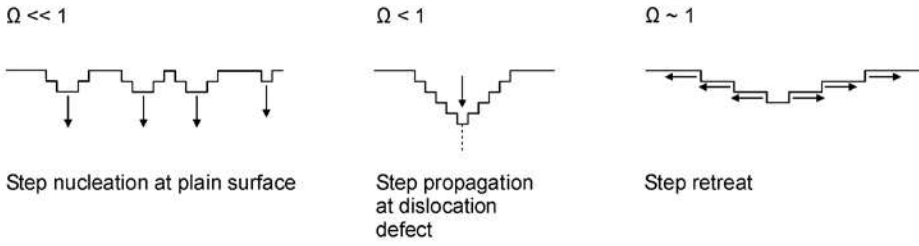

Figure 26. The dominant dissolution mechanism depends on the level of undersaturation. At very high undersaturations two-dimensional pits or vacancy islands can nucleate at perfect surfaces, at lower levels of undersaturation step nucleation can still proceed at dislocation defects. Eventually near equilibrium step nucleation ends and step retreat becomes the dominant dissolution mechanism. Ω identifies with the saturation degree (modified after Dove et al. 2005 and Juilland et al. 2010).

approaches equilibrium. However, the step nucleation mechanism and rate depend also on the nature of the crystal and the crystal face, especially in terms of the liquid-solid interface energy (Dove et al. 2005). Furthermore, dissolution rates near equilibrium increase with increasing defect density as exemplified for alite by Juilland et al. (2010) or for quartz by Blum et al. (1990). The suggestion by *ab initio* cluster studies that the precursor molecules of silicate dissolution should generally have a connectedness lower than 3 is consistent with a steady-state silicate dissolution mechanism dominated by step retreat.

II. Induction period. In the pozzolanic reaction the reaction rate decreases rapidly during period I and remains low during the ensuing induction period (Fig. 21). In most models this evolution is linked to the formation of a protective barrier layer on the reacting pozzolan particles (Takemoto and Uchikawa 1980; Glasser et al. 1987; Fraay et al. 1989). This barrier layer is expected to shield the pozzolan from the surrounding basic solution and to hamper its dissolution. Two distinct hypotheses are put forward regarding the nature of the protective layer. 1) The leached layer hypothesis is based on the incongruent dissolution of the pozzolan (cf. Livingston et al. 2001 for alite). As alkalis are leached from the surface an amorphous layer consisting of Si and Al remains, meanwhile Ca^{2+} is adsorbed at the surface and a double layer is created, inhibiting further dissolution. Eventually Si and Al dissolve and recombine with the adsorbed Ca^{2+} to form C-S-H and C-A-H phases (Takemoto and Uchikawa 1980). 2) The protective precipitate hypothesis is based on a dissolution-reprecipitation process, in which the pozzolan first releases Si and Al which then subsequently reprecipitate at the pozzolan surface as a coating of stable or metastable C-S-H and C-A-H reaction products (Greenberg 1961; Glasser et al. 1987). Alternatively, the reaction rate can also decrease sharply because of a decrease in the degree of undersaturation of the solution as suggested by the mechanistic model for mineral dissolution. If the degree of undersaturation would drop below the threshold for step nucleation at dislocation edges, the dissolution rate would be considerably lowered. The latter mechanism could of course also take place together with the formation of a barrier layer at the pozzolan-liquid interface.

The end of the induction period is marked by the massive nucleation and subsequent growth of reaction products. Several theories have been proposed to explain the sudden transition from the induction to the main period of reaction. The suggested theories were mainly derived from concepts developed to explain the hydration behavior of alite (cf. Gartner et al. 2002; Bullard et al. 2011). Takemoto and Uchikawa (1980) have suggested that the protective membrane would be semi-permeable, allowing osmosis of water from the outer solution to the concentrated inner solution. The rising osmotic pressure due to the ongoing dissolution of the pozzolan would eventually result in a rupture of the membrane, release of dissolved silica and alumina and the start of the main period of C-S-H and C-A-H precipitation. This theory was based on the osmotic pump model for the hydration of alite by Double et al. (1978) and the observation of relict hollow shells of reaction products by electron microscopy. Also more recent Nuclear Resonance Reaction Analysis results that indicate the development of a depleted silica gel layer at the surface of alite grains during the induction period have been linked to the existence of a semi-permeable layer (Livingston et al. 2001). A different, more widely accepted mechanism was first suggested by Stein and Stevels (1964) for the hydration of alite in the presence of silica. They proposed that the conversion of the protective layer of metastable C-S-H(m) or disordered gel type phases to a more stable C-S-H form would result in the acceleration of the hydration reaction of alite. The same mechanism can be applied to the pozzolanic reaction, the transformation would be triggered by the reaching of a certain degree of supersaturation with respect to the stable C-S-H assemblage. However, detailed studies on the evolution of the fluid saturation degree during the first stages of the pozzolanic reaction are still lacking.

III. Main reaction period. At the end of the induction period, typically only a very limited amount of reaction products has been formed and the pozzolan has barely reacted (Snellings

et al. 2009). The initiation of the main reaction period can be observed by an exponentially increasing heat release rate (Fig. 21) related to the large-scale nucleation and growth of the reaction products as the rate-controlling steps. The exponential reaction rate increase is short-lived, and eventually the reaction rate starts decreasing again. It has been widely considered that the decrease in rate is due to the onset of a diffusion-controlled process. Many observations of the formation of an enveloping layer of reaction products on the pozzolan grains supported the interpretation that the reaction rate becomes limited by the diffusion of reactants through the reaction product layer (Držaj et al. 1978; Türker and Yeginobali 2003; Mertens et al. 2009). Other processes may also cause a deceleration of the reaction rate. Consumption of the smallest particles will leave coarse particles that react more slowly. Also a lack of space or densification of the C-S-H rim can hinder the growth of C-S-H particles and thus decrease the reaction rate (Bishnoi and Scrivener 2009). Finally, the growing competition for a dwindling supply of water can lead to the deceleration of the reaction (Bullard et al. 2011).

In the traditional view of reaction rate deceleration due to diffusion control, several mathematical models have been used to fit the evolution of the degree of reaction α. In $Ca(OH)_2$-pozzolan systems the degree of reaction is usually quantified by the direct determination by X-ray diffraction or thermogravimetry of the amount of $Ca(OH)_2$ reacted (Kondo et al. 1976; Takemoto and Uchikawa 1980; Shi and Day 2000) or by the evolution of the overall heat release curve measured by calorimetry. Most kinetic models are based on the Jander equation developed to describe three-dimensional diffusion control during solid-state sintering of a contracting reactant sphere (Jander 1927):

$$\left[1-\left(1-\alpha\right)^{1/3}\right]^2=\frac{2kt}{r^2}=Kt \tag{3}$$

Where α identifies with the fractional reaction, k with the rate constant for the diffusion process, t equals to the time since the onset of the diffusion controlled reaction process, r is the initial radius of the spherical reactant and K represents a constant proportional to k. In the original Jander equation the thickness of the interface layer or equivalently, its diffusion coefficient is taken not to change over time. However, in cementitious systems the interface layer is expected to grow or densify gradually with the proceeding reaction. Therefore, a modified, more general form of this equation has been used more frequently (Kondo et al. 1976; Shi and Day 2000; Mertens et al. 2009).

$$\left[1-\left(1-\alpha\right)^{1/3}\right]^N=Kt \tag{4}$$

This equation allows the classification of the ongoing reaction based on the value of the exponent of reaction N. If $N = 1$, then dissolution or nucleation/precipitation processes at the surface of the grains are the rate-limiting step. With $N > 1$, three-dimensional diffusion through a layer of reaction products is considered to be the rate-limiting step. A decreasing permeability of the interface layer induced by thickening or densification by reaction product precipitation would correspond with $N < 2$. In all studies a conspicuous increase in N was observed over the course of hydration, implying a decreasing permeability of the reaction product interface layer (Takemoto and Uchikawa 1980; Shi and Day 2000; Mertens et al. 2009). Cabrera and coworkers have successfully applied both the original Jander equation on metakaolin-$Ca(OH)_2$ systems (Cabrera and Rojas 2001) as well as the modification developed by Ginstling and Brounshtein (1950) to allow for the decreasing permeability of the interface layer on silica fume-$Ca(OH)_2$ and trass-$Ca(OH)_2$ systems. The Ginstling-Brounhstein equation is formulated as follows:

$$\left[1-\left(1-\alpha\right)^{1/3}\right]^2-\frac{2}{3}\left[1-\left(1-\alpha\right)^{1/3}\right]^3=Kt \tag{5}$$

Villar-Cociña et al. (2003) have applied a decreasing nucleus model to model the decrease in

electrical conductivity of a saturated $Ca(OH)_2$ solution upon the addition of a pozzolan. The model was used to determine diffusion coefficients of the interlayer and overall reaction rate constants to indicate the activity of the added pozzolans.

It should be noted that the fitting of the presented kinetic models can only give general information of the reaction mechanism and that the results should be interpreted cautiously. Variations in reaction product morphology, thickening or densification of the interface layer will influence the permeability and diffusion coefficient of the barrier layer. Additionally, obtained reaction rate constants should be considered as overall apparent values because the apparent rate constant will encompass a series of processes which are considered to be combined in a pseudo-first order reaction. Averaging occurs also over the reaction rates of inner and outer product formation. Additionally, finer fractions of a pozzolan will react more rapidly than the coarser ones and an overall value will be obtained.

Pozzolanic activity

The reaction rate during and the timing and duration of the described stages of the pozzolanic reaction are highly dependent on the intrinsic activity and characteristics of the pozzolan. Highly active pozzolans such as metakaolin will increase heat release during the initial dissolution period and significantly shorten the duration of the induction period (Massazza 2001). Additional to intrinsic pozzolan properties such as specific surface area, chemical composition or active phase content, the consumption of $Ca(OH)_2$ over time is also depending on external factors such as mix design and curing conditions.

Intrinsic pozzolan properties. It is generally accepted that a first-order relationship exists between the rate of dissolution and the total or reactive mineral surface area under far-from-equilibrium conditions (Brantley 2008). However, the determination of the specific surface area is not entirely straightforward. It can be measured by geometric calculations departing form the particle size distribution curve or by the BET N_2 adsorption technique. Both techniques have drawbacks. Geometric calculations demand the assumption of particle shapes and in the BET technique the internal particle porosity is often included (White and Brantley 2003). Both mineral dissolution and the initial stages of the pozzolanic reaction consist of processes taking place at the liquid-solid interface. Therefore, at least initially, a linear relationship is expected between the activity of a pozzolan and the available surface area for reaction. Correlations between the Blaine fineness or the BET specific surface of a specific pozzolan and its activity or even the evolution of compressive strength have been reported frequently for the early reaction period, varying in duration from 7 days up to 3 months (Ludwig and Schwiete 1963; Costa and Massazza 1974; Takemoto and Uchikawa 1980; Day and Shi 1994, Mertens et al. 2009). However, inconsistencies arise when the activity dependence on specific surface of materials of different origins are compared. The absence of a single encompassing relationship points to the fact that the pozzolanic activity is dependent on more factors. To illustrate the effect of particle shape and internal porosity, for similar particle size distributions or fineness the complex structure and highly porous nature of rice husk ash or diatomite constituents may result in very different activities compared to that of spherical non-porous fly ash particles.

To enhance the specific surface area and thus the activity of a pozzolan, grinding is a commonly used technique. Even materials which are commonly not regarded to behave pozzolanically, such as quartz, can become reactive when ground below a certain critical particle diameter (Benezet and Benhassaine 1999). The particle diameter or the curvature of the surface of a pozzolan particle also affects the surface energy or surface tension through the Gibbs-Thomson effect and results in a higher solubility of smaller particles (cf. Ostwald ripening) (Iler 1979).

Additional to increasing the total surface area, grinding also results in the creation of surface defects, i.e., sites experiencing lattice strain or sites partially disconnected from the underlying undisturbed material (Alexander 1960). The lowered activation energy of hydrolysis of the Si-

O_{br}-Si bonds at these sites has a definite positive effect on the pozzolanic activity. Activation of pozzolans by acid treatment results in an etched surface and the enhanced activity relies on a similar creation of abundant surface pits and steps. More generally, the bulk density of defects in a material exerts a significant influence on the activity of both minerals and vitreous materials (Shi 2001; Nair et al. 2008). Highly-crystalline materials showing very few linear or planar defects are generally observed to be much more stable in $Ca(OH)_2$ saturated solutions than amorphous materials with large concentrations of bulk and surface defects. This can be illustrated by the higher pozzolanic activity of metakaolin produced from paper sludge ash compared to regularly produced metakaolin of higher purity and larger specific surface area. The increased reactivity of the former was related to an increased concentration of surface defects (Péra and Amrouz 1998). Bich et al. (2009) characterized the presence of surface defects in kaolinite based on the asymmetry of the DTA peak of dehydroxylation. Thermally activated disordered kaolinite with many surface defects was shown to be more reactive than burned ordered kaolinite showing few defects. Activation of kaolinite by prolonged grinding was related to surface defect creation. This is illustrated by the disappearance of the DTA peak of dehydroxylation and the remarkable increase in weight loss over the lower temperature range of 100-500 °C in Figure 27, indicating the presence of disordered weakly bonded hydroxyl and water groups (Vizcayno et al. 2009).

In determining the pozzolanic and cementitious properties of SCMs also the mineralogical composition plays a prominent role. The proneness to reaction of the amorphous and crystalline phases is linked to their structural stability in an alkaline $Ca(OH)_2$ saturated solution. The effect of crystal structural properties on the mineral stability can be illustrated by variations in

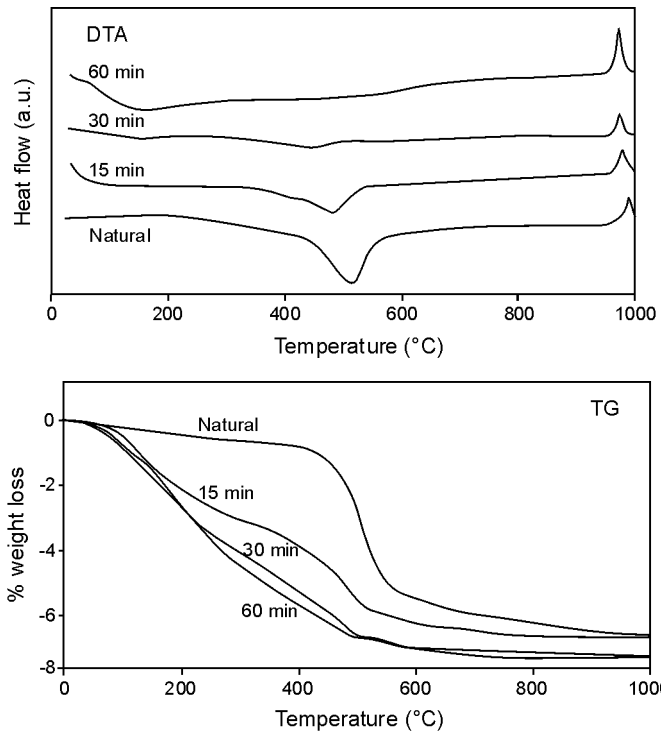

Figure 27. DTA (*top*) and TG (*bottom*) curves for natural kaolinite and kaolinite ground for 15, 30, and 60 min. in a Herzog-mill (modified after Vizcayno et al. 2009).

enthalpy of formation of pure-silica polymorph structures. Besides the naturally occurring silica polymorphs, α- and β-quartz, cristobalite, tridymite, coesite and stishovite, a large diversity of synthesized all-silica molecular sieves or zeolites exists and is used in industrial processes. Petrovic et al. (1993) and Piccione et al. (2000) experimentally determined the enthalpies of transition from the stable α-quartz structure to the metastable polymorph structures. The range of energies is quite narrow at only 6.8-14.4 kJ/mol SiO_2 above quartz, and a strong linear correlation between enthalpy and framework density (the number of tetrahedral framework atoms per nm³) was observed (Fig. 28). Both experimental and theoretical (Henson et al. 1994; Sastre and Corma 2006; Zwijnenburg et al. 2007) results indicate that for the pure silica polymorphs the quality of packing of the SiO_4 tetrahedra is the most important parameter controlling silica stability. Furthermore, the formation enthalpy of an amorphous silica glass was only 7 kJ/mol higher than quartz and lower by 0-7 kJ/mol than the zeolitic structures (Petrovic et al. 1993). On purely crystal structural grounds, this difference may serve as an explanation of the observed higher activity of natural zeolites compared to volcanic glass of similar composition and origin (Mortureux et al. 1980; Sersale 1980). The higher enthalpy of formation of less dense structures is expected to increase the difference in Gibbs energy between reactants and reaction products. Nevertheless, the effect of framework density on dissolution activation energy and thus on reaction kinetics remains unclear.

The situation becomes more complicated when typical SCMs consisting of several mixed oxide phases are considered. In general, the pozzolanic activity of minerals thermodynamically stable at ambient conditions is low when compared on an equal specific surface basis to less stable mineral assemblages. Volcanogenic deposits containing large amounts of volcanic glass or zeolites are more reactive than quartz sands or detrital clays. In this respect, the thermodynamic driving force behind the pozzolanic reaction may serve as a rough indicator of the potential reactivity of a specific crystalline or non-crystalline phase (Takemoto and Uchikawa 1980). Obviously, the content of active phases in a specific SCM is a factor of primary importance (Millet and Hommey 1974; Sersale 1993).

Many studies have suggested that a correlation exists between the long term performance in terms of compressive strength or durability and the bulk chemistry of the SCM without reference to the mineralogical composition (e.g., Watt and Thorne 1965; Costa and Massazza 1974;

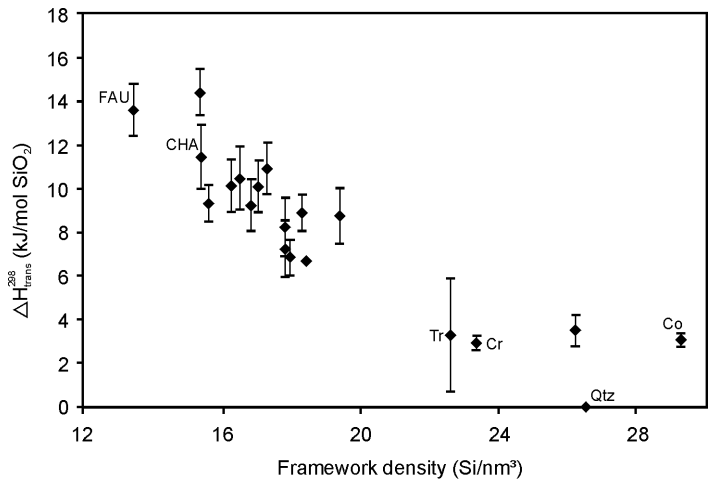

Figure 28. Experimental transition enthalpy from quartz compared to framework density of pure-silica polymorphs (Piccione et al. 2000). Qtz stands for quartz, Co for coesite, Cr for cristobalite, Tr for tridymite, CHA for chabazite and FAU for faujasite.

Hanna and Afify 1974; Cavdar and Yetgin 2006). The pozzolanic activities and blended cement or pozzolan-lime binder performance showed positive linear correlations of varying statistical significance with the sum of bulk SiO_2 and Al_2O_3, in some cases also Fe_2O_3 was added. The sum $SiO_2 + Al_2O_3 + Fe_2O_3 \geq 70$ wt% remains one of the fulfillment criteria for pozzolans in ASTM C618. In case of a one phase material the chemical composition can be considered as a meaningful parameter. However most natural and artificial SCMs consist of a heterogeneous mixture of phases and then a direct relationship between overall chemical composition and pozzolanic activity becomes less obvious. The fact that all correlations were reported for long term pozzolanic activity and/or performance indicates that the characteristics and the distribution of the reaction products should relate SCM chemistry and long term performance. The eventual, long term reaction product assemblage is controlled by the overall chemistry of the active phases (Massazza 2001). Addition of blast furnace slag or metakaolin has been observed to change the Ca/Si ratio, the silicate polymerization and the morphology of the main C-S-H reaction products and can thus alter the permeability of the reaction product barrier layer and the eventual performance of the binder (Richardson 1999, 2004). As the main reaction products are calcium-silicate-hydrates (with some Al incorporation) and calcium-aluminate-hydrates (containing additional Si and Fe), the total $SiO_2 + Al_2O_3 + Fe_2O_3$ content of the active phases may be considered as an indication of the $Ca(OH)_2$ binding potential of an SCM.

In practice, it is very difficult to separate the contributions to the SCM activity of physical particle characteristics and mineralogical properties. This is considered one of the primary reasons of contradictory findings in literature concerning the relative activities of SCM phases. Furthermore, because SCMs of comparable origin often show broad similarities in physical particle properties if not in mineralogical and chemical composition, the widespread adoption of the genetic classification scheme of SCMs can be considered to remain sensible.

External factors. The rate of the pozzolanic reaction also depends on the mix design, larger water/binder ratios will result in increased pozzolanic activity but will inevitably decrease the performance of the binder due to the increased overall porosity.

The ratio of SCM over $Ca(OH)_2$, or equivalently the ratio of SCM over Portland cement obviously affects the pozzolanic activity in increasing or decreasing the frequency of fulfillment of the reaction configuration. The $Ca(OH)_2$:pozzolan ratio for optimal performance and activity is depending on the overall content, composition and activity of the constituent phases of the SCM, but is usually situated in between 1:1 (Murat 1983; Bakolas et al. 2006) and 2:1 (Takemoto and Uchikawa 1980; Costa and Massazza 1974). Pozzolans rich in Al_2O_3 generally need higher $Ca(OH)_2$:SCM ratios for optimal reactivity, and SCMs displaying hydraulic activity usually need much less $Ca(OH)_2$ to activate the hydration reactions (Lang 2002). In terms of Portland cement over SCM ratio optimal replacement percentages are often defined based on the desired properties of the hardened cement. In general, the optimal replacement ratio depends on the water demand, i.e., surface roughness and specific surface, and the activity of the SCM. The higher the water demand and activity, the lower the optimal replacement ratio is, typically 10-15 wt% for silica fume or metakaolin. Optimal replacement ratios defined for durability properties tend to be somewhat higher than ratios for optimal strength performance. At excessive replacement levels the pozzolanic activity is lowered because of the premature depletion of the solution alkalinity by the reacting SCM. A significant drop in solution pH below 10 may not only effectuate a decrease in pozzolanic reaction rate, but can also lead to the destabilization of AFm and AFt reaction products in the blended cement (Lothenbach et al. 2011).

To increase the pozzolanic reaction rate, curing at elevated temperatures can be applied. The temperature dependence of the pozzolanic reaction on the short term can be described by the Arrhenius equation, implying an exponential dependence of the reaction rate on temperature (Snellings et al. 2009). The curing temperature should however not exceed the stability field of the C-S-H phase and result in the precipitation of more crystalline phases (typically above

80-100 °C; Taylor 1990). The acceleration induced by elevated curing temperatures is much more pronounced for the pozzolanic reaction compared to the hydration of Portland cement constituents due to the higher activation energy of the pozzolanic reaction (Shi and Day 1993).

Hydration mechanism and kinetics of blended cements

In blended Portland cements the hydration reactions of the clinker phases are complemented by the pozzolanic or hydraulic reactions of the added SCM. Although the hydration processes of the clinker phases follow different mechanisms and rates than the pozzolanic or hydraulic reactions of the SCM, the clinker hydration in blended cements is influenced by the presence of SCMs. Reaction kinetics, products and the properties of fresh and hardened pastes can be manipulated by the replacement of a fraction of the Portland cement by SCMs. Both the properties of the SCM as the mix design are determining factors with the potential to affect all stages of the hydration and pozzolanic reactions in the blended cement.

Influence of SCMs on the hydration of clinker phases. To eliminate the interference of simultaneously occurring reactions in a blended cement, the effect of SCM addition on the hydration kinetics of single clinker compounds has been investigated by numerous researchers. The hydration mechanisms of the individual clinker components have been recently reviewed by Gartner et al. (2002) and Bullard et al. (2011). Similar to the pozzolanic reaction mechanism, the hydration of C_3A in the presence of gypsum and the hydration of C_3S experience both a brief initial phase of high reactivity followed by a dormant period and an eventual main reaction stage.

C_3S. The main component of Portland cement is C_3S, constituting 60-70 wt% of the cement. In general, the addition of an SCM has an accelerating effect on the hydration of C_3S (Ogawa et al. 1980). The heat evolution rate during the main reaction period and the cumulative amount of heat released over the complete reaction are increased, especially when recalculated to the C_3S content in the samples (Massazza 2001). The effect of the SCM on the early reaction is mainly governed by its fineness, as illustrated in Figure 29. The initial dissolution period is

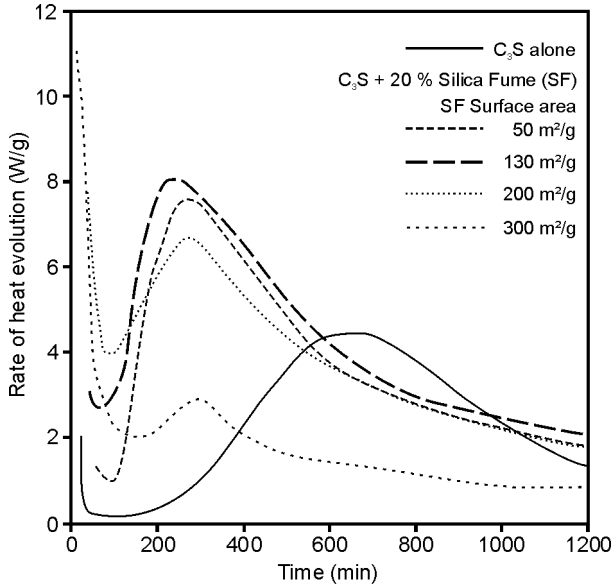

Figure 29. The effect of the silica fume specific surface area on the heat evolution rate curves in hydrating pastes of C_3S with 20 wt% silica fume (Beedle et al. 1989).

lengthened and the induction stage shortened, when SCMs of increasing fineness are introduced (Stein and Stevels 1964; Kurdowski and Nocun-Wczelik 1983; Beedle et al. 1989; Korpa et al. 2008). This phenomenon is usually termed the filler effect. The addition of extremely fine particles results however in a decreased hydration rate because the high water demand of the particles limits the amount of water that can participate in the hydration and pozzolanic reactions (Beedle et al. 1989; Korpa et al. 2008). SCMs with low specific surface area such as certain fly ashes have been observed to lengthen the induction period, but increase the cumulative heat released during the main reaction stage (Watt and Thorne 1965, 1966). This dependence on the SCM specific surface has been attributed to Ca^{2+} adsorption and C-S-H nucleation at the SCM surface. In consequence, the layer of reaction products on the C_3S particles would be thinner and C_3S dissolution would thus last longer (Wu and Young 1984). In addition, the lowered Ca^{2+} and hydroxyl concentrations at the C_3S surface may accelerate the conversion of an initially precipitated impermeable metastable C-S-H(m) to a more stable and permeable C-S-H form (Stein and Stevels 1964). Eventually $Ca(OH)_2$ formed as a result of the C_3S hydration, will be partially or completely consumed by the pozzolanic reaction.

C_3A. The hydration of C_3A in the presence of gypsum is an important regulator of the setting of the blended cement. Contrary to the effect of SCMs on C_3S hydration, the heat evolution rate of the main C_3A hydration stage is lowered in the presence of SCMs (Collepardi et al 1978; Uchikawa and Uchida 1980). The reasons underlying the decreased C_3A hydration rate remain unclear. A correlation seems to exist with the SCM specific surface; the higher the specific surface, the lower the hydration rate (Collepardi et al. 1978). Other factors could be the alteration of solution composition by SCM addition, the adsorption of sulfate at the pozzolan surface or the altered hydration product assemblage.

Blended cements. The hydration behavior of blended cements is dominated by the hydration of its main component. In the case of pozzolan containing blended cements, C_3S is the most prominent constituent. In cements consisting of a large fraction (50-90 wt%) of a hydraulic SCM, e.g., granulated blast furnace slag, the long term behavior is governed by the hydration of the SCM. In consequence, for pozzolanic SCMs, the early hydration behavior is mainly affected by the specific surface of the SCM. On the condition that sufficient water remains available for hydration, an increase in specific surface results in an accelerated cement hydration, lengthened early dissolution stage and shortened induction period (Takemoto and Uchikawa 1980). To the contrary, slag dominated cements are known to hydrate more slowly and expel less heat than Portland cement and are therefore suitable for applications in mass concrete structures such as dams, reservoir, quays etc. (Lang 2002). However, when recalculated to the actual clinker content, the heat liberated by the slag-cement over a longer time period is higher than that released by the Portland cement (Hooton and Emery 1983). Obviously, the added SCMs consume $Ca(OH)_2$ released by clinker hydration to form supplementary cementitious reaction products. In addition the reaction product composition, structure, morphology and in some cases also the assemblages are considerably changed.

REACTION PRODUCTS

Compared to the wide variability in supplementary cementitious materials, there exists only a relatively small range of compounds formed in the pozzolanic, hydraulic or hydration reactions. This is mainly due to the similarity in overall chemical composition of the hydrating mixtures of pozzolans and lime or blended cements, regardless of the type of SCM. In consequence, only a limited number of phases will be thermodynamically stable or metastable at ambient conditions. This observation enabled the application of thermodynamic models to calculate the ultimate hydrate mineralogy from chemistry by Lothenbach and coworkers (e.g., Lothenbach and Winnefeld 2006; Matschei et al. 2007b). Combined with quantitative kinetic

data or models on reactant consumption or product formation, thermodynamic calculations have also been used to study evolving hydration processes (e.g., Lothenbach et al. 2007, 2008a; Winnefeld and Lothenbach 2010). Although kinetic barriers may impede the attainment of ultimate thermodynamic equilibrium, or formation of products may not conform to the predicted assemblage due to locally prevailing chemical conditions. The thermodynamic approach has shown to be successful in predicting the behavior of many product assemblages in function of variable pH, sulfate, carbonate or temperature conditions (e.g., Lothenbach and Gruskovnjak 2007; Pelletier et al. 2010; Matschei and Glasser 2010). Hence, reported observations on product assemblages of the pozzolan-lime reaction or the hydration of blended cements may be compared at least in a qualitative way with thermodynamic predictions.

Product assemblages

The chemical composition of the mix, more specifically the amount and composition of the pozzolanically or hydraulically active phases together with the pozzolan - lime or pozzolan - Portland cement ratio are primary factors in the determination of the reaction product assemblage. In addition, the presence of soluble sulfate, carbonate or chloride may provoke the formation of AFt and AFm phases incorporating the corresponding anion groups (Matschei et al. 2007c; Balonis et al. 2010). Curing conditions are equally important, partial CO_2 pressure and curing temperature may affect the product assemblage considerably (Lothenbach et al. 2008a). Evolving reaction conditions, e.g., the depletion of $Ca(OH)_2$ by the pozzolanic reaction or decreasing released heat of hydration, may result in changes in the product assemblage during ageing.

Pozzolan-lime reaction products. In $Ca(OH)_2$ saturated solutions silica released from the pozzolan in combination with Ca^{2+} primarily forms C-S-H. Dissolved alumina can be incorporated into the C-S-H phase (Richardson et al. 1993) or can be precipitated in combination with Ca^{2+} as calcium-aluminate-hydrates. The Ca/Si ratio of the C-S-H phase is variable both in space as in time and also depends on the activity and composition of the pozzolan and the mix design. Increasing polymerization of the silicate groups in the C-S-H is observed upon prolonged curing—the silicate monomer and dimer contents decrease while the polymer content increases (Massazza and Testolin 1983; Brough et al. 1995).

In the absence of sulfate, carbonate or chlorides $C_4AH_{13\text{-}19}$ forms as main calcium aluminate hydrate (Taylor 1990). If general or local deficiency of $Ca(OH)_2$ occurs, often encountered when metakaolin is added as SCM, the recombination of alumina and silica with Ca^{2+} to form strätlingite (hydrated gehlenite), C_2ASH_8, can be observed (Serry et al. 1984; Ambroise et al. 1994). Strätlingite allows structural substitution of Na^+ and K^+ for Ca^{2+} (Jones 2002). At later stages of reaction, higher water/solid ratio or in the presence of abundant alkalis, hydrogarnet or katoite, C_3AH_6, is stabilized (Takemoto and Uchikawa 1980; Serry et al. 1984; Sersale 1993). Hydrogarnet can incorporate Si in a solid solution series between katoite $Ca_3Al_2(OH)_{12}$ and grossularite $Ca_3Al_2Si_3O_{12}$. In metakaolin-lime pastes the formation of hydrogarnet is mostly observed at elevated curing temperatures above 40 °C (De Silva and Glasser 1992). Although C_4AH_{13} and strätlingite are considered to be thermodynamically unstable towards hydrogarnet and $Ca(OH)_2$, no evidence of the transformation of strätlingite and C_4AH_{13} to hydrogarnet was observed to occur at 60 °C (Rojas and Cabrera 2002; Rojas 2006). At temperatures below 40 °C, typically only traces of hydrogarnet can be observed. Hydrogarnet forms very slowly at low temperatures, probably due to kinetic reasons (Takemoto and Uchikawa 1980; Massazza 2001). C_4AH_{13} can possibly be stabilized by the incorporation of small amounts of carbonate or sulfate (Pöllmann 2006).

SCMs containing soluble sulfate such as fly ashes or blast furnace slags will react with $Ca(OH)_2$ to form ettringite, $C_6A\bar{S}_3H_{32}$, or monosulfoaluminate (kuzelite), $C_4A\bar{S}H_{12}$, or a combination of both depending on the sulfate over alumina ratio (Mortureux et al. 1980). A

limited solid solution of sulfate into C_4AH_{13} up to SO_4/2OH of 0.5 was observed at 25 °C (Matschei et al. 2007c). Addition of Na_2SO_4 accelerates the pozzolanic reaction. Removal of dissolved sulfate by ettringite precipitation is compensated by an increase in hydroxide concentration and pH to maintain electroneutrality (Shi and Day 2000). Ettringite initially formed transforms partially or completely into kuzelite when all soluble sulfate is consumed. If excess alumina is present also other hexagonal calcium aluminate hydrates or hydrogarnet may be encountered (De Silva and Glasser 1992). The considerable amount of MgO present in blast furnace slags can also give rise to hydrotalcite-type phases with an ideal composition of $Mg_4Al_2(OH)_{14}{\cdot}3H_2O$ but allowing extensive cationic and anionic substitution. Virtually no Mg^{2+} was observed to enter the C-S-H phase (Richardson et al. 1994; Richardson and Groves 1997). Upon exposure to air or in binders with very low carbonate contents, carbonation of the C_4AH_{13} to hemicarboaluminate, $C_4A\overline{C}_{0.5}H_{12}$, will occur. More extensive carbonation due to prolonged exposure or due to substantial amounts of carbonates such as calcite present in the binder results in the formation of monocarboaluminate, $C_4A\overline{C}H_{11}$ (Matschei et al. 2007c). In Figure 30 the phase assemblages of the AFm-type structure are presented in a ternary diagram with at the apices OH-AFm (C_4AH_{13}), SO_4-AFm (kuzelite) and CO_3-AFm (monocarboaluminate).

Except from the limited solid solution between C_4AH_{13} and kuzelite, the end members behave as separate phases from a mineralogical point of view. The carbonation of C_4AH_{13} prevents the conversion of ettringite into kuzelite (Kuzel 1996), therefore at high levels of carbonation often ettringite can be found, while at low levels kuzelite is present (Massazza and Daimon 1992; Atkins et al. 1993). In the presence of calcite and at temperatures below 20 °C, also ettringite was observed to show substantial solid solution between the ideal SO_4-ettringite and the CO_3-ettringite end members (Barnett et al. 2001).

Blended cement reaction products. The reaction product assemblages formed in the hydration of blended cements are similar to the compounds formed in the reaction between SCMs

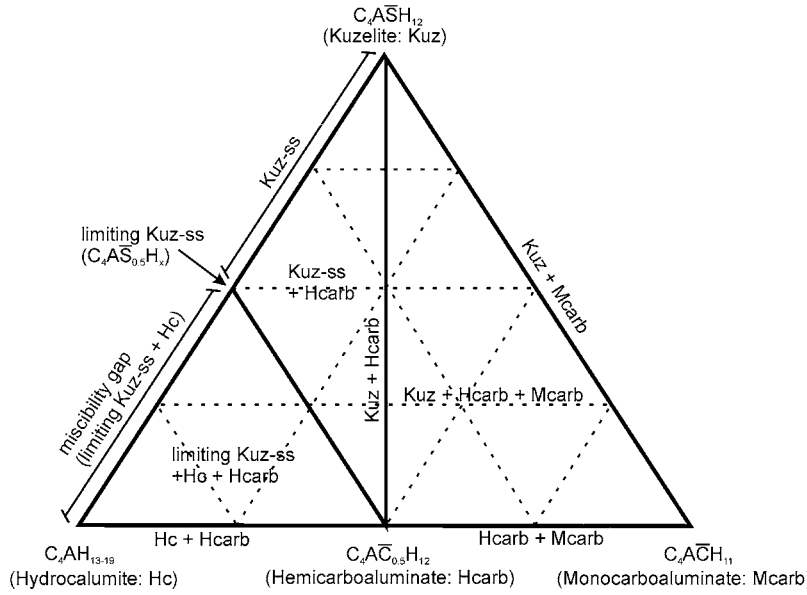

Figure 30. Calculated phase assemblage between different AFm phases at 25 °C. A possible range of stoichiometry of hemicarboaluminate and the limited formation of ternary solid solutions are not shown (Pöllmann 2006) (modified after Matschei et al. 2007c).

and lime. The underlying reason is that in most cases the overall bulk chemical composition of the binders are comparable, with the exception that Portland cement usually contains calcium sulfates and commonly incorporates some carbonate from adsorption of atmospheric CO_2 or interblending with a limited amount of limestone. Compared to the hydration product assemblage of ordinary Portland cement, SCM addition mostly results in a variation in the relative proportions of the reaction products. At ambient conditions the hydration products in blended cements commonly comprise C-(A)-S-H and AFm-type phases, ettringite and when substantial MgO is available, hydrotalcite-type phases. The $Ca(OH)_2$ content depends mainly on the blending ratio of SCM over Portland cement and the composition and activity of the SCM (Massazza 2001). When all $Ca(OH)_2$ is consumed in the pozzolanic reaction, strätlingite may develop.

The C-S-H phase in blended cements usually displays Ca/Si ratios in the range of lower than 1 to 1.8, i.e., lower than the observed C-S-H Ca/Si range in ordinary Portland cement of 1.2 to 2.1 (Richardson 1999). This is generally accepted to be due to the larger availability of Si and Al originating from the dissolving SCMs (Richardson 2008). Conjointly the mean (alumino)silicate chain length is increased from values between 2 to 5 in respectively young and mature PC pastes to 10 or more in some blended cements (Richardson 1999). The extent to which mean chain lengths are affected depends on the activity and composition of the SCM and the curing conditions. The C-S-H phase nanostructure in blended cements is considered to be most compatible with a defect-tobermorite structure, rather than a jennite-based structure (Cong and Kirkpatrick 1996a, 1996b; Richardson 2004). Tetrahedral substituent ions such as Al^{3+} can be incorporated into C-S-H only in the bridging tetrahedron (Richardson and Groves 1993; Andersen et al. 2006). Sorption or incorporation of alkali and sulfate ions at the C-(A)-S-H surface is related to its Ca/Si ratio and Al content. Alkali sorption increases with decreasing Ca/Si ratio and increasing Al content (Hong and Glasser 1999), while sulfate adsorption decreases with decreasing Ca/Si (Matschei et al. 2007b). In addition to sorption behavior, also the morphology of the C-S-H phase is dependent on its composition (Richardson 2004). As Ca/Si decreases and Al/Ca increases in C-A-S-H in GGBFS and MK blended cements a transition occurs from fibrillar, thin particles to sheet-like two-dimensional foils (Richardson and Groves 1997; Richardson 1999).

Due to the presence of easily soluble calcium sulfates, ettringite is able to form in the initial hydration stages. At more advanced stages of hydration ettringite can be partially or completely transformed to kuzelite. This transformation is obviously controlled by the overall bulk SO_3/Al_2O_3 ratio, but also, as mentioned before, by the CO_2/Al_2O_3 ratio. Calculated phase assemblage variations in function of changing sulfate and carbonate levels as expected to occur in Portland cement hydrated at 25 °C are given in Figure 31. At low carbonate and sulfate levels hydrogarnet was calculated to be present in the product assemblage, at higher carbonate and sulfate levels hydrogarnet is destabilized (Matschei and Glasser 2010). In blended cements, strätlingite can be encountered when $Ca(OH)_2$ is not present and SO_3/Al_2O_3 is low (Grutzeck et al. 1981).

Hydration thermodynamics

The recent development of a comprehensive and internally consistent thermodynamic database for cement hydrate compounds allows clarifying and eventually predicting the response of product assemblages on compositional changes of the binder (Matschei et al. 2007b). To illustrate the ultimate binder mineralogy, the product assemblages in the ternary CaO-SiO_2-Al_2O_3 system at 25 °C and water over solid ratio of 1:1 were explored following the methodology outlined by Lothenbach and Winnefeld (2006) based on a Gibbs energy minimization. For illustration, two different cases were considered. In one case calcium sulfates were absent, in the other 5 wt% of gypsum was added to the system. To visualize the phase relationships between the hexagonal hydrates and the C-S-H, the precipitation of the hydrogarnet solid solution series

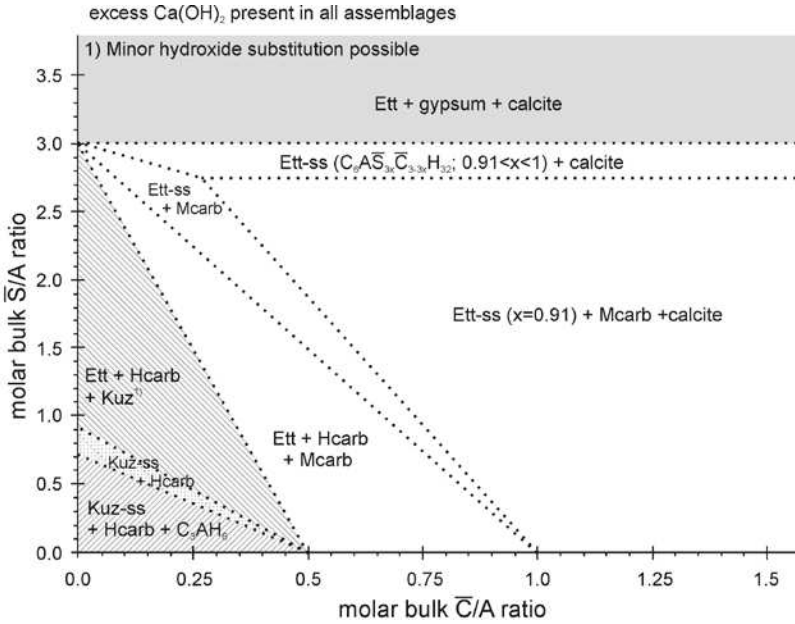

Figure 31. Calculated phase assemblage of a hydrated mixture consisting of C_3A, $Ca(OH)_2$ and varying initial sulfate and carbonate ratios at 25 °C (modified after Matschei and Glasser 2010).

needed to be suppressed. Ideal solid solution between C-S-H of tobermorite type (Ca/Si = 0.83) and jennite (Ca/Si = 1.6) was assumed. No incorporation of Al into C-S-H was accounted for. Obviously, this model is a simplification and serves mainly to highlight the expected changes in product assemblages. Incorporation of sulfate, carbonate, chloride, alkali or magnesium or iron compounds would definitely alter the nature and extent of the product stability fields.

CaO-SiO_2-Al_2O_3. Upon inspection of the ternary diagram in Figure 32, the phases containing silica are C-S-H and strätlingite. Alumina is distributed over the C_4AH_{13} and strätlingite phases. C-S-H is the most stable phase at low Ca levels and excess silica and alumina can be considered as unreacted SCM material. Increasing the Ca content from the field where C-S-H is the sole reaction product, a tieline is crossed connecting C-S-H of tobermorite composition (Ca/Si = 0.83) with the Al_2O_3 apex. In the corresponding field the C/S ratio of the mix is sufficiently high to allow the precipitation of strätlingite in the presence of alumina. When augmenting the Ca proportion eventually excess alumina will combine with Ca to form C_4AH_{13}, in addition strätlingite will start decomposing into C-S-H and C_4AH_{13}. Finally, at high Ca levels strätlingite disappears and the ultimate product assemblage is predicted to consist of C-S-H, C_4AH_{13} and excess $Ca(OH)_2$. In the rare case that alumina is prevalent over silica and sufficient Ca is available, C-S-H is destabilized in favor of strätlingite, C_4AH_{13} and excess alumina.

The presented ternary diagram confirms the observed incompatibility of $Ca(OH)_2$ and strätlingite. Takemoto and Uchikawa (1980) indicated that the Ca^{2+} concentration needed for the precipitation of C-A-H phases is in general higher than for C-S-H phases, possibly explaining why C-A-H phases can usually be found outside the C-S-H layer enveloping the reacting SCM or clinker particles.

CaO-SiO_2-Al_2O_3-SO_4. In the presence of sulfate the topology of the ternary diagram remains essentially unchanged (Fig. 33), only ettringite and kuzelite are stabilized over C_4AH_{13}. In the presence of C_4AH_{13}, a solid-solution member of the kuzelite-C_4AH_{13} series

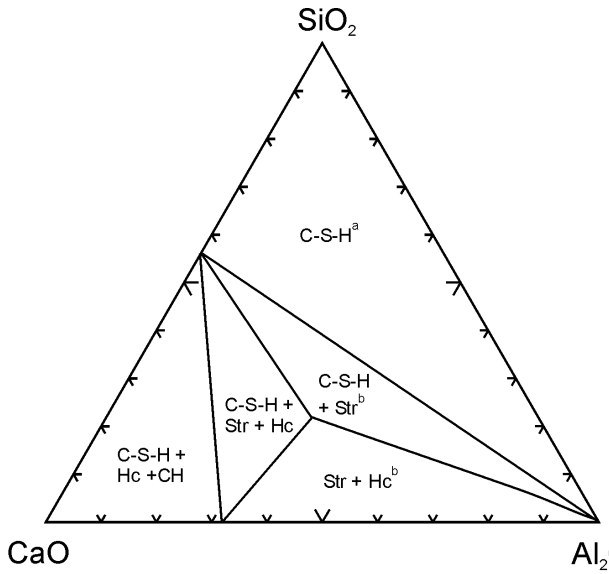

Figure 32. Reaction product assemblages in the CaO-SiO_2-Al_2O_3 ternary system (wt% based) at 25 °C and w/s ratio of 1:1. Str stands for strätlingite, Hc for C_4AH_{13}, CH and C-S-H are cement shorthand for $Ca(OH)_2$ and calcium-silicate-hydrates. In a) excess silica and alumina is present respectively as quartz and gibbsite, in b) excess alumina is present as gibbsite.

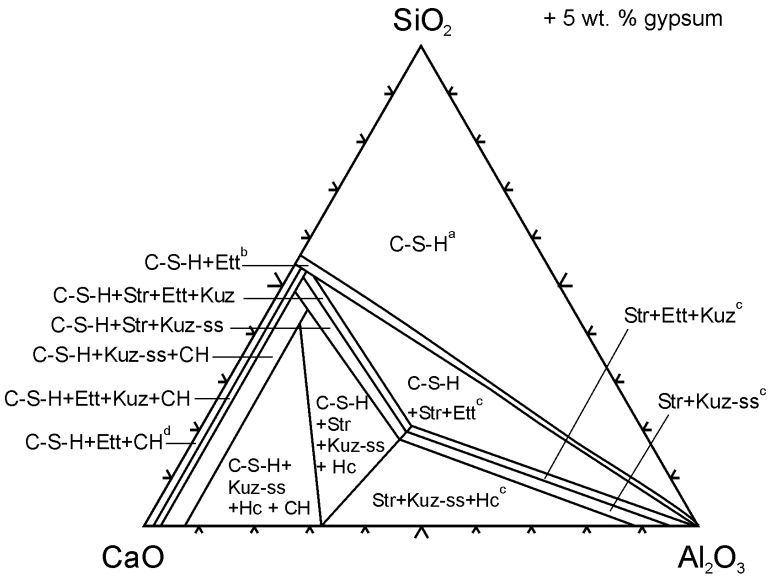

Figure 33. Reaction product assemblages in the CaO-SiO_2-Al_2O_3 ternary system (wt% based) at 25 °C and w/s ratio of 1:1, 5 wt% gypsum was added to the system. Str stands for strätlingite, Hc for C_4AH_{13} and Ett for ettringite. Kuz corresponds with kuzelite and Kuz-ss with a solid solution member of the kuzelite-C_4AH_{13} solid solution series. CH and C-S-H are cement shorthand for $Ca(OH)_2$ and calcium-silicate-hydrates. In a) excess silica, alumina and gypsum are present, in b) excess alumina and gypsum, in c) excess alumina and d) excess gypsum.

is predicted to be present. Strätlingite is predicted to precipitate in the absence of $Ca(OH)_2$. Higher CaO/SO_3 and Al_2O_3/SO_3 favor the formation of kuzelite over ettringite as corroborated by Figure 31.

In general, at higher curing temperatures denser and more heterogeneously distributed hydrates are formed resulting in a coarser porosity (Kjellsen et al. 1991). Above 50 °C kuzelite is increasingly stabilized over ettringite and monocarboaluminate (Thomas et al. 2003; Christensen et al. 2004; Lothenbach et al. 2008b). The product assemblage formed in concrete cured at elevated temperature may thus change when temperatures are lowered under service. The stabilization of ettringite over kuzelite at lower temperatures may thus be a primary cause of delayed ettringite formation and the associated concrete deterioration (Famy et al. 2002). Matschei and Glasser (2010) reported that above 25 °C kuzelite formation is favored over C_4AH_{13} or a solid solution member of the kuzelite-C_4AH_{13} series.

One of the benefits of thermodynamic calculations of the hydration processes is the prediction of the volume of solids present in the cement. Coupled with kinetic data on the consumption of reactants an evolving picture of the hydrate assemblage in a binder can be established. Assuming that the total volume of the binder paste remains constant, the increase in volume of the solid phases due to the formation of hydrated compounds allows evaluation of the total porosity of the system (Lothenbach et al. 2008a). Properties known to be roughly correlated with total porosity such as compressive strength or permeability can as such be estimated. The calculated solid phase evolution of a hydrating slag-silica fume cement as displayed in Figure 34 was shown to correspond well with experimental observations on the product assemblage (Lothenbach et al. 2009).

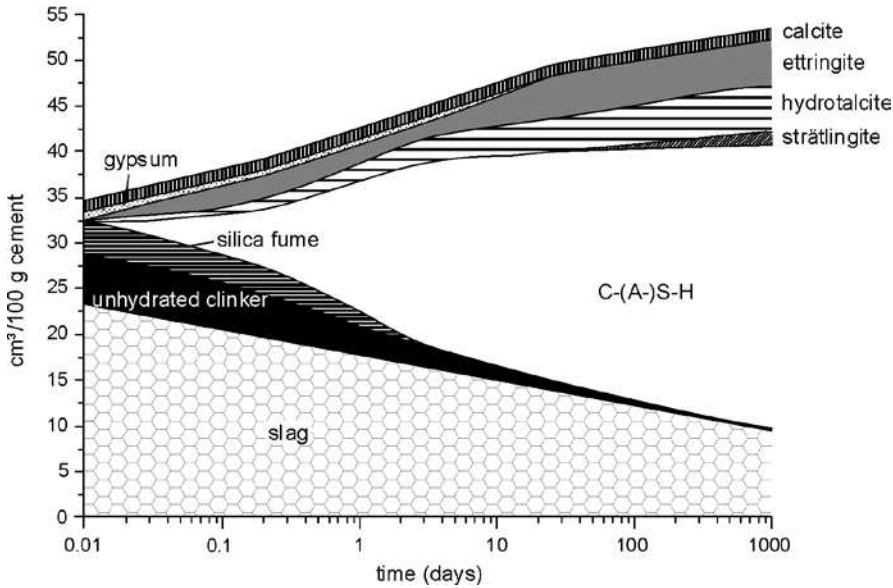

Figure 34. Modeled volume changes (cm³/100 g of unhydrated binder) during the hydration of low alkali blended cement containing 66.6% ground granulated blast furnace slag, 10% of silica fume and less than 23.3% of Portland cement (Lothenbach et al. 2009).

PROPERTIES OF MORTAR AND CONCRETE CONTAINING SUPPLEMENTARY CEMENTITIOUS MATERIALS

The physical bulk properties of SCM blended lime or cement binders depend both on mix design and curing conditions and on the inherent characteristics of the SCM. Therefore, the literature on performance shows a myriad of studies evaluating the effect of one or more of these factors. Variations in the inherent SCM characteristics often preclude direct comparisons between different studies, but some general trends can be observed. The emerging view is that the utilization of SCMs is regarded as beneficial in terms of performance, durability and sustainability. Instead of going into detail on these aspects for all separate SCMs, this section rather presents a brief generic overview of the effect of SCM addition on lime and Portland cement binders illustrated by specific examples. More comprehensive reviews centered on the effect of addition of different SCMs on the performance and durability of SCM-lime or SCM blended cements binders can be found in Malhotra and Mehta (1996), Hewlett (2001), Bensted and Barnes (2002) and Siddique (2008).

Properties of uncured mortar and concrete containing SCMs

The properties of the freshly mixed and early cured mortar and concrete are important because they can exert a significant control on the ultimate performance and durability of the binder. In this respect the particle characteristics and the initial reactivity of SCMs can influence the water demand and setting time of the mortar or concrete. This is for instance of importance when low water/binder ratios are needed in the preparation of high-performance concrete and the use of superplasticizers becomes necessary.

Water demand. The effect of SCMs on the amount of water needed for the binder to reach a specified workability or fluidity is largely depending on the particle characteristics of the SCM and its proportion in the mortar or concrete. Both the particle size distribution and the particle shape and porosity determine the specific surface and fineness of the SCM. In general, the higher the fineness or specific surface area and the more irregular the particle shape of SCM, the higher the water requirement of the blended binder is. SCMs such as silica fume, metakaolin or diatomite earths that show large specific surface areas typically increase the water demand substantially. Obviously, the higher the proportion of fine SCM particles added to the mix, the higher the water demand as illustrated in Table 4 for metakaolin blended cements (Badogiannis et al. 2005). To the contrary, the spherical particles and relatively low specific surface area encountered in fly ashes may result in lowered water requirements. Since the water/binder ratio is directly related to the binder porosity, increased binder water requirement commonly results in lowered strength performance and vice versa. Especially at higher replacement levels it may thus be essential to introduce superplasticizers to reduce the water/binder ratio.

Setting time. SCMs can both increase and decrease the setting in blended cements. The end of setting is generally conceived to be related to the end of the induction period and the start of hardening due to C-S-H reaction product formation. In this respect the acceleration of alite hydration can decrease setting times in blended cements. However, this acceleration effect is neutralized when at higher cement replacement ratios the overall content in clinker hydration products is lowered due to the dilution effect of the SCM. Also increased water requirements at higher replacement ratios may extend the setting time. In metakaolin blended cement the initial and final setting times at low replacement ratios and low water demand were observed to be slightly reduced, while at higher replacement ratios and water demand the rate of setting was slowed down (Table 4, Badogiannis et al. 2005).

Heat evolution. The heat evolved during hydration of blended cements strongly depends on the early reactivity of SCMs. Highly reactive SCMs such as silica fume or metakaolin increase the heat released during the initial dissolution period and the subsequent main hydration period (cf. Fig. 21). This has been attributed in part to the acceleration of clinker hydration and in part

Table 4. Variation of water demand and initial and final setting times for cements blended with metakaolin from differing sources. MK identifies with metakaolin in the sample index, followed by the respective replacement percentages of 10 or 20 wt% (Badogiannis et al. 2005).

Sample	Metakaolin (wt%)	Water demand (water/solid)	Setting time (min)	
			Initial	Final
PC	–	27.5	105	140
MK1-10	10	29	75	130
MK2-10	10	29	85	130
MK3-10	10	32	105	160
MK4-10	10	32.5	155	180
MKC-10	10	31	95	130
MK1-20	20	32	105	160
MK2-20	20	31.5	110	165
MK3-20	20	38.5	120	160
MK4-20	20	41	205	230
MKC-20	20	37.5	140	170

to the extensive formation of supplementary products of the pozzolanic reaction. However, most SCMs of lower activity can be effectively used to reduce the hydration heat in large structures. The combined effect of clinker dilution and a more sluggish pozzolanic reaction lowers the maximum temperature reached and minimizes the risk of cracking as exemplified in Figure 35 for ground granulated blast furnace slag cement.

Properties of hardened mortar and concrete containing SCMs

The properties of hardened SCM blended binders are strongly related to the development of the binder microstructure, i.e., to the distribution, type, shape and dimensions of both reaction products and pores. The general beneficial effects of SCM addition in terms of both strength performance and durability are mostly attributed to the pozzolanic reaction in which $Ca(OH)_2$ is consumed to produce additional C-S-H and C-A-H reaction products. The formation of

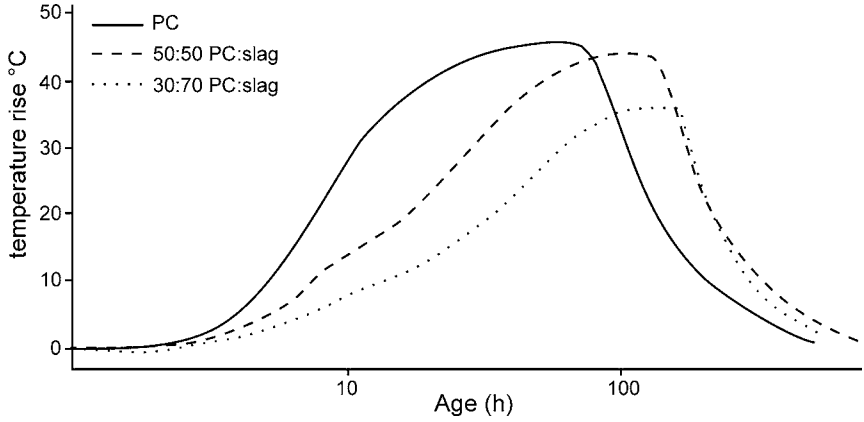

Figure 35. Influence of ground granulated blast furnace slag replacement ratio on adiabatic temperature rise (modified after Wainwright and Tolloczko 1986). PC stands for Portland cement. PC stands for Portland cement.

pozzolanic reaction products results in infilling of interstitial porosity and a refining of the pore size distribution or pore structure.

Pore structure. The pore structure is one of the most important factors governing the durability in terms of attack by aggressive agents such as CO_2, sulfates and chlorides (Luke 2002). It is generally observed that the addition of SCMs results in an increase of total porosity, but a consistent decrease in mean pore sizes. Capillary porosity, larger than 30-40 nm, is generally reduced and "gel porosity" increased, the latter being smaller than 10 nm and related to the typical distances between C-S-H particles (Takemoto and Uchikawa 1980). This can be explained by the infilling of coarse and capillary pores by C-S-H phases. In Table 5 the total pore volume and volume of pores smaller than 20 μm are compared for ordinary Portland cement and Portland cement blended with metakaolin. An overall increase of both pore volume and proportion of fine pores can be observed. Also the threshold pore radius, the radius below which the porosity sharply increases, is lowered considerably (Fig. 36) (Khatib and Wild 1996). The refinement of the pore structure generally results in lowered permeability and ionic diffusion coefficients, thus effectively improving the durability of the binder.

Moreover, the coarse and capillary porosity have been observed to be closely correlated with the compressive strength, increasing porosities leading to decreased binder strength

Table 5. The effect of blending Portland cement with metakaolin on the pore volume and proportion of small pores in a blended cement (Khatib and Wild 1996).

	Pore volume (mm^3/g)				% of fine pores (radii < 20 μm)			
	Metakaolin (%)				Metakaolin (%)			
Age (days)	0	5	10	15	0	5	10	15
3	262	257.6	284.1	277.6	22.2	28.3	31	39.9
7	229.6	261.7	268.8	251.6	26.5	32.1	41	50.4
14	209.9	203.4	221	212.1	30.3	43	53.9	55.7
28	189.1	205.3	237.1	222.7	33.7	43.5	48.7	54.9
90	181.4	180.8	219.6	198.9	37.3	44.7	49.9	57.6

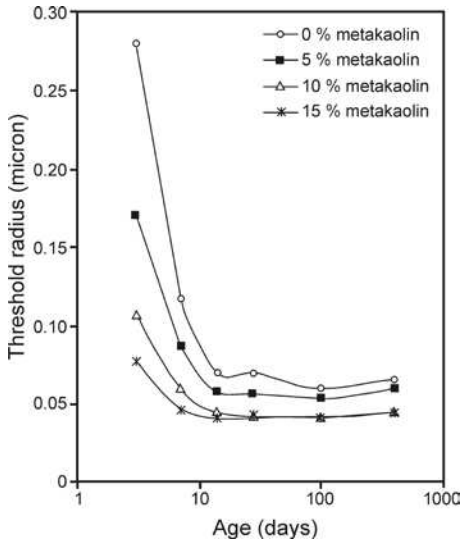

Figure 36. The introduction of metakaolin reduces the threshold pore radius significantly. The threshold radius is the pore radius below which the porosity sharply increases (Khatib and Wild 1996).

(Takemoto and Uchikawa 1980; Papayianni and Stefanidou 2006). The improvement of the cement microstructure is also visible at the interface zone between aggregate and binder in mortars and concrete. The interface zone in ordinary Portland cement is a region of low C-S-H and high ettringite and $Ca(OH)_2$ concentrations between 25 and 100 μm in thickness with decreased microhardness. In blended cements both the amount of $Ca(OH)_2$ and its preferential orientation is reduced (Larbi and Bijen 1990). Instead additional C-S-H replaces $Ca(OH)_2$, fills porosity and reduces the thickness of the interface zone (Shannag 2000). The microhardness of the interface zone is increased (Asbridge et al. 2002) and the adhesion between binder and aggregate improved.

Strength. The water/binder ratio is a factor of primary importance in governing strength development and ultimate strength of both SCM-lime and SCM-Portland cement based binders. As mentioned earlier, a close relationship exists between water/binder ratio and binder porosity on the one hand and binder porosity and strength on the other hand. The high water demand of very fine pozzolans such as silica fume may necessitate the use of water-reducing agents to lower the water requirement of the blend and improve the eventual binder strength.

Strength development in SCM-lime binders depends on the one hand on the mix design, the SCM/lime and water/binder ratio, and the curing conditions, elevated temperature curing increases the rate of strength development but often lowers final strength, and on the other hand on the SCM reactivity. The latter can widely differ from SCM-type to SCM-type as exemplified in Figure 37 (Shi and Day 1995), depending on the particle characteristics, active phase content and chemical and mineralogical composition of the SCM. The ultimate strength of SCM-lime binders may exceed 20 MPa, which is high enough to serve for many common applications (Massazza 2002).

In blended cement pastes, mortars and concrete the result of SCM incorporation on the development of strength is conceived to be controlled by the dilution effect, the filler effect, the hydration acceleration effect and the pozzolanic or hydraulic reaction. The first three

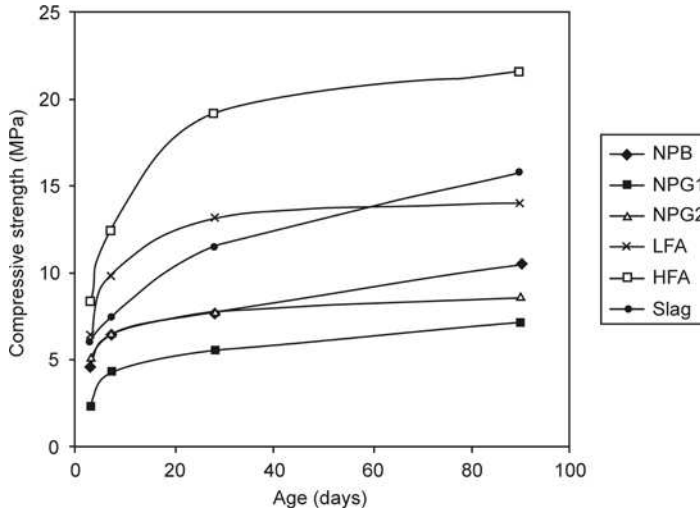

Figure 37. Compressive strength development of blends of lime (20%) and a variety of SCMs (80%). SCMs with hydraulic properties develop the highest strengths over time (Shi and Day 1995). NPB stands for natural vitreous pozzolan from Bolivia, NPG for natural vitreous pozzolan from Guatemala, LFA for low-lime fly ash, HFA for high-lime fly ash, the slag used was a typical ground granulated blast furnace slag.

factors have similar effects as an inert filler and dominate the initial strength development. The contribution of the pozzolanic or hydraulic reactions to cement strength is usually developed in a later curing stage, depending on the SCM reactivity. In the large majority of blended cements initial lower strengths can be observed compared to the parent Portland cement. However, especially in the case of SCMs of higher fineness than the Portland cement, the decrease in early strength is usually less than what can be expected based on the dilution factor. This can be explained on the one hand by the contribution of the filler effect, in which small SCM grains fill in the interstitial space between the cement particles, resulting in a much denser binder matrix. On the other hand, the acceleration of the clinker hydration reactions (cf. Fig. 29) can also at least partially accommodate the loss of early strength.

At later curing ages blended cements typically show a higher rate of strength development due to the supplementary formation of products of the pozzolanic or hydraulic reactions. Depending on the mix design and the SCM activity, in many cases the ultimate strength can become higher than that of the parent Portland cement as illustrated in Figure 38 for ground granulated slag cement. The rate of the pozzolanic and hydraulic reactions principally determines the moment when the blended cement strength exceeds the parent Portland cement strength. Highly reactive SCMs such as metakaolin or silica fume were observed to enhance even early strengths within one day (Sabir et al. 2001), while slags of much lower reactivity typically present positive strength contributions only after 14 to 28 days of curing (Lang 2002). It should be noted that because hydrated ordinary Portland cement only contains about 20 wt% of $Ca(OH)_2$, at high cement replacement percentages of 40% or more by pozzolans, strength development may be hampered because of a general lack of $Ca(OH)_2$ (e.g., Yilmaz et al. 2007).

Durability of mortar and concrete containing SCMs

One of the main advantages of SCMs, and one of the early incentives to introduce SCMs into blended cements, is the significantly increased chemical resistance of the binder to the ingress and deleterious action of aggressive solutions. The improved durability of SCM-blended binders enables to lengthen the service life of structures and reduces the costly and inconvenient need to replace deteriorated constructions. In general, one of the principal reasons of increased durability in SCM-blended cements is the lowered $Ca(OH)_2$ content available to take part in deleterious reactions. Furthermore, the higher content in C-S-H binder phase with a reduced Ca/Si ratio results in finer pore size distributions and lower permeabilities

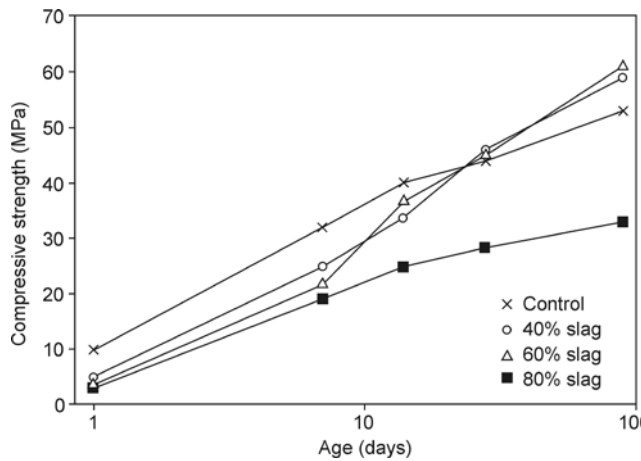

Figure 38. Development of compressive strength in concrete blended with various amounts of ground granulated blast furnace slag (Khatib and Hibbert 2005).

and in a thermodynamically more stable and chemically more resistant C-S-H phase with increased bonding capability of chlorine and alkaline ions. It is apparent that the replacement ratios of Portland cement by SCMs required for optimal durability are usually higher than the replacement ratios needed for optimal strength.

Sulfate attack. The interaction of sulfate containing solutions with concrete structures can result in swelling, cracking and eventual structural failure. Sulfate attack involves the formation of expansive compounds in the reaction of sulfate with $Ca(OH)_2$ to form gypsum or in combination with aluminates to form ettringite. The intensity of sulfate attack depends on the associated cation, increasing in the order $Ca^{2+} < Na^{+} < Mg^{2+}$. In addition of ettringite formation induced by interaction with Ca-sulfate solutions, Na-sulfate leads to the additional formation of gypsum when reacted with $Ca(OH)_2$. $MgSO_4$ is very aggressive, not only leading to the formation of gypsum and ettringite but also to the disintegration of the C-S-H phase into brucite, gypsum and silica.

SCM addition can reduce or eliminate the deleterious formation of expansive compounds by lowering the overall amount of $Ca(OH)_2$, by reducing the diffusion rate of sulfate in the pore solution and possibly by increasing the chemical resistance of the C-S-H phase. Replacement percentages of 30-40% of Portland cement by vitreous natural pozzolans were observed to be very effective in reducing expansion upon sulfate attack (Fig. 39) (Massazza and Costa 1979). Lower additions do not completely consume $Ca(OH)_2$, leaving a potential for expansion. Resistance to $MgSO_4$ attack can only be improved at low (2%) concentrations of $MgSO_4$.

Chloride attack. Exposure to de-icing salts, seawater or salt-bearing groundwater may result in increased leaching of $Ca(OH)_2$, higher binder porosity and lower strength. In addition, crystallization of salts in pores may cause expansion. In reinforced concrete, increased $Cl^-/(OH)^-$ ratios can lead to steel passivation and rebar corrosion. The lowered permeability of SCM-blended cements strongly reduces the diffusion rate of chloride ions into the binder matrix. Moreover, relatively large amounts of Cl^- can be bound to C-S-H and AFm phases giving blended cements that contain higher amounts of these reaction products a larger chloride binder capacity (Balonis et al. 2010). Lowered Cl^- concentrations in the depth profiles from a surface exposed to a chlorine bearing solutions in Figure 40 illustrate the improved resistance of blended concrete to chlorine attack (Chan and Ji 1999).

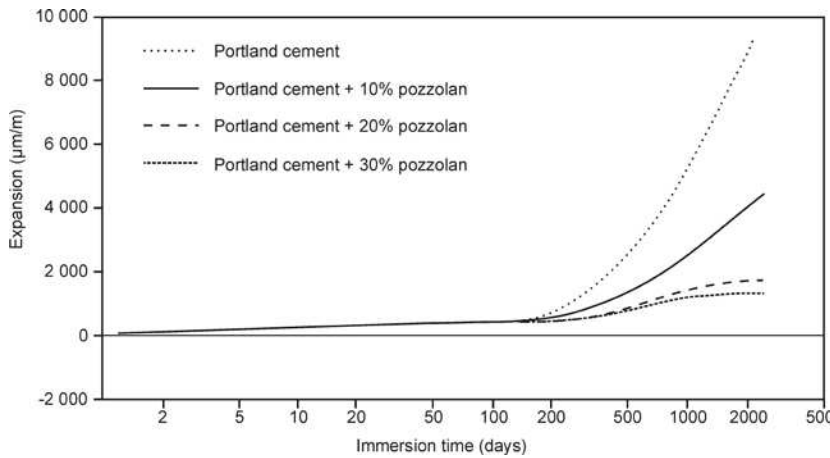

Figure 39. Reduction of mortar expansion due to attack of a 1% $MgSO_4$ solution decreases with increasing Portland cement replacement by a vitreous natural pozzolan (modified after Massazza and Costa 1979).

Carbonation. Reaction of hydration products with carbonate bearing solutions results in the formation of $CaCO_3$ and silica and/or alumina gel. In porous binders, intense carbonation can result in a decreased pore solution pH, possibly leading to steel passivation in reinforced concrete. However, in relatively impermeable binders, carbonation is usually confined to the upper surface and does not progress into the binder matrix. Although a depleted reserve of $Ca(OH)_2$ might render blended cements more susceptible to carbonation, in general the reduced permeability effectively counteracts the loss of buffering $Ca(OH)_2$.

Alkali-silica reaction. Alkali-silica reactions cause severe damage to concrete structures. Expansion is generally caused by the formation of an alkali-calcium-silica gel due to the interaction of alkalis present in the concrete pore solution with $Ca(OH)_2$ and reactive silica from the aggregate. The expansion risk is especially high when cements containing high levels of alkali are used in combination with reactive aggregates. The utilization of SCMs can prevent alkali-silica reactions by reducing the availability of alkalis, lowering the pH and depleting $Ca(OH)_2$. Although SCMs can contain relatively large amounts of alkali, in most cases the effective soluble amount of alkalis is rather low. Furthermore, the increased alkali-binding capability of the hydration products (i.e., C-A-S-H) enables to lower the alkalinity of the pore solution. However, it should be noted that at low replacement ratios below 20% the addition of SCMs can increase alkali-silica reactions with respect to the parent Portland cement. This pessimum behavior can be related to the supplementary release of alkalis from SCMs combined with an incomplete consumption of $Ca(OH)_2$ (Hobbs 2002). More than 20% replacement is usually sufficient to avoid expansion. Figure 41 illustrates the expansion abatement in zeolite tuff blended cements, showing that expansion is strongly reduced when 20% or more zeolite tuff is added to the high-alkali cement (Feng and Peng 2005). In general, low-alkali SCMs containing both silica and alumina are observed to be most effective in minimizing expansion. Alumina-poor SCMs have less potential to reduce the alkali-silica reaction.

CONCLUSIONS

The benefits of supplementary cementitious materials utilization in the cement and construction industry are threefold. First is the economic gain obtained by replacing a substantial part of the Portland cement by cheap natural pozzolans or industrial by-products. Second is the lowering of the blended cement environmental cost associated with the greenhouse gases emitted during Portland cement production. A third advantage is the durability improvement of the end product. Additionally, the increased blending of SCMs with Portland cement is of limited interference in the conventional production process and offers the opportunity to valorize and immobilize vast amounts of industrial and societal waste into construction materials.

Supplementary cementitious materials can be conveniently classified according to a genetic classification scheme. A distinction is made between naturally occurring and artificial SCMs. The latter category is subdivided into intentionally thermally activated materials and by-products of industrial processes. Detailed accounts on the physical, chemical and mineralogical characteristics for the various SCM groups and subgroups corroborate the view that there exists a close relationship between the material properties and their hydraulic and pozzolanic reactivity that promises to be quantified and predicted.

To identify the material properties of importance and when they become essential in the pozzolanic reaction, a detailed knowledge on the pozzolanic reaction mechanism is needed. Recent developments regarding the dissolution kinetics and mechanisms of aluminosilicates in high pH environments are illustrated to be instrumental in obtaining more fundamental insights into the pozzolanic reaction. Improved knowledge on the kinetics and mechanism of the pozzolanic reaction will allow making better thermodynamic predictions of evolving reaction product assemblages over the course of hydration.

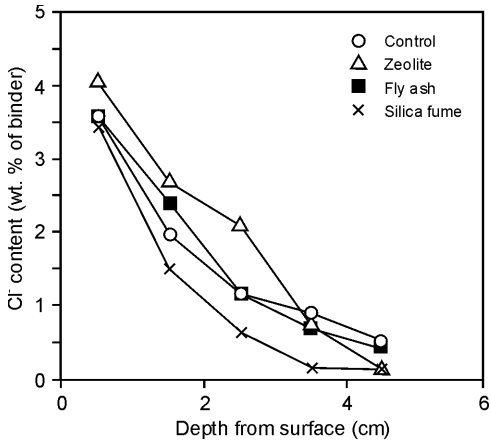

Figure 40. Chloride concentrations in function of depth from the concrete surface exposed to a Cl^- rich solution after 30 days of exposure. The concrete water to binder ratio was 0.33 (modified after Chan and Ji 1999).

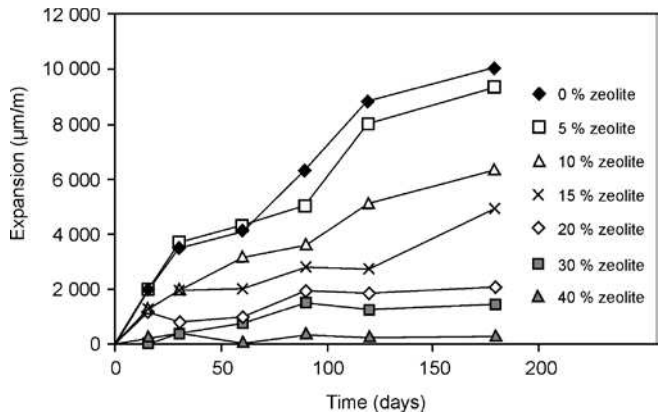

Figure 41. Alkali-silica expansion abatement in natural zeolite blended concrete at various Portland cement replacement percentages (Feng and Peng 2005).

The reaction product assemblages are observed to be mainly a function of the chemical composition of the reactive components in the reactant mixture. In contrast to the wide variability in SCMs, there exists only a relatively small range of thermodynamically stable or metastable compounds formed in the pozzolanic, hydraulic or hydration reactions. Recent developments in thermodynamic modeling allow an improved, more quantitative understanding of the parameters controlling the assemblage of reaction products to be obtained.

A synopsis of the technological effects of using blended cements is included in the present paper. Properties of fresh and hardened mortar and concrete incorporating SCMs are compared. The effects of SCM incorporation are obviously strongly linked to the specific physical characteristics and can differ widely from slowly reacting blast furnace slag to highly reactive metakaolin. The emerging image is that the appropriate use of SCMs should be regarded as beneficial in terms of performance, durability and sustainability of the end product.

ACKNOWLEDGMENTS

R. Snellings extends his gratitude towards the Research Foundation - Flanders (FWO) for financial support.

REFERENCES

Ahmadi B, Shekarchi M (2010) Use of natural zeolite as a supplementary cementitious material. Cem Concr Comp 32:134-141

Akman MS, Mazlum F, Esenli F (1992) Comparative study of natural pozzolans used in blended cement production. ACI Special Publication 132:471-494

Alexander KM (1960) Reactivity of ultrafine powders produced from siliceous rocks. J Am Concr I 57:557-569

Al-Rawas AA, Hago AW, Corcoran TC, Al-Ghafri KM (1998) Properties of Omani artificial pozzolana (sarooj). Appl Clay Sci 13:275-292

Ambroise J, Gniewek J, Dejean J, Péra J (1987) Hydration of synthetic pozzolanic binders obtained by thermal activation of montmorillonite. Ceram Bull 66:1731-1733

Ambroise J, Maximilien S, Péra J (1994) Properties of metakaolin blended cements. Adv Cem Based Mater 1:161-168

Ambroise J, Murat M, Péra J (1985) Hydration reaction and hardening of calcined clays and related minerals. V. Extension of the research and general conclusions. Cem Concr Res 15:261-268

Andersen MD, Jakobsen HJ, Skibsted J (2006) A new aluminium-hydrate species in hydrated Portland cements characterized by ^{27}Al and ^{29}Si MAS NMR spectroscopy. Cem Concr Res 36:3-17

Asbridge AH, Page CL, Page MM (2002) Effects of metakaolin, water/binder ratio and interfacial transition zones on the microhardness of cement mortars. Cem Concr Res 32:1365-1369

Asher RR (1965) Volcanic construction materials in Idaho. Idaho Bureau of Mines and Geology 135:1-94

Atkins M, Lachowski EE, Glasser FP (1993) Investigation of solid and aqueous chemistry of 10-year-old Portland cement pastes; with and without silica modifier. Adv Cem Res 5:97-102

Ayub M, Yusuf M, Beg A, Faruqi FA (1988) Pozzolanic properties of burnt clays. Pakistan J Sci Ind R 31:1-5

Badogiannis E, Kakali G, Dimopoulou G, Chaniotakis E, Tsivilis S (2005) Metakaolin as a main cement constituent. Exploitation of poor Greek kaolins. Cem Concr Comp 27:197-203

Bakharev T (2005) Geopolymeric materials prepared using Class F fly ash and elevated temperature curing. Cem Concr Res 35:1224-1232

Bakolas A, Aggelakopoulou E, Moropoulou A, Anagnostopoulou S (2006) Evaluation of pozzolanic activity and physico-mechanical characteristics in metakaolin-lime pastes. J Therm Anal Calorim 84:157-163

Balonis M, Lothenbach B, Le Saout G, Glasser FP (2010) Impact of chloride on the mineralogy of hydrated Portland cement systems. Cem Concr Res 40:1009-1022

Baris YL, Simonato L, Saracci R, Skidmore JW, Artvinli M (1981) Malignant mesothelioma and radiological chest abnormalities in two villages in central Turkey: An epidemiological and environmental investigation. Lancet 317:984-987

Barnett SJ, Adam CD, Jackson A (2001) XRPD profile fitting investigation of the solid solution between ettringite, $Ca_6Al_2(SO_4)_3(OH)_{12}{\cdot}26H_2O$, and carbonate ettringite, $Ca_6Al_2(CO_3)_3(OH)_{12}{\cdot}26H_2O$. Cem Concr Res 31:13-17

Baronio G, Binda L (1997) Study of the pozzolanicity of some bricks and clays. Constr Build Mater 11:41-46

Battaglino G, Schippa G (1968) On a new method for evaluating the aptitude of a material to be employed as pozzolanic addition. Ind Ital Cem 38:175-178

Beedle SS, Groves GW, Rodger SA (1989) The effect of fine pozzolanic and other particles on hydration of C_3S. Adv Cem Res 2:3-8

Bellotto M, Gualtieri A, Artioli A, Clark SM (1995) Kinetic study of the kaolinite-mullite reaction sequence. Part I: Kaolinite dehydroxylation. Phys Chem Miner 22:207-217

Benezet JC, Benhassaine A (1999) Grinding and pozzolanic reactivity of quartz powders. Powder Technol 105:167-171

Bensted J, Barnes P (2002) Structure and Performance of Cements. 2nd edition. Spon Press, London

Bich C, Ambroise J, Péra J (2009) Influence of degree of dehydroxylation on the pozzolanic activity of metakaolin. Appl Clay Sci 44:194-200

Bijen J (1996) Benefits of slag and fly ash. Constr Build Mater 10:309-314

Biricik H, Aköz F, Berktay I, Tulgar AN (1999) Study of pozzolanic properties of wheat straw ash. Cem Concr Res 29:637-643

Blezard RG (2001) The history of calcareous cements. *In*: Lea's Chemistry of Cement and Concrete. 4th edition. Hewlett P (ed) Butterworth-Heinemann, Oxford, p 1-24

Blum AE, Yund RA, Lasaga AC (1990) The effect of dislocation density on the dissolution rate of quartz. Geochim Cosmochim Acta 54:283-297

Bougara A, Lynsdale C, Milestone NB (2010) Reactivity and performance of blast furnace slags of different origin. Cem Concr Comp 32:319-324

Brady PV, Walther JV (1990). Kinetics of quartz dissolution at low temperatures. Chem Geol 82:253-264

Brantley SL (2008) Kinetics of mineral dissolution. *In*: Kinetics of Water-Rock Interaction. Brantley SL, Kubicki JD, White AF (eds) Springer, New York, p 151-210

Brough AR, Dobson CM, Richardson IG, Groves GW (1995) A study of the pozzolanic reaction by solid-state ^{29}Si nuclear magnetic resonance using selective isotopic enrichment. J Mater Sci 30:1671-1678

Bullard JW, Jennings HM, Livingston RA, Nonat A, Scherer GW, Schweitzer JS, Scrivener KL, Thomas JJ (2011) Mechanisms of cement hydration. Cem Concr Res 41:1208-1223

Cabrera J, Rojas MF (2001) Mechanism of hydration of the metakaolin-lime-water system. Cem Concr Res 31:177-182

Cameron WE (1977) Mullite: a substituted alumina. Am Mineral 62:747-755

Canpolat F, Yilmaz K, Köse MM, Sümer M, Yurdusev MA (2004) Use of zeolite, coal bottom ash and fly ash as replacement materials in cement production. Cem Concr Res 34:731-735

Caputo D, Liguori B, Colella C (2008) Some advances in understanding the pozzolanic activity of zeolites: The effect of zeolite structure. Cem Concr Comp 30:455-462

Cara S, Carcangiu G, Massidda L, Meloni P, Sanna U, Tamanini M (2006) Assessment of pozzolanic potential in lime-water systems of raw and calcined kaolinic clays from the Donnigazza Mine (Sardinia-Italy). J Appl Clay Sci 33:66-72

Çavdar A, Yetgin Ş (2007) Availability of tuffs from northeast of Turkey as natural pozzolan on cement, some chemical and mechanical relationships. Constr Build Mater 21:2066-2071

Chakchouk A, Trifi L, Samet B, Bouaziz S (2009) Formulation of blended cement: effect of process variables on clay pozzolanic activity. Constr Build Mater 23:1365-1373

Chan SYN, Ji X (1999) Comparative study of the initial surface absorption and chloride diffusion of high performance zeolite, silica fume and PFA concretes. Cem Concr Comp 21:293-300

Chen Y, Shah N, Huggins FE, Huffman GP (2005) Transmission electron microscopy investigation of ultrafine coal fly ash particles. Environ Sci Technol 39:1144-1151

Cheriaf M, Cavalcante Rocha J, Péra J (1999) Pozzolanic properties of pulverized coal combustion bottom ash. Cem Concr Res 29:1387-1391

Chipera SJ, Apps JA (2001) Geochemical stability of natural zeolites. Rev Mineral Geochem 45:117-161

Christensen AN, Jensen TR, Hanson JC (2004) Formation of ettringite, $Ca_6Al_2(SO_4)_3(OH)_{12}{\cdot}26H_2O$, AFt, and monosulphate, $Ca_4Al_2O_6(SO_4){\cdot}14H_2O$, AFm-14, in hydrothermal hydration of Portland cement and of calcium aluminum oxide—calcium sulphate dihydrate mixtures studied by in situ synchrotron X-ray powder diffraction. J Solid State Chem 177:1944-1951

Chung DDL (2002) Review: Improving cement-based materials by using silica fume. J Mater Sci 37:673-682

Chusilp N, Jaturapitakkul C, Kiattikomol K (2009) Utilization of bagasse ash as a pozzolanic material in concrete. Constr Build Mater 23:3352-3358

Colella C, de Gennaro M, Aiello R (2001) Use of zeolitic tuff in the building industry. Rev Mineral Geochem 45:551-587

Coles DG, Ragaini RC, Ondov JM, Fisher GL, Silberman D, Prentice BA (1979) Chemical studies of stack fly ash from a coal-fired power plant. Environ Sci Technol 13: 455-459

Collepardi M, Baldini G, Pauri M, Corradi M (1978) The effect of pozzolanas on the tricalcium aluminate hydration. Cem Concr Res 8:741-751

Cong X, Kirkpatrick RJ (1996b) ^{29}Si MAS NMR study of the structure of calcium silicate hydrate. Adv Cem Based Mater 3:144-156

Cong X, Kirkpatrick RJ (1996a) ^{29}Si and ^{17}O NMR investigation of the structure of some crystalline calcium silicate hydrates. Adv Cem Based Mater 3:133-143

Cook DJ (1986a) Natural pozzolanas. *In*: Cement Replacement Materials. Swamy RN (ed) Surrey University Press, London, p 1-39

Cook DJ (1986b) Calcined clay, shale and other soils. *In*: Cement Replacement Materials. Swamy RN (ed) Surrey University Press, London, p 40-72

Cook DJ (1986c) Rice husk ash. *In*: Cement Replacement Materials. Swamy RN (ed) Surrey University Press, London, p 171-196

Cordeiro GC, Filho RDT, Fairbairn EMR (2009b) Use of ultrafine rice husk ash with high-carbon content as pozzolan in high performance concrete. Mater Struct 42:983-992

Cordeiro GC, Filho RDT, Tavares LM, Fairbairn EMR (2008) Pozzolanic activity and filler effect of sugar cane bagasse ash in Portland cement and lime mortars. Cem Concr Res 30:410-418

Cordeiro GC, Filho RDT, Tavares LM, Fairbairn EMR (2009a) Ultrafine grinding of sugar cane bagasse ash for application as pozzolanic admixture in concrete. Cem Concr Res 39:110-115

Costa U, Massazza F (1974) Factors affecting the reaction with lime of pozzolans. Proceedings of the 6th International Congress on the Chemistry of Cement III-6:1-17

Criscenti LJ, Kubicki JD, Brantley SL (2006) Silicate glass and mineral dissolution: calculated reaction paths and activation energies for hydrolysis of a Q^3 Si by H_3O^+ using a*b initio* methods. J Phys Chem A 110:198-206

Damtoft JS, Lukasik J, Herfort D, Sorrentino D, Gartner EM (2008) Sustainable development and climate change initiatives. Cem Concr Res 38:115-127

Davraz M, Gündüz L (2005) Engineering properties of amorphous silica as a new natural pozzolan for use in concrete. Cem Concr Res 35:1251-1261
Davraz M, Gündüz L (2008) Reduction of alkali silica reaction risk in concrete by natural (micronized) amorphous silica. Constr Build Mater 22:1093-1099
Day RL (1990) Pozzolans for use in low-cost housing. International Development Research Centre, Ottawa, Canada
Day RL, Shi C (1994) Influence of the fineness of pozzolan on the strength of lime natural-pozzolan cement pastes. Cem Concr Res 24:1485-1491
De Sensale GR (2006) Strength development of concrete with rice-husk ash. Cem Concr Comp 28:158-160
De Silva PS, Glasser FP (1992) Pozzolanic activation of metakaolin. Adv Cement Res 4:167-178
Degirmenci N, Yilmaz A (2009) Use of diatomite as partial replacement for Portland cement in cement mortars. Constr Build Mater 23:284-288
Demoulian E, Gourdin P, Hawthorn, F, Vernet C (1980) Influence de la composition chimique et de la texture des laitiers sur leur hydraulicité. Proceedings of the 7th International Congress on the Chemistry of Cement II-III:105-111
Dihr RK (1986) Pulverised-fuel ash. *In:* Cement Replacement Materials. Swamy RN (ed) Surrey University Press, London, p 197-255
Divet L, Randriambololona R (1998) Delayed ettringite formation: the effect of temperature and basicity on the interaction of sulphate and C-S-H phase. Cem Concr Res 28:357-363
Double DD, Hellawell A, Perry SJ (1978) The hydration of Portland cement. Proc R Soc London A 359:435-451
Douglas E, Elola A, Malhotra VM (1990) Characterisation of ground granulated blast furnace slag and fly ashes and their hydration in Portland cement blends. Cem Concr Aggr 12:38-46
Dove PM (1999) Dissolution kinetics of quartz in aqueous mixed cation solutions. Geochim Cosmochim Acta 63:3715-3727
Dove PM, Crerar DA (1990) Kinetics of quartz dissolution in electrolyte solutions using a hydrothermal mixed flow reactor. Geochim Cosmochim Acta 54:955-969
Dove PM, Han N, De Yoreo JJ (2005) Mechanisms of classical crystal growth theory explain quartz and silicate dissolution behavior. P Natl Acad Sci USA 102:15357-15362
Drits VA, Besson G, Muller F (1995) An improved model for structural transformations of heat-treated aluminous dioctahedral 2:1 layer silicates. Clays Clay Miner 43:718-731
Držaj B, Hočevar S, Slokan M, Zajc A (1978) Kinetics and mechanism of reaction in the zeolitic tuff-CaO-H_2O systems at increased temperature. Cem Concr Res 8:711-720
Dudas MJ, Warren CJ (1987) Submicroscopic model of fly ash particles. Geoderma 40:101-114
Efstathiadis E (1978) Greek Concrete of Three Millenniums. Hellenic Ministry of Public Works, Athens.
Emmerich K (2010) Thermal analysis for characterization and processing of industrial minerals. *In:* Industrial Mineralogy. EMU Notes in Mineralogy, 9. Christidis G (ed) Eötvös University Press, Budapest, p 129-170
Erdem TK, Meral Ç, Tokyay M, Erdogan TY (2007) Use of perlite as a pozzolanic addition in producing blended cements. Cem Concr Comp 29:13-21
Erdoğdu K, Türker P (1998) Effects of fly ash particle size on strength of Portland cement fly ash mortars. Cem Concr Res 28: 1217-1222
Escalante JI, Gomez LY, Johal KK, Mendoza G, Mancha H, Mendez J (2001). Reactivity of blast furnace slag in Portland cement blends hydrated under different conditions. Cem Concr Res 31:1403-1409
Famy C, Scrivener KL, Atkinson A, Brough AR (2002) Effects of an early or a late heat treatment on the microstructure and composition of inner C-S-H products of Portland cement mortars. Cem Concr Res 32:269-278
Felipe MA, Xiao Y, Kubicki JD (2001) Molecular orbital modeling and transition state theory in geochemistry. Rev Miner Geochem 42:485-531
Feng NQ, Chan SYN, He ZS, Tsang MKC (1997) Shale ash concrete. Cem Concr Res 27:279-291
Feng NQ, Peng GF (2005) Applications of natural zeolite to construction and building materials in China. Constr Build Mater 19:579-584
Fernandez R, Martirena F, Scrivener KL (2011) The origin of the pozzolanic activity of calcined clay minerals: A comparison between kaolinite, illite and montmorillonite. Cem Concr Res 41:113-122
Ferreira C, Ribeiro A, Ottosen L (2003) Possible applications for municipal solid waste fly ash. J Hazard Mater B96:201-216
Fidjestol P, Lewis R (2001) Microsilica as an addition. *In*: Lea's Chemistry of Cement and Concrete. Hewlett PC (ed) Butterworth-Heinemann, Oxford, p 679-712
Filippidis A, Georgakopoulos A (1992) Mineralogical and chemical investigation of fly ash from the Main and Northern lignite fields in Ptolemais, Greece. Fuel 1992:373-376
Fraay ALA, Bijen JM, De Haan YM (1989) The reaction of fly ash in concrete a critical examination. Cem Concr Res 19:235-246

Fragoulis D, Chaniotakis E, Stamatakis MG (1997) Zeolitic tuffs of Kimolos island, Aegean Sea, Greece and their industrial potential. Cem Concr Res 27:889-905

Fragoulis D, Stamatakis MG, Papageorgiou D, Chaniotakis E (2005) The physical and mechanical properties of composite cements manufactured with calcareous and clayey Greek diatomite mixtures. Cem Concr Res 27:205-209

Frearson JPH, Uren JM (1986) Investigation of a granulated blast furnace slag containing merwinite crystallisation. Proc 2nd Int Conf Use of Fly Ash, Silica Fume, Slag and Natural Pozzolans in Concrete II:1401-1421

Frias M, Rodriguez O, Vegas I, Vigil R (2008) Properties of calcined clay waste and its influence on blended cement behavior. J Am Ceram Soc 91:1226-1230

Gartner EM (2004) Industrially interesting approaches to 'low-CO_2' cements. Cem Concr Res 34:1489-1498

Gartner EM, Young JF, Damidot DA, Jawed I (2002) Hydration of Portland cement. *In*: Structure and Performance of Cements. Bensted J, Barnes P (eds) Spon Press, London, p 57-113

Gieré R, Carleton LE, Gregory RL (2003) Micro- and nanochemistry of fly ash from a coal-fired power plant. Am Mineral 88:1853-1865

Ginstling AM, Brounhstein BI (1950) On diffusion kinetics in chemical reactions taking place in spherical powder grains. Zhur Priklad Khim 23:1249-1259 (in Russian)

Glasser FP, Diamond S, Roy DM (1987) Hydration reactions in cement pastes incorporating fly ash and other pozzolanic materials. Proc Mater Res Soc Symp 86:167-186

Gomes S, François M (2000) Characterization of mullite in silicoaluminous fly ash by XRD, TEM, and ^{29}Si MAS NMR. Cem Concr Res 30:175-181

Gomes S, François M, Abdelmoula M, Refait Ph., Pellisier C, Evrard O (1999) Characterization of magnetite in silico-aluminous fly ash by SEM, TEM, XRD, magnetic susceptibility, and Mössbauer spectroscopy. Cem Concr Res 29:1705-1711

Goodarzi F (2006) Characteristics and composition of fly ash from Canadian coal-fired power plants. Fuel 85:1418-1427

Goto S, Fujimori H, Tsuda T, Ooshiro K, Yamamoto S, Ioku K (2007) Structure analysis of glass of CaO-Al_2O_3-SiO_2 system by means of NMR. Proc 12th Int Congr Chem Cement Concrete

Gottardi G, Obradovic J (1978) Sedimentary zeolites in Europe. Fortschr Mineral 56:316-366

Greenberg SA (1961) Reaction between silica and calcium hydroxide solutions, I. Kinetics in the temperature range 30 to 85 °C. J Phys Chem 65:12-16

Grubb DG, Guimaraes MS, Valencia R (2000) Phosphate immobilization using an acidic type F fly ash. J Hazard Mater 76:217-236

Grutzeck MW, Roy DM, Scheetz BE (1981) Hydration mechanisms of high-lime fly ash in Portland-cement composites. Proc Mater Res Symp MRS-N 92–101

Grzeszczyk S, Lipowski G (1997) Effect of content and particle size distribution of high-calcium fly ash on the rheological properties of cement pastes. Cem Concr Res 27:907-916

Habert G, Billard C, Rossi P, Chen C, Roussel N (2010) Cement production technology improvement compared to factor 4 objectives. Cem Concr Res 40:820-826

Habert G, Choupay N, Escadeillas G, Guillaume D, Montel JM (2009) Clay content of argillites: Influence on cement based mortars. Appl Clay Sci 43:322-330

Hamdan H, Muhid MNM, Endud S, Listiorini E, Ramli Z (1997) ^{29}Si MAS NMR, XRD and FESEM studies of rice husk silica for the synthesis of zeolites. J Non-cryst Solids 211:126-131

Hamilton JP, Brantley SL, Pantano CG, Criscenti LJ, Kubicki JD (2001) Dissolution of nepheline, jadeite and albite glasses: Toward better models for aluminosilicate dissolution. Geochim Cosmochim Acta 65:3683-3702

Hanna KM, Afify A (1974) Evaluation of the activity of pozzolanic materials. J Appl Chem Biotechn 24:751-757

Hay RA, Sheppard RL (2001) Formation of zeolites in open hydrologic systems. Rev Mineral Geochem 45:261-275

He C, Mackovicky E, Osbaeck B (1996) Thermal treatment and pozzolanic activity of Na- and Ca-montmorillonite. Appl Clay Sci 10:351-368

He C, Mackovicky E, Osbaeck B (2000) Thermal stability and pozzolanic activity of raw and calcined mixed-layer mica/smectite. Appl Clay Sci 17:141-161

He C, Makovicky E, Osbaeck B (1994) Thermal stability and pozzolanic activity of calcined kaolin. Appl Clay Sci 9:165-187

He C, Makovicky E, Osbaeck B (1995) Thermal stability and pozzolanic activity of raw and calcined illite. Appl Clay Sci 9:337-354

He C, Osbaeck B, Makovicky E (1995) Pozzolanic reactions of six principal clay minerals: activation, reactivity assessment and technological effects. Cem Concr Res 25:1691-1702

Henson NJ, Cheetham AK, Gale JD (1994) Theoretical calculations on silica frameworks and their correlation with experiment. Chem Mater 6:1647-1650
Hewlett PC (2001) Lea's Chemistry of Cement and Concrete. 4th edition. Butterworth-Heinemann, Oxford
Hilali EA, Jeannette A, Nataf M (1981) Pozzolanas. Mines, Geologie et Energie, Maroc 49:195-208
Hobbs DW (2002) Alkali-silica reaction in concrete. *In*: Structure and Performance of Cements. Bensted J, Barnes P (eds) Spon Press, London, p 265-281
Hong SY, Glasser FP (1999) Alkali binding in cement pastes: Part I. The C-S-H phase. Cem Concr Res 29:1893-1903
Hooton RD (2008) Bridging the gap between research and standards. Cem Concr Res 38:247-258
Hooton RD, Emery JJ (1983) Glass content determination and strength development predictions for vitrified blast furnace slag. ACI Special Publication 79:943-962
Hower JC, Rathbone RF, Robertson JD, Peterson G, Trimble AS (1999) Petrology, mineralogy, and chemistry of magnetically-separated sized fly ash. Fuel 78:197-203
Hower JC, Trimble AS, Eble CF, Palmer CA, Kolker A (2000) Characterization of fly ash from low-sulfur coal sources: Partitioning of carbon and trace elements with particle size. Energ Source 21:511-525
Huizhen L (1992) Effect of structure and composition on reactivity of zeolite-tuff used as blending material of Portland cement. Proceedings of the 9th International Congress on the Chemistry of Cement 128-134
Idorn MG (1997) Concrete Progress from Antiquity to the Third Millenium. Telford, London
Iler RK (1979) The Chemistry of Silica: Solubility, Polymerization, Colloid and Surface Properties, and Biochemistry. John Wiley and Sons, New York
Ilic M, Cheeseman Ch, Sollars Ch, Knight J (2003) Mineralogy and microstructure of sintered lignite coal fly ash. Fuel 82:331-336
Ish-Shalom M, Bentur A, Grinberg T (1980) Cementing properties of oil-shale ash: I. Effect of burning method and temperature. Cem Concr Res 10:799-807
James J, Rao MS (1986) Reactivity of rice husk ash. Cem Concr Res 16:296-302
Jander W (1927) Reaktionen im festen Zustande bei höheren Temperaturen. Reaktionsgeschwindigkeiten endotherm verlaufender Umsetzungen. Z Anorg Allg Chem 163:1-30
Janotka I, Krajči L, Dzivak M (2003) Properties and utilization of zeolite-blended Portland Cements. Clays Clay Miner 51:616-624
Jauberthie R, Rendell F, Tamba S, Cisse I (2000) Origin of the pozzolanic effect of rice husks. Constr Build Mater 14:419-423
Jo BW, Kim CH, Tae GH, Park JB (2007) Characteristics of cement with nano-SiO_2 particles. Constr Build Mater 21:1351-1355
Johansson S, Andersen PJ (1990) Pozzolanic activity of calcined moler clay. Cem Concr Res 20:447-452
Jones TR (2002) Metakaolin as a pozzolanic addition to concrete. *In*: Structure and Performance of Cements. Bensted J, Barnes P (eds) Spon Press, London, p 372-398
Joshi RC, Lohtia RP (1997) Fly ash in concrete production, properties and uses. Advances in Concrete Technology 2. Gordon and Breach Science Publishers, Amsterdam
Juilland P, Gallucci E, Flatt R, Scrivener K (2010) Dissolution theory applied to the induction period in alite hydration. Cem Concr Res 40:831-844
Justnes H (2002) Condensed silica fume as a cement extender. *In*: Structure and Performance of Cements. Bensted J, Barnes P (eds) Spon Press, London, p 399-408
Justnes H (2007) Silica fume in high-quality concrete - A review of mechanism and performance. Proc 9th CANMET/ACI Int Conf on Fly Ash, Silica Fume, Slag and Natural Pozzolans in Concrete, p 63-78
Justnes H, Meland I, Bjoergum JO (1990) Nuclear magnetic resonance (NMR) - a powerful tool in cement and concrete research. Adv Cem Res 3:105-110
Kaid N, Cyr M, Julien S, Khelafi H (2009) Durability of concrete containing a natural pozzolan as defined by a performance-based approach. Constr Build Mater 23:3457-3467
Kakali G, Perraki T, Tsivilis S, Badogiannis E (2001) Thermal treatment of kaolin: the effect of mineralogy on the pozzolanic activity. Appl Clay Sci 20:73-80
Kantsepolsky IS, Terekhovich SV, Khlebo AP Ronchinsky EM (1969) Frost and atmosphere resistance of solutions in pozzolan Portland cements. Tr Alma-At Nauk Issled Proekt Inst Stroit Mater 9:119-125 (in Russian)
Khatib JM, Hibbert JJ (2005) Selected engineering properties of concrete incorporating slag and metakaolin. Constr Build Mater 19:460-472
Khatib JM, Wild S (1996) Pore size distribution of metakaolin paste. Cem Concr Res 26:1545-1553
Kirby CS, Rimstidt JD (1993) Mineralogy and surface properties of municipal solid waste ash. Environ Sci Technol 27:652-660
Kitsopoulos KP, Dunham AC (1996) Heulandite and mordenite-rich tuffs from Greece: a potential source for pozzolanic materials. Mineral Deposita 31:576-583

Kjellsen KO, Detwiler RJ, Gjørv OE (1991) Development of microstructures in plain cement pastes hydrated at different temperatures. Cem Concr Res 21:179-189
Kjellsen KO, Wallevik OH, Hallgren M (1999) On the compressive strength development of high performance concrete and paste - effect of silica fume. Mater Struct 32:63-69
Knauss KG, Wolery TJ (1988) The dissolution kinetics of quartz as a function of pH and time at 70 °C. Geochim Cosmochim Acta 52:43-53
Kolay PK, Singh DN (2001) Physical, chemical, mineralogical, and thermal properties of cenospheres from an ash lagoon. Cem Concr Res 31:539-542
Kondo R, Lee K, Diamon M (1976) Kinetics and mechanisms of hydrothermal reaction in lime-quartz-water systems. J Ceram Soc Jpn 84:573-578
Korpa A, Kowald T, Tretting R (2008) Hydration behavior, structure and morphology of hydration phases in advanced cement-based systems containing micro and nanoscale pozzolanic additives. Cem Concr Res 38:955-962
Koukouzas N, Hämäläinen J, Papanikolaou D, Tourunen A, Jäntti T (2007) Mineralogical and elemental composition of fly ash from pilot scale fluidised bed combustion of lignite, bituminous coal, wood chips and their blends. Fuel 86:2186-2193
Kurdowski W, Nocun-Wczelik W (1983) The tricalcium silicate hydration in the presence of active silica. Cem Concr Res 13:341-348
Kutchko BG, Kim AG (2006) Fly ash characterization by SEM-EDS. Fuel 85:2537-2544
Kuzel HJ (1996) Initial hydration reactions and mechanisms of delayed ettringite formation in Portland cements. Cem Concr Comp 18:195-203
Lang E (2002) Blast furnace cements. *In*: Structure and Performance of Cements. 2nd edition. Bensted J, Barnes P (eds) Spon Press, London, 310-325
Larbi JA, Bijen JM (1990) Orientation of calcium hydroxide at the Portland cement paste-aggregate interface in mortars in the presence of silica fume: A contribution. Cem Concr Res 20:461-470
Lasaga AC (1998) Kinetic theory in the earth sciences. Princeton University Press, Chichester.
Lasaga AC, Lüttge A (2005) Kinetic justification of the solubility product: application of a general kinetic dissolution model. J Phys Chem B 109:1635-1642
Lavat AE, Trezza MA, Poggi M (2009) Characterization of ceramic roof tile wastes as pozzolanic admixture. Waste Manage 29:1666-1674
Le Maître RW, Bateman P, Dudek A, Keller J, Lameyre J, Le Bas MJ, Sabine PA, Schmid R, Sorensen H, Streckeisen A, Woolley AR, Zanettin B (1989). A Classification of Igneous Rocks and Glossary of Terms, Recommendations of the International Union of Geological Sciences, Subcommission on the Systematics of Igneous Rocks. Blackwell Scientific, Oxford
Lea FM (1970) The Chemistry of Cement and Concrete. 3rd Edition. Chemical Publishing, New York
Liebig E, Althaus E (1997) Kaolinite and montmorillonite as pozzolanic components in lime mortars: untreated and after thermal activation. ZKG Int 50:282-290
Liebig E, Althaus E (1998) Pozzolanic activity of volcanic tuff and suevite: effects of calcination. Cem Concr Res 28:567-575
Liguori B, Caputo D, Marroccoli M, Colella C (2003) Evaluation of zeolite-bearing tuffs as pozzolanic addition for blended cements. ACI Special Publications 221:319-333
Lilkov V, Dimitrova E, Petrov OE (1997) Hydration process of cement containing fly ash and silica fume: the first 24 hours. Cem Concr Res 1997:577-588
Lindgreen H, Geiker M, Krøyer H, Springer N, Skibsted J (2008) Microstructure engineering of Portland cement pastes and mortars through addition of ultrafine layer silicates. Cem Concr Comp 30:686-699
Livingston RA, Schweitzer JS, Rolfs C, Becker HW, Kubsky S (2001) Characterization of the induction period in tricalcium silicate hydration by nuclear resonance reaction analysis. J Mater Res 16:687-693
Lothenbach B, Gruskovnjak A (2007) Hydration of alkali-activated slag: thermodynamic modelling. Adv Cem Res 19:81-92
Lothenbach B, Le Saout G, Gallucci E, Scrivener K (2008b) Influence of limestone on the hydration of Portland cements. Cem Concr Res 38:848-860
Lothenbach B, Matschei T, Möschner G, Glasser FP (2008a) Thermodynamic modelling of the effect of temperature on the hydration and porosity of Portland cement. Cem Concr Res 38:1-18
Lothenbach B, Scrivener K, Hooton RD (2011) Supplementary cementitious materials. Cem Concr Res 41:1244-1256
Lothenbach B, Winnefeld F (2006) Thermodynamic modelling of the hydration of Portland cement. Cem Concr Res 36:209-226
Lothenbach B, Winnefeld F, Alder C, Wieland E, Lunk P (2007) Effect of temperature on the pore solution, microstructure and hydration products of Portland cement pastes. Cem Concr Res 37:483-491
Ludwig U, Schwiete HE (1963) Lime combination and new formations in the trass-lime reactions. Zem-Kalk-Gips 10:421-431

Luke K (2002) Pulverized fuel ash as a cement extender. *In*: Structure and Performance of Cements, 2nd edition. Bensted J, Barnes P (eds.) Spon Press, London, p 353-371
Luke K (2007) The effect of natural zeolites on the composition of cement pore fluids at early ages. Proceedings of the 11th International Congress on the Chemistry of Cement
Malhotra VM (1993) Fly ash, slag, silica fume, and rice-husk ash in concrete: a review. Concr Int 15:23-28
Malhotra VM, Mehta PK (1996) Pozzolanic and Cementitious Materials. Overseas Publishers Association, Amsterdam
Maltais Y, Marchand J (1997) Influence of curing temperature on cement hydration and mechanical strength development of fly ash mortars. Cem Concr Res 27:1009-1020
Manz OE (1998) Coal fly ash: A retrospective and future look. Energeia 9:1-3 *http://www.caer.uky.edu/energeia/PDF/vol9-2.pdf*
Massazza F (1974) Chemistry of pozzolanic additions and mixed cements. Proceedings of the 6th International Congress on the Chemistry of Cement, 1-65
Massazza F (2001) Pozzolana and pozzolanic cements. *In*: Lea's Chemistry of Cement and Concrete. Hewlett PC (ed) Butterworth-Heinemann, Oxford, p 471-636
Massazza F (2002) Properties and applications of natural pozzolanas. *In*: Structure and Performance of Cements, 2nd edition. Bensted J, Barnes P (eds.) Spon Press, London, p 326-352
Massazza F, Costa U (1979) Aspects of the pozzolanic activity and properties of pozzolanic cements. Il Cemento 76:3-18
Massazza F, Daimon M (1992) Conference report: Chemistry of hydration of cements and cementitious systems. Proceedings of the 9th International Congress on the Chemistry of Cement p 383-446
Massazza F, Testolin M (1983) Trimethylsilylation in the study of pozzolana-containing pastes. Il Cemento 80:49-62
Matschei T, Glasser FP (2010) Temperature dependence, 0 to 40 °C, of the mineralogy of Portland cement paste in the presence of calcium carbonate. Cem Concr Res 40:763-777
Matschei T, Lothenbach B, Glasser FP (2007a) The role of calcium carbonate in cement hydration. Cem Concr Res 37:551-558
Matschei T, Lothenbach B, Glasser FP (2007b) Thermodynamic properties of Portland cement hydrates in the system CaO-Al_2O_3-SiO_2-$CaSO_4$-$CaCO_3$-H_2O. Cem Concr Res 37:1379-1410
Matschei T, Lothenbach B, Glasser FP (2007c) The AFm phase in Portland cement. Cem Concr Res 37:118-130
Mehta PK (1977) Properties of blended cements, cements made from rice-husk ash. J Am Concrete I 74:440-442
Mehta PK (1981) Studies on blended Portland cements containing Santorin earth. Cem Concr Res 11:507-518
Mehta PK (1986) Condensed silica fume. *In*: Cement Replacement Materials. Swamy RN (ed) Surrey University Press, London, p 134-170
Mehta PK (1987) Natural pozzolans: Supplementary cementing materials for concrete. CANMET Special Publication 86:1-33
Mehta PK (1989) Pozzolanic and cementitious by-products in concrete. Another look. ACI Special Publication 114:1-44
Mertens G, Snellings R, Van Balen K, Bicer-Simsir B, Verlooy P, Elsen J (2009) Pozzolanic reactions of common natural zeolites with lime and parameters affecting their reactivity. Cem Concr Res 39:233-240
Meyer C (2009) The greening of the concrete industry. Cem Concr Comp 31:601-605
Mielenz RC, White LP, Glantz OJ (1950) Effect of calcination on natural pozzolanas. Symp on Use of Pozzolanic Materials in Mortars and Concrete. ASTM Special Technical Publication 99:43-92
Millet J, Hommey R (1974) Etude minéralogique des pâtes pouzzolanes-chaux. Bull Liaison Ponts et Chaussées 74:59-63
Mondragon F, Rincon F, Sierra L, Escobar J, Ramirez J, Fernandez J (1990) New perspectives for coal ash utilization: synthesis of zeolitic materials. Fuel 69:263-266
Morales EV, Villar-Cociña E, Frias M, Santos SF, Savastano H (2009) Effects of calcining conditions on the microstructure of sugar cane waste ashes (SCWA): Influence in the pozzolanic activation. Cem Concr Comp 31:22-28
Morrow CP, Nangia S, Garrison J (2009) *Ab initio* investigation of dissolution mechanisms in aluminosilicate minerals., J Phys Chem A 113:1343-1352
Mortureux B, Hornain H, Gautier E, Regourd M (1980) Comparaison de la réactivité de differentes pouzzolanes. Proceedings of the 7th International Congress on the Chemistry of Cement IV:110-115
Mostafa NY, El-Helamy SAS, Al-Wakeel EI, El-Korashy SA, Brown PW (2001) Characterization and evaluation of the pozzolanic activity of Egyptian industrial by-products. I: Silica fume and dealuminated kaolin. Cem Concr Res 31:467-474
Murat M (1983) Hydration reaction and hardening of calcined clays and related minerals. I.Preliminary investigation on metakaolinite. Cem Concr Res 13:259-266
Murayama N, Yamamoto H, Shibata J (2002) Mechanism of zeolite synthesis from coal fly ash by alkali hydrothermal reaction. Int J Miner Process 64:1-17

Naidenov V (1991) Rapid hardening cement-gypsum composites for shotcreting on the base of Bulgarian raw materials: Part I. Introduction, materials, design of the compositions, strength and deformability. Cem Concr Res 21:896-904

Nair DG, Fraaij A, Klaassen AAK, Kentgens APM (2008) A structural investigation relating pozzolanic activity of rice husk ashes. Cem Concr Res 38:861-869

Nangia S, Garrison BJ (2008) Reaction rates and dissolution mechanisms of quartz as a function of pH. J Phys Chem A 112:2027-2033

Nathan Y, Dvorachek M, Pelly I, Mimran U (1999) Characterization of coal fly ash from Israel. Fuel 78:205-213

Oelkers EH (2001) General kinetic description of multioxide silicate mineral and glass dissolution. Geochim Cosmochim Acta 65:3703-3719

Ogawa K, Uchikawa H, Takemoto K, Yasui I (1980) The mechanism of the hydration in the system C_3S pozzolanas. Cem Concr Res 10:683-696

Pal SC, Mukherjee A, Pathak SR (2003) Investigation of hydraulic activity of ground granulated blast furnace slag in concrete. Cem Concr Res 33:1481-1486

Papadakis VG (1999) Effect of fly ash on Portland cement systems Part I. Low-calcium fly ash. Cem Concr Res 29:1727-1736

Papadakis VG (2000) Effect of fly ash on Portland cement systems Part II. High-calcium fly ash. Cem Concr Res 30:1647-1654

Papayianni I, Stefanidou M (2006) Strength-porosity relationships in lime-pozzolan mortars. Constr Build Mater 20:700-705

Papayianni I, Stefanidou M (2007) Durability aspects of ancient mortars of the archeaological site of Olynthos. J Cult Herit 8:193-196

Payá J, Monzó J, Borrachero MV, Peris E, González-López E (1997) Mechanical treatments of fly ashes. Part III: studies on strength development of ground fly ashes (GFA) - cement mortars. Cem Concr Res 27:1365-1377

Pelletier L, Winnefeld F, Lothenbach B (2010) The ternary system Portland cement-calcium sulphoaluminate clinker-anhydrite: Hydration mechanism and mortar properties. Cem Concr Comp 32:497-507

Pelmenschikov A, Leszczynski J, Petterson LGM (2001) Mechanism of dissolution of neutral silica surfaces: Including effect of self-healing. J Phys Chem A 105:9528-9532

Pelmenschikov A, Strandh H, Petterson LGM, Leszczynski J (2000) Lattice resistance to hydrolysis of Si-O-Si bonds of silicate minerals: *Ab initio* calculations of a single water attack onto the (001) and (111) β cristobalite surfaces. J Phys Chem B 104:5779-5783

Péra J, Ambroise J, Messi A (1998) Pozzolanic activity of calcined laterite. Silicates Industriels 7-8:87-106

Péra J, Amrouz A (1998) Development of highly reactive metakaolin from paper sludge. Adv Cem Based Mater 7:49-56

Péra J, Boumaza R, Ambroise J (1997) Development of a pozzolanic pigment from red mud. Cem Concr Res 27:1513-1522

Perraki Th, Kakali G, Kontoleon F (2003) The effect of natural zeolites on the early hydration of Portland cement. Microporous Mesoporous Mater 61:205-212

Petrovic I, Navrotsky A, Davis ME, Zones SI (1993) Thermochemical study of the stability of frameworks in high silica zeolites. Chem Mater 5:1805-1813

Piccione PM, Laberty C, Sanyuan Y, Camblor MA, Navrotsky A (2000) Thermochemistry of pure silica zeolites. J Phys Chem B 104:10001-10011

Pöllmann H (2006) Syntheses, properties and solid solution of ternary lamellar calcium aluminate hydroxy salts (AFm-phases) containing SO_4^{2-}, CO_3^{2-} and OH^-. Neues JB Miner Abh 128:173-181.

Puertas F, Fernández-Jiménez A (2003) Mineralogical and microstructural characterization of alkali-activated fly ash/slag pastes. Cem Concr Res 25:287-292

Queralt I, Querol X, López-Soler A, Plana F (1997) Use of coal fly ash for ceramics: a case study for large Spanish power station. Fuel 76:787-791

Ramsden AR, Shibaoka M (1982) Characterization and analysis of individual fly-ash particles fom coal-fired power stations by a combination of optical microscopy, electron microscopy and quantitative electron microprobe analysis. Atmos Environ 16: 2191-2206

Regourd M (1986) Slags and slag cements. *In*: Cement Replacement Materials. Swamy RN (ed) Surrey University Press, London, p 73-99

Regourd M (2001) Cements made from blast furnace slag. *In*: Lea's Chemistry of Cement and Concrete. 4th edition. Hewlett PC (ed) Butterworth-Heinemann, Oxford, p 637-678

Richardson IG (1999) The nature of C-S-H in hardened cements. Cem Concr Res 29:1131-1147

Richardson IG (2004) Tobermorite/jennite and tobermorite/calcium hydroxide-based models for the structure of C-S-H: applicability to hardened pastes of tricalcium silicate, β-dicalcium silicate, Portland cement, and blends of Portland cement with blast furnace slag, metakaolin, or silica fume. Cem Concr Res 34:1733-1777

Richardson IG (2008) The calcium silicate hydrates. Cem Concr Res 38:137-158
Richardson IG, Brough AR, Brydson R, Groves GW, Dobson CM (1993) Substituted calcium silicate hydrate (C-S-H) gels as determined by ^{29}Si and ^{27}Al NMR and EELS. J Am Ceram Soc 76:2285-2288
Richardson IG, Brough AR, Groves GW, Dobson CM (1994) The characterization of hardened alkali-activated blast furnace slag pastes and the nature of the calcium silicate hydrate (C-S-H) phase. Cem Concr Res 24:813-829.
Richardson IG, Groves GW (1992) Models for the composition and structure of calcium silicate hydrate (C-S-H) gel in hardened tricalcium silicate pastes. Cem Concr Res 22:1001-1010
Richardson IG, Groves GW (1993) The incorporation of minor and trace elements into calcium silicate hydrate (C-S-H) gel in hardened cement pastes. Cem Concr Res 23:131-138
Richardson IG, Groves GW (1997) The structure of the calcium silicate hydrate phases present in hardened pastes of white Portland cement/blast furnace slag blends. J Mater Sci 32:4793-4802
Rocha J, Klinowski J (1990) ^{29}Si and ^{27}Al magic-angle-spinning NMR studies of the thermal transformation of kaolinite. Phys Chem Miner 17:179-186
Rodriguez-Camacho RE, Uribe-Afif R (2002) Importance of using the natural pozzolans on concrete durability. Cem Concr Res 32:1851-1858
Rojas MF (2006) Study of hydrated phases present in a MK-lime system cured at 60 °C and 60 months of reaction. Cem Concr Res 36:827-831
Rojas MF, Cabrera J (2002) The effect of temperature on the hydration rate and stability of the hydration phases of metakaolin-lime-water systems. Cem Concr Res 32:133-138
Roy A (2009) Sulfur speciation in granulated blast furnace slag: an X-ray absorption spectroscopic investigation. Cem Concr Res 39:659-663
Roy DM, Arjunan P, Silsbee MR (2001) Effect of silica fume, metakaolin, and low-calcium fly ash on chemical resistance of concrete. Cem Concr Res 31:1809-1813
Roy WR, Thiery RG, Schuller R, Suloway J (1981) Coal fly ash: a review of the literature and proposed classification system with emphasis on environental impacts. Illinois Geol Surv Environ Geol Notes EGN 96:1-69
Sabir BB, Wild S, Bai J (2001) Metakaolin and calcined clays as pozzolans for concrete: a review. Cem Concr Comp 23:441-454
Sakai E, Miyahara S, Ohsawa S, Lee S-H, Daimon M (2005) Hydration of fly ash cement. Cem Concr Res 35:1135-1140
Sastre G, Corma A (2006) Rings and strain in pure silica zeolites. J Phys Chem B 110:17949-17959
Satarin VI (1974) Slag portland cement. Proeedings of the 6th International Congress on the Chemistry of Cement, principal paper 1-51
Scheetz BE, Earle R (1998) Utilization of fly ash. Curr Opin Solid State Mater Sci 3:510-520
Schott J, Petit JC (1987) New evidence for the mechanisms of dissolution of silicate minerals. *In*: Aquatic Surface Chemistry: Chemical Processes at the Particle-Water Interface. Stumm W (ed) John Wiley and Sons, New York, p 293-315
Scott PW, Critchley SR, Wilkinson FCF (1986) The chemistry and mineralogy of some granulated and pelletized blast furnace slags. Mineral Mag 50:141-147
Scrivener KL, Kirkpatrick RJ (2008) Innovation in use and research in cementitious material. Cem Concr Res 38:128-136
Sear LKA (2001) Properties and Use of Coal Fly Ash: A Valuable Industrial By-Product. Thomas Telford, London
Sear LKA, Weatherley AJ, Dawson A (2003) The environmental impacts of using fly ash - the UK producers' perspective. International Ash Utilization Symposium, Center for applied Energy Research , University of Kentucky. *http://www.ukqaa.org.uk/Papers/KentuckyAshSymposiumLKASearEtAl2003.pdf*
Serry MA, Taha AS, El-Hemaly SAS, El-Didamony H (1984) Metakaolin-lime hydration products. Thermochim Acta 79:103-110
Sersale R (1980) Structure et charactérisation des pouzzolanes et des cendres volantes. Proceedings of the 7th International Congress on the Chemistry of Cement IV-1:3-21
Sersale R (1993) Advances in Portland and blended cements. Proceedings of the 9th International Congress on the Chemistry of Cement 261-302
Sersale R, Frigione G (1987) Portland-zeolite cement for minimizing alkali-aggregate expansion. Cem Concr Res 17:404-410
Shannag MJ (2000) High strength concrete containing natural pozzolan and silica fume. Cem Concr Comp 22:399-406
Sharma RL, Pandey SP (1999) Influence of mineral additives on the hydration characteristics of ordinary Portland cement. Cem Concr Res 29:1525-1529
Shi C (2001) An overview on the activation of reactivity of natural pozzolans. Can J Civil Eng 28:778-786

Shi C, Day RL (1995) Microstructure and reactivity of natural pozzolans, fly ash and blast furnace slag, Proceedings of the 17th International Conference on Cement Microscopy 150-161
Shi C, Day RL (2000) Pozzolanic reaction in the presence of chemical activators. Part I. Reaction kinetics. Cem Concr Res 30:51-58
Siddique R (2008) Waste Materials and By-products in Concrete. Springer, Berlin
Sjöberg L (1989) Kinetics and non-stoichiometry of labradorite dissolution. *In*: Proceedings of the 6th International Symposium on Water-Rock Interaction. Miles DL (ed) p 639-642
Smadi MM, Haddad RH (2003) The use of oil shale ash in Portland cement concrete. Cem Concr Comp 25:43-50
Smolczyk HG (1980) Slag structure and identification of slag. Proceedings of the 7th International Congress on the Chemistry of Cement I:III1-17
Snellings R, Mertens G, Cizer Ö, Elsen J (2010a) Early age hydration and pozzolanic reaction in natural zeolite blended cements: Reaction kinetics and products by in situ synchrotron X-ray powder diffraction. Cem Concr Res 40:1704-1713
Snellings R, Mertens G, Elsen J (2010b) Calorimetric evolution of the pozzolanic reaction of zeolites. J Therm Anal Calorim 101:97-105
Snellings R, Mertens G, Hertsens S, Elsen J (2009) The zeolite-lime pozzolanic reaction: Reaction kinetics and products by in situ synchrotron X-ray powder diffraction. Microporous Mesoporous Mater 126:40-49
Spence RJS, Cook DJ (1983) Building Materials in Developing Countries. Wiley and Sons, London
Stamatakis MG, Fragoulis D, Csirik G, Bedelean I, Pedersen S (2003) The influence of biogenic micro-silica-rich rocks on the properties of blended cements. Cem Concr Comp 25:177-184
Stamatakis MG, Fragoulis D, Papageorgiou A, Chaniotakis E (1998) Zeolitic tuffs from Greece and their commercial potential in the cement industry. World Cem 29:98-102
Steenari B-M, Lindqvist O (1999) Fly ash characteristics in co-combustion of wood with coal, oil or peat. Fuel 78:479-488
Stein HN, Stevels JM (1964) Influence of silica on the hydration of $3CaO.SiO_2$. J Appl Chem 14:338-346
Stillings LL, Brantley SL (1995) Feldspar dissolution at 25 °C and pH 3: Reaction stoichiometry and the effect of cations. Geochim Cosmochim Acta 59:1483-1496
Strandh H, Petterson LGM, Sjöberg L, Wahlgren U (1997) Quantum chemical studies of the effects on silicate mineral dissolution rates by adsorption of alkali metals. Geochim Cosmochim Acta 61:2577-2587
Swaddle TW, Rosenqvist J, Yu P, Bylaska E, Phillips BL, Casey WH (2005) Kinetic evidence for five-coordination in $AlOH(aq)^{2+}$ ion. Science 308:1450-1453
Swamy RN (1986) Cement Replacement Materials. Surrey University Press, London
Takemoto K, Uchikawa H (1980) Hydratation des ciments pouzzolaniques. Proceedings of the 7th International Congress on the Chemistry of Cement IV-2:1-29
Tangchirapat W, Buranasing R, Jaturapitakkul C, Chindaprasirt P (2008) Influence of rice husk-bark ash on mechanical properties of concrete containing high amount of recycled aggregates. Constr Build Mater 22:1812-1819
Tangchirapat W, Jaturapitakkul C, Chindaprasirt P (2009) Use of palm oil fuel ash as a supplementary cementitious material for producing high-strength concrete. Constr Build Mater 23:2641-2646
Taylor HFW (1990) The Chemistry of Cement. Academic Press, London
Taylor R, Richardson IG, Brydson RMD (2010) Composition and microstructure of 20-year-old ordinary Portland cement-ground granulated blast furnace slag blends containing 0 to 100% slag. Cem Concr Res 40:971-983
Tazaki K, Fyfe WS, Sahu KC, Powell M (1989) Observations on the nature of fly ash particels. Fuel 68:727-734
Thomas JJ, Rothstein D, Jennings HM, Christensen BJ (2003) Effect of hydration temperature on the solubility behavior of Ca-, S-, Al-, and Si-bearing solid phases in Portland cement pastes. Cem Concr Res 33:2037-2047
Tsipursky SI, Drits VA (1984) The distribution of octahedral cations in the 2:1 layers of dioctahedral smectites by oblique electron diffraction. Clay Miner 19:177-193
Türker P, Yeginobali A (2003) Comparison of hydration products of different pozzolanic systems. Proceedings of the 25th International Conference on Cement Microscopy 1-9
Türkmenoğlu AG, Tankut A (2002) Use of tuffs from central Turkey as admixture in pozzolanic cements Assessment of their petrographical properties. Cem Concr Res 32:629-637
Uchikawa H, Uchida S (1980) Influence of pozzolana on the hydration of C_3A. Proceedings of the 7th International Congress on the Chemistry of Cement IV:24-29
Uzal B, Turanli L, Yücel H, Göncüoğlu MC, Culfaz A (2010) Pozzolanic activity of clinoptilolite; A comparative study with silica fume, fly ash and a non-zeolitic natural pozzolan. Cem Concr Res 40:398-404
Vassilev SV, Mendez R, Borrego AG, Diaz-Somoano M, Martinez-Tarazona MR (2004) Phase-mineral and chemical composition of coal fly ashes as a basis for their multicomponent utilization. 3. Characterization of magnetic and char concentrates. Fuel 83:1563-1583

Vassilev SV, Menendez R, Alvarez D, Diaz-Somoano M, Martinez-Tarazona MR (2003): Phase-mineral and chemical composition of coal fly ashes as a basis for their multicomponent utilization. 1. Characterization of feed coals and fly ashes. Fuel 82:1793-1811

Vassilev SV, Menendez R, Diaz-Somoano M, Martinez-Tarazona MR (2004): Phase-mineral and chemical composition of coal fly ashes as a basis for their multicomponent utilization. 2. Characterization of ceramic cenosphere and salt concentrates. Fuel 83:585-603

Vassilev SV, Vassileva CH (1996) Mineralogy of combustion wastes from coal-fired power stations. Fuel Process Technol 47:261-280

Vempati RK, Rao A, Hess TR, Cocke DL, Lauer Jr. HV (1994) Fractionation and characterization of Texas lignite class 'F' fly ash by XRD, TGA, FTIR and SEM. Cem Concr Res 24:1153-1164

Villar-Cociña E, Valencia-Morales E, Gonzalez-Rodriguez R, Hernandez-Ruiz J (2003) Kinetics of the pozzolanic reaction between lime and sugar cane straw ash by electrical conductivity measurement: A kinetic-diffusive model. Cem Concr Res 33:517-524

Villar-Cociña E, Valencia-Morales E, Gonzalez-Rodriguez R, Hernandez-Ruiz J (2003) Kinetics of the pozzolanic reaction between lime and sugar cane straw ash by electrical conductivity measurement: A kinetic-diffusive model. Cem Concr Res 33:517-524

Vizcayno C, De Gutierrez RM, Castello R, Rodriguez E, Guerrero CE (2009) Pozzolan obtained by mechanochemical and thermal treatments of kaolin. Appl Clay Sci 49:405-413

Walther JV (1996) Relation between rates of aluminosilicate mineral dissolution, pH, temperature, and surface charge. Am J Sci 296:693-728

Ward CR, French D (2006) Determination of glass content and estimation of glass composition in fly ash using quantitative X-ray diffractometry. Fuel 85:2268-2277

Watt JD, Thorne DJ (1965) Composition and pozzolanic properties of pulverised-fuel ashes, Part 1-2. J Appl Chem 15:585-604

Watt JD, Thorne DJ (1966) Composition and pozzolanic properties of pulverised-fuel ashes, Part 3. J Appl Chem 16:33-39

Westrich HR, Cygan RT, Casey WH, Zemitis C, Arnold GW (1993) The dissolution kinetics of mixed-cation orthosilicate minerals. Am J Sci 293:869-893

White AF, Brantley SL (2003) The effect of time on the weathering of silicate minerals: why do weathering rates differ in the laboratory and the field? Chem Geol 202:479-506

Wild S, Gailius A, Hansen H, Pederson L, Szwabowski J (1997) Pozzolanic properties of a variety of European clay bricks: Comparative study of pozzolanic, chemical and physical properties of clay bricks in four European countries for utilization of pulverized waste clay brick in production of mortar and concrete. Build Res Inf 25:170-175

Winburn RS, Grier DG, McCarthy GJ, Peterson RB (2000) Rietveld quantitative X-ray diffraction analysis of NIST fly ash standard reference materials. Powder Diffraction 15:163-172

Winnefeld F, Lothenbach B (2010) Hydration of calcium sulfoaluminate cements - Experimental findings and thermodynamic modelling. Cem Concr Res 40:1239-1247

Wong RCK, Gillott JE, Law S, Thomas MJ, Poon CS (2004) Calcined oil sands fine tailings as a supplementary cementing material for concrete. Cem Concr Res 34:1235-1242

Wu ZQ, Young JF (1984) The hydration of tricalcium silicate in the presence of colloidal silica. J Mater Sci 19:3477-3486

Xiao Y, Lasaga AC (1994) *Ab initio* quantum mechanical studies of the kinetics and mechanisms of silicate dissolution: $H^+(H_3O^+)$ catalysis. Geochim Cosmochim Acta 58:5379-5400

Xiao Y, Lasaga AC (1996) *Ab initio* quantum mechanical studies of the kinetics and mechanisms of quartz dissolution: OH^- catalysis. Geochim Cosmochim Acta 60:2283-2295

Yilmaz B, Uçar A, Öteyaka B, Uz V (2007) Properties of zeolitic tuff (clinoptilolite) blended Portland cement. Build Environ 42:3808-3815

Yu LH, Ou H, Lee LL (2003) Investigation on pozzolanic effect of perlite in concrete. Cement Concr Res 33:73-76

Zain MFM, Islam MN, Mahmud F, Jamil M (2010) Production of rice husk ash for use in concrete as a supplementary cementitious material. Constr Build Mater, doi:10.1016/j.conbuildmat.2010.07.003

Zendri E, Lucchini V, Biscontin G, Morabito ZM (2004) Interaction between clay and lime in "cocciopesto" mortars: a study by ^{29}Si MAS spectroscopy. Appl Clay Sci 25:1-7

Zwijnenburg MA, Corá F, Bell RG (2007) On the performance of DFT and interatomic potentials in predicting the energetic of (three-membered ring-containing) siliceous materials. J Phys Chem B 111:6156-6160